A DISSERTATION FOR THE DEGREE OF DOCTOR OF PHILOSOPHY IN FOOD AND NUTRITION

Anti-inflammatory effect of isoegomaketone isolated from radiation mutant *Perilla frutescens* var. *crispa*

방사선육종 차조기에서 분리한 이소에고마케톤의 항염증 효능

August 2017

Department of Food and Nutrition

Graduate School

Seoul National University

Chang Hyun Jin

Anti-inflammatory effect of isoegomaketone isolated from radiation mutant *Perilla frutescens* var. *crispa*

방사선육종 차조기에서 분리한
이소에고마케톤의 항염증 효능

지도교수 한 성 림

이 논문을 생활과학박사 학위논문으로 제출함
2017년 4월

서울대학교 대학원
식품영양학과
진 창 현

진 창 현의 생활과학박사 학위논문을 인준함
2017년 6월

위 원 장 _____ (인)

부위원장 _____ (인)

위 원 _____ (인)

위 원 _____ (인)

위 원 _____ (인)

Abstract

Anti-inflammatory effect of isoegomaketone isolated from radiation mutant *Perilla frutescens* var. *crispa*

Chang Hyun Jin

Department of Food and Nutrition

Graduate School

Seoul National University

About 165 lines of radiation-induced mutant *P. frutescens* var. *crispa* were screened for their anti-inflammatory activities. Among those screened, the one mutant with the highest inhibitory activity on NO production in lipopolysaccharide (LPS)-treated RAW264.7 cells was selected. The enhanced anti-inflammatory activity of the mutant seemed to be due to the increase in isoegomaketone (IK) content. IK has been shown to exhibit several biological activities including anti-inflammatory, anti-cancer, and anti-obesity effects. The induction of heme oxygenase-1 (HO-1) seemed to contribute to anti-inflammatory activity of IK in RAW264.7 cells. However, there were no studies which investigated the mechanism of HO-1 induction by IK. In the present study, anti-inflammatory effect of IK isolated from radiation mutant *P. frutescens* var. *crispa* ("Antisperill") was investigated using *in vitro* and *in vivo* models. In addition, in an effort to investigate any potentiality of radiation mutant *P. frutescens* var. *crispa* as functional food, optimal extraction method was chosen, as well as anti-arthritic properties of the extracts was investigated in CAIA model.

In **Study 1**, the mechanism of IK-induced HO-1 expression was investigated using RAW264.7 cells. RAW264.7 cells were treated with IK (5, 10, 15 μM) to study the mechanism of IK-induced HO-1 expression. IK upregulated HO-1 mRNA and protein expression in a dose dependent manner. IK-induced HO-1 mRNA expression was suppressed only by SB203580, a specific inhibitor of p38 MAPK. ROS scavengers (N-acetyl-L-cysteine, NAC, and glutathione, GSH) also blocked the IK-induced ROS production and HO-1 expression. Both NAC and SB203580 suppressed the IK-induced Nrf2 activation.

In **Study 2**, whether IK has an anti-arthritic activity in collagen antibody-induced arthritis (CAIA) animal model was investigated. Rheumatoid arthritis was induced in male Balb/c mice by collagen-antibody injection. Experimental animals were randomly divided into five groups: normal, CAIA, CAIA + IK (5 mg/kg/day), CAIA + IK (10 mg/kg/day), and CAIA + apigenin (16 mg/kg/day) and respective treatments were administered via oral gavage once per day for 4 days. Mice treated with IK (10 mg/kg/day) showed improvement in disease outcome. Arthritic score, paw volume, and paw thickness were significantly lower compared to the control CAIA mice at day 7 (73%, 15%, and 14% lower, respectively). Furthermore, histopathological examination of ankle for inflammation showed that infiltration of inflammatory cells and edema formation were reduced by IK treatment. Similarly, neutrophil to lymphocyte ratio (NLR) in whole blood was lower in mice treated with IK (10 mg/kg/day) by 51.9% compared to the control CAIA mice.

In **Study 3**, to determine the optimal extraction method for developing radiation mutant *P. frutescens* var. *crispa* as functional food, extracts were

obtained by two methods: extract obtained by supercritical carbon dioxide extraction (SFE) and extract obtained by ethanol extraction (EE). SFE contained 5-fold higher levels of IK compared with EE. When LPS-induced RAW264.7 cells were treated with extracts at 25 μg/mL, the SFE inhibited the expression of inflammatory mediators such as nitric oxide (NO), monocyte chemoattractant protein-1 (MCP-1), interleutkin-6 (IL-6), interferon-β (IFN-β), and inducible nitric oxide synthase (iNOS) to a much greater extent compared with EE.

In **Study 4**, whether SFE (in Study 3) has an anti-arthritic activity in collagen antibody-induced arthritis (CAIA) animal model was investigated. Extracts were obtained by supercritical carbon dioxide extraction method from radiation mutant *P. frutescens* var. *crispa* leaf (SFE-M) and from wild type species leaf (SFE-W). Experimental animals were randomly divided into four groups: normal, CAIA, CAIA + SFE-M (100 mg/kg/day), and CAIA + SFE-W (100 mg/kg/day) and respective treatments were administered via oral gavage once per day for 4 days. Mice treated with SFE-M showed improvement in disease outcome. Arthritic score, paw volume, and paw thickness were significantly lower compared to the control CAIA mice from day 3 to day 7. Furthermore, histopathological examination of ankle for inflammation showed that infiltration of inflammatory cells and edema formation were reduced by SFE-M treatment. Similarly, NLR in whole blood was lower in mice treated with SFE-M by 37% compared to the control CAIA mice. However, SFE-W didn’t show any significant effect compared to the control CAIA group.

IK showed anti-inflammatory properties by HO-1 expression via ROS/p38 MAPK/Nrf2 pathway in RAW264.7 cells, as well as real, actual, and

palpable anti-arthritic effect in CAIA animal model. Furthermore, supercritical carbon dioxide extraction was found to be the better method compared with the ethanol extraction method for the presentation of extract from leaves of radiation mutant *P. frutescens* var. *crispa* to be used as functional food because of higher IK content. Efficacy of the extract from radiation mutant *P. frutescens* var. *crispa* by SFE was confirmed as the treatment with the extract reduced the incidence of clinically evident signs and symptoms in CAIA animal model. Taken together, the results of this study encourage the commercial use of the extract of radiation mutant *P. frutescens* var. *crispa* as a functional food in the chronic inflammatory situation like RA.

Key words: isoegomkatone, anti-inflammation, supercritical carbon dioxide extraction, radiation mutant *P. frutescens*, collagen antibody-induced arthritis

Student Number: 2011-31095

Contents

Abstract i

Contents v

List of Tables x

List of Figures xi

List of Abbreviations xiv

I. Introduction 1

1. Background 2

2. Objectives of the study 5

II. Literature review 7

1. Radiation breeding 8

2. Characteristics of *Perilla frutescens* 13

2.1. Bioactivity 13

2.2. Active constituents 16

2.3. Extraction method 18

3. Pharmacological activities of isoegomaketone 20

4. Mouse model of rheumatoid arthritis 21

4.1. Collagen-induced arthritis (CIA) 22

4.2. Collagen antibody-induced arthritis (CAIA) 23

4.3. Zymosan-induced arthritis 23

5. Previous study 24

III. Study 1: Isoegomaketone upregultes heme oxygenase-1 in RAW264.7 cells via ROS/p38 MAPK/Nrf2 pathway 28

1. Abstract 29

2. Introduction 30
3. Materials and Methods 32
3.1. Reagents 32
3.2. Isolation of IK 32
3.3. Cell culture 38
3.4. Cytotoxicity assay 38
3.5. Determination of NO concentration 38
3.6. Preparation of cell extracts and western analysis 39
3.7. Quantitative real-time PCR 40
3.8. Statistical analysis 43
4. Results 44
4.1. Effect of IK on HO-1 expression in RAW264.7 cell 44
4.2. Effect of kinase inhibitors on HO-1 expression by IK treatment 46
4.3. Effect of ROS scavengers on HO-1 expression by IK treatment 49
4.4. Effect of ROS scavenger and p38 MAPK inhibitor on Nrf2 activation by IK treatment 51
4.5. Effect of NAC on NO production in LPS-treated RAW264.7 cells 53
4.6. Effect of ROS scavengers on the production of antioxidant enzymes 55
5. Discussion 57

IV. Study 2: Isoegomaketone alleviates the development of collagen antibody-induced arthritis in male Balb/c mice 61
1. Abstract 62

2. Introduction 63
3. Materials and Methods 65
3.1. Animals 65
3.2. Sample preparation 65
3.3. Collagen antibody-induced arthritis 65
3.4. Assessment of clinical signs of inflammation 68
3.5. Histopathological assessment 68
3.6. Analysis of neutrophil and lymphocyte 69
3.7. Statistical analysis 69
4. Results 70
4.1. Effect of IK treatment on development of RA in CAIA model 70
4.2. Effect of IK treatment on paw volume in CAIA model 74
4.3. Effect of IK treatment on paw thickness in CAIA model 76
4.4. Effect of IK treatment on arthritic score in CAIA model 78
4.5. Effect of IK treatment on blood cell population in CAIA model 80
5. Discussion 82

V. Study 3: Comparison of the anti-inflammatory activities of supercritical carbon dioxide versus ethanol extracts from leaves of radiation mutant *Perilla frutescens* var. *crispa* 86
1. Abstract 87
2. Introduction 88
3. Materials and Methods 90
3.1. Materials 90
3.2. Cell culture 90

3.3. Ethanol extraction 91
3.4. SC-CO_2 extraction 91
3.5. HPLC analysis 92
3.6. Cytotoxicity assay 92
3.7. Determination of NO concentration 93
3.8. Preparation of cell extracts and western blot analysis 93
3.9. Quantitative real-time PCR 95
3.10. Measurement of MCP-1, IFN-β, and IL-6 by ELISA 97
3.11. Statistical analysis 97
4. Results 98
4.1. Yield and composition of SFE (supercritical carbon dioxide extract) and EE (ethanol extract) 98
4.2. Effect of SFE and EE on cell viability 102
4.3. Effect of SFE and EE on LPS-stimulated NO production in RAW264.7 cells 104
4.4. Effect of SFE and EE on production of inflammatory mediators in LPS-stimulated RAW264.7 cells 107
5. Discussion 110

VI. Study 4: Anti-arthritic activities of the supercritical carbon dioxide extract from radiation mutant *Perilla frutescens* var. *crispa* in collagen antibody-induced arthritis 113
1. Abstract 114
2. Introduction 115
3. Materials and Methods 118
3.1. Animals 118
3.2. SC-CO_2 extraction 118

3.3. HPLC analysis 119
3.4. Sample preparation and treatment 119
3.5. Collagen antibody-induced arthritis 120
3.6. Assessment of clinical signs of inflammation 122
3.7. Histopathological assessment 122
3.8. Analysis of neutrophil and lymphocyte 123
3.9. Statistical analysis 123
4. Results 124
4.1. Composition of SFE-M (supercritical carbon dioxide extract from radiation mutant *P. frutescens*) and SFE-W (supercritical carbon extract from wild type *P. frutescens*) 124
4.2. Effect of SFE-W and SFE-M treatment on development of RA in CAIA model 126
4.3. Effect of SFE-W and SFE-M treatment on paw volume in CAIA model 131
4.4. Effect of SFE-W and SFE-M treatment on paw thickness in CAIA model 133
4.5. Effect of SFE-M and SFE-W treatment on arthritic score in CAIA model 135
4.6. Effect of SFE-M and SFE-W treatment on blood cell population in CAIA model 137
5. Discussion 139

VII. Overall Discussion 142
References 147
국문초록 163

List of Tables

Table 2.1	Milestones in the development of induced mutagenesis.	9
Table 2.2	The constituents and their effects of *P. frutescens*	17
Table 2.3	The several extraction methods from *P. frutescens*	19
Table 3.1	Primers sequences for Real Time-PCR analysis	42
Table 4.1	Histopathological scores of the groups	72
Table 5.1	Primers sequences for Real Time-PCR analysis	96
Table 5.2	Extraction yield and HPLC data of samples extracted with ethanol and SC-CO_2 from *P. frutescens* var. *crispa* leaves	100
Table 6.1	Histopathological scores of the groups	128

List of figures

Figure 2.1	Breeding process of radiation mutant *P. frutescens* var. *crispa*	12
Figure 2.2	The selection process of "Antisperill", a radiation mutant *P. frutescens* var. *crispa* contained higher IK content	26
Figure 2.3	Putative model for the inhibition of NO production by IK in LPS-induced RAW264.7 cells	27
Figure 3.1	Isolation scheme for isoegomaketone	35
Figure 3.2	Purity of isoegomaketone measured by HPLC analysis	36
Figure 3.3	Chemical structure of isoegomaketone	37
Figure 3.4	The expression of HO-1 by IK treatment in RAW264.7 cells.	45
Figure 3.5	Effect of specific kinase inhibitors on cell viability.	47
Figure 3.6	Effect of specific kinase inhibitors on HO-1 expression in IK-treated RAW274.7 cells.	48
Figure 3.7	Effect of ROS scavengers on HO-1 expression in IK-treated RAW264.7 cells.	50
Figure 3.8	Effect of NAC and p38 MAPK inhibitor on Nrf2 activation in IK-treated RAW264.7 cells.	52
Figure 3.9	Effect of NAC on NO production in LPS-treated RAW264.7 cells.	54
Figure 3.10	Effect of ROS scavengers on the production of antioxidant enzymes in IK-treated RAW264.7 cells.	56

Figure 4.1	The scheme of induction of CAIA and sample treatment	67
Figure 4.2	Image of representative microscopic features of knee joint and mice joint.	71
Figure 4.3	Effect of IK and API on mean histopathological arthritis score in CAIA mice.	73
Figure 4.4	Effect of IK and API on paw volume in CAIA mice.	75
Figure 4.5	Effect of IK and API on paw thickness in CAIA mice.	77
Figure 4.6	Effect of IK and API on arthritic score in CAIA mice.	79
Figure 4.7	Effect of IK and API on neutrophil-to-lymphocyte ratio in CAIA mice.	81
Figure 5.1	HPLC chromatograms.	101
Figure 5.2	Effect of SFE and EE on cell viability.	103
Figure 5.3	Effect of SFE and EE on NO production and iNOS expression levels in RAW264.7cells.	106
Figure 5.4	Effect of SFE and EE on the production of inflammatory mediators in RAW264.7cells.	108
Figure 5.5	Effect of SFE and EE on IL-6 and MCP-1 expression levels in RAW264.7cells.	109
Figure 6.1	The scheme of induction of CAIA and sample treatment	121
Figure 6.2	HPLC chromatograms	125
Figure 6.3	Image of representative microscopic features of	127

knee joint and mice joint.

Figure 6.4 Effects of SFE-M and SFE-W on mean histopathological arthritis score in CAIA mice. 129

Figure 6.5 Effect of SFE-M and SFE-W on weight in CAIA mice. 130

Figure 6.6 Effect of SFE-M and SFE-W on paw volume in CAIA mice. 132

Figure 6.7 Effect of SFE-M and SFE-W on paw thickness in CAIA mice. 134

Figure 6.8 Effect of SFE-M and SFE-W on arthritic score in CAIA mice. 136

Figure 6.9 Effect of SFE-M and SFE-W on neutrophil-to-lymphocyte ratio in CAIA mice. 138

List of Abbreviations

API	Apigenin
ARE	antioxidant response element
CAIA	Collagen antibody-induced arthritis
CAT	Catalase
CIA	Collagen-induced arthritis
CO	Carbon monoxide
EE	Ethanol extract of Perilla leaf
EK	Egomaketone
GSH	Glutathione
GST	Glutathione S-transferase
HO-1	Heme oxygenase-1
IFN-β	Interferon-β
IK	Isoegomaketone
IL-1	Interleukin-1
IL-6	Interleukin-6
LPS	Lipopolysaccharide
MCP-1	Monocyte chemoattractant protein-1
iNOS	Inducible nitric oxide synthase
NAC	N-acetyl-L-cysteine
LET	Linear energy transfer
NLR	Neutrophil to lymphocyte ratio

NO	Nitric oxide
Nrf2	Nuclear factor E2-related factor 2
NSAID	Nonsteroidal anti-inflammatory drugs
NQO-1	NADH quinone oxidoreductase
PI3K	Phosphoinositide 3-kinase
PK	Perilla ketone
PKC	Protein kinase C
RA	Rheumatoid arthritis
ROS	Reactive oxygen species
SC-CO_2	Supercritical carbon dioxide extraction
SFE	Supercritical carbon dioxide extract
SFE-M	SC-CO_2 extract of radiation mutant *P. frutescens*
SFE-W	SC-CO_2 extract of wild type *P. frutescens*
TNFα	Tumor necrosis factor α

I. Introduction

1. Background

Perilla frutescens (L.) Britt. is an annual herbaceous plant in the Lamiaceae family. Its leaves are used as food in Asian cuisines and its seeds are used for the extraction of edible oil in Korea. In traditional medicine practices, *P. frutescens* is also used for treatment of various illnesses including cough, phlegm, back pain, and diabetes (Han *et al*., 1994; Kim *et al*., 2007). In previous studies, *P. frutescens* extracts were prepared using diverse methods to examine the pharmacological activities: the ethanol extract (Lee and Han, 2012) showed anti-inflammatory effect; the water and ethanol extracts had antioxidant effect (Cho *et al*., 2011b); the methanol extract exerted a preventative action against Alzheimer's *disease* (Choi *et al*., 2004). Supercritical carbon dioxide (SC-CO_2) extraction has been used for seeds of *P. frutescens* (Jung *et al*., 2012; Kim *et al*., 1998), but SC-CO_2 extraction method has not been used for the extraction of isoegomaketone (IK) from *P. frutescens* leaves.

Induction of mutation and selection of mutants have been considered as powerful tools for plant breeding and researches for the past 80 years. X-ray, γ (gamma) ray irradiation, and chemical treatments have been used for breeding of mutants in a wide range of plants (Nakano *et al*., 2010). Over the past 40 years, the use of γ rays for the induction of mutation has become

particularly prevalent, while the use of X-rays has been significantly decreased. Gamma rays is a type of ionizing radiation that interacts with atoms to induce free radicals in cells which damage or modify important components of plant cells such as chromosome.

IK, an oil component in *P. frutescens*, has been shown to have numerous biological activities. It has been shown to have inhibitory activity on NO production in LPS-treated RAW264.7 cells (Jin *et al*., 2010). IK induced apoptosis in several cancer cells through caspase-dependent and -independent pathways (Cho *et al*., 2011a; Kwon *et al*., 2014a). Furthermore, IK has the potential for increasing the effectiveness of prostate cancer therapy with TRAIL (Lee *et al*., 2014). Previously, it was shown that IK induced the HO-1 expression in RAW264.7 cells (Jin *et al*., 2010), however, the detailed mechanism is yet to be elucidated.

SC-CO_2 extraction is a novel and powerful technique for extracting lipophilic components (Guan *et al*., 2007; Sookwong *et al*., 2016). SC-CO_2 extraction has several advantages over the use of organic solvents, because CO_2 is non-toxic, non-reactive, non-corrosive, and inexpensive.

Rheumatoid arthritis (RA) is a systemic autoimmune disease in which chronic joint inflammation leads to cartilage destruction and bone erosion (Scott *et al*., 2010). About 1% of US population is affected by RA, and RA

increases the risk for cardiovascular disease, lymphoma, and death (Yang *et al*., 2013). Typically, RA is treated with steroidal/nonsteroidal anti-inflammatory drugs (NSAID) or biological modulators such as tumor necrosis factor alpha (TNF-α) inhibitors and interleutkin-1 (IL-1) receptor antagonists (Smolen *et al*., 2014). Acetaminophen, a kind of NSAID, is frequently used in very high doses (4 g/day) (Dragos *et al*., 2017). However, the use of standard drugs in RA caused numerous side effects: infusion hypersensitivity reactions with the use of TNF-α inhibitors (Matucci *et al*., 2016); gastrointestinal ulcerations and hemorrhagic events triggered by NSAID (McAlindon *et al*., 2014); higher risk of infection due to the use of biological drugs (Cabral *et al*., 2016); etc. Therefore, the renewed interest in botanical origin remedies which lack severe side effects and have millennia-proven efficacy is growing (Umar *et al*., 2014). These remedies maybe have a beneficial effect not only on the symptoms but also on the development of the disease (Akhtar *et al*., 2011). Previously, it was reported that IK reduced NO production and iNOS protein levels in LPS-treated Balb/c mice (Jin *et al*., 2010). Although there is strong evidence that IK has anti-inflammatory effect, whether IK can exert a treatment effect on inflammatory disease such as RA has not been investigated. Furthermore, the studies using the extract containing IK will be needed to apply into functional food.

2. Objectives of the study

Hypotheses

It is hypothesized that (1) IK will induce HO-1 expression via ROS/MAPK/Nrf2 pathway in RAW 264.7 cells, (2) IK treatment will delay the development of the arthritis and alleviate the symptoms of arthritis, (3) SC-CO_2 extraction method will be more suitable method for acquiring extracts containing higher IK content from radiation mutant *P. furtescens* var. *crispa*, and (4) SFE-M treatment will delay the development of the arthritis and alleviate the symptoms of arthritis in CAIA model.

Specific aims

Study 1: To test the hypothesis, changes in HO-1 expression with the treatment of specific MAPK inhibitors and ROS scavengers were determined in IK-treated RAW 264.7 cells.

Study 2: To test the hypothesis, effects of IK treatment were determined in CAIA mouse model and arthritic score, paw volume, paw thickness, histopathological changes, and NLR were compared between the treatment and the control group.

Study 3: To test the hypothesis, two extracts prepared using SC-CO_2 extraction method and ethanol extraction method from *P. frutescens* leaves were compared for IK concentration and anti-inflammatory activities.

Study 4: To test the hypothesis, effects of SFE-M treatment were determined in CAIA mouse model and arthritic score, paw volume, paw thickness, histopathological changes, and NLR were compared between the treatment and the control group.

II. Literature review

1. Radiation breeding

Plant breeding methods have contributed immensely to the development of genetically improved crop varieties. These methods continue to enrich the crop germplasm base by evolving genetically superior varieties for cultivation. Existing germplasm resources may not be adequate to meet the food needs of an ever-increasing human population, estimated to swell to nine billion by 2050 (Green *et al*., 2005). The use of induced mutations has played a key role in the improvement of superior plant varieties (Ahloowalia and Maluszynski, 2001). A large number of improved mutant varieties have been released for commercial cultivation in different crop species demonstrating economic value of the mutation breeding technology (Kharkwal and Shu, 2009). Induced mutations provide a viable option by generation of a novel source of resistance to biotic/abiotic stress factors whereby a new resistant variety can be developed. Since the very early part of the twentieth century, several experimental breakthroughs were made in the area of induced mutagenesis (Table 2.1).

Table 2.1. Milestones in the development of induced mutagenesis (Suprasanna *et al*., 2015)

Year	Induced mutagenesis
1901-1904	de Vries: radiation induced mutations in plants and animals
1927	Muller: Drosophila-proof of mutation induced by X-rays opened a new avenue in genetics and breeding
1928	Stadler: first report on induced mutation in crop plants-barley, maize, wheat and oat
1936	The first induced mutant variety released-tobacco var. 'Chlorina' using X-ryas
1942	First report of induced disease resistance in a crop plant; X-ray induced mildew resistance in barley
1944	The term 'Mutation Breeding' coined; First report of chemically induced mutation
1949	First plant mutation experiment using ^{60}Co gamma ray installation; ^{60}Co became a standard tool in mutation induction of crop plants
1964	The FAO/IAEA Joint Division was set up with a mandate to support and encourage the production of induced mutations for crop production particularly for food security issues in developing countries
1966	First chemically induced mutant variety, Luther of barley
1993	Register of plant mutant varieties set up by the FAO/IAEA, which became the mutant variety genetic stock database (http://mvgs.iaea.org) in 2008
2000-2009	Development of high-throughput genotyping and phenotyping using automated, robotic and computerized systems

Several types of mutagenic agents are used extensively to create genetic variation for use in genetics and/or crop improvement. Ionizing radiation can be divided into two classes according to differences in linear energy transfer (LET). Alpha particles, neutrons, and heavy ion beams have high LET, while gamma rays, X-rays, and electron beams have low LET. These radiation sources were used to produce mutant in several plants. Since the discovery in Drosophila (Muller, 1927) and in barley (Stadler, 1928) that X rays can induce mutations, radiation-induced mutants have been extensively studied and utilized in various ways, such as in the analysis of gene function and for mutation breeding. Over the past 40 years, the use of gamma rays in mutation induction has become prevalent, while the use of X-rays has been reduced. Recent study has shown that heavy ion beams, also classified as high LET radiation, tend to induce structural changes in the chromosomes (Shikazono *et al*, 2000). Among the physical mutagens, gamma rays are the most popular among mutation breeders because of the convenience of use and their ability to penetrate deep into a biological matter. Gamma rays induce nucleotide substitutions and small deletions of 2-16 bp and the mutation frequency is estimated to be one mutation/6.2 Mb (Sato *et al*., 2006). In previous reports, several mutant crops were acquired using gamma irradiation; a rice mutant with altered seed tocopherols (Hwang *et al*., 2014),

soybean mutant lines with a low lipoxygenase content (Lee *et al*., 2014), Perilla mutant with variation of leaf flavor components (Lee *et al*., 1999).

The radiation mutant *P. frutescens* var. *crispa* was acquired using gamma ray irradiation. The seeds of *P. frutescens* var. *crispa* were irradiated with 200 Gy using gamma ray and then 2,000 seeds were gathered (M1 generation). Through sowing seeds every year, 165 seeds were acquired in M3 generation. And then 165 seeds were cultivated in the field every year for uniformity and stability (Figure 2.1).

Year	**‘95**	**‘96**	**‘97**	**‘98**	**‘99**	**‘00**	**‘01**	**’02**	**‘03**	**‘04**
Generation	Irradiation of seeds	M1	M2	M3	M4	M5	M6	M7	M8	M9
P. Frutescens var. *crispa*	200 Gy irradiation	1 2,000	1 2,000	CJ-1 . . . . . . CJ-165	Confirm of uniformity and stability					
	Irradiation	Group Selection		Line Selection						

Figure 2.1. Breeding process of radiation mutant *P. frutescens* var. *crispa*

2. Characteristics of *Perilla frutescens*

P. frutescens belongs to the annual herbaceous plant in the Lamiaceae family and is an edible` plant frequently used in Asian countries including Korea, Japan and China. It has a pleasant flavor and taste and is used as a food ingredient. The herb is about 1 m high with small flowers, a gray-brown fruit, and glossy, downy-haired leaves. Cultivation of the crop is grown from seed and sown in May. Harvesting is usually between the end of September and beginning of October. The applicable parts of perilla plants are the leaves and seeds. There are two different leaf colors caused by their differing accumulation of anthocyanins (Gong *et al*., 1997): a red-purple type (red perilla, *P. frutescens* var. *acuta* (Odash.) Kudo and *crispa* (Benth.) W. deane, Jasoyeop in Korea, Aka-jiso in Japanese) and a green-purple type (green perilla, *P. frutescens* f. *viridis* Makino, ‘Chungsoyeop’ in Korean, ‘Ao-jiso’ in Japanese).

2.1 Bioactivity

P. frutescens has been used as an oriental medicine for many years in Asia and has been passed on through generations by experience. Recent studies demonstrated the pharmacological activities of *P. frutescens*.

Long-term secondary diabetic complications are the main cause of morbidity and mortality in diabetic patients. The aldose reductase gene has been a drug target in the clinical management of diabetes, because it involved in diabetic complication. The EtOAc-soluble fractions of *P. frutescens* leaves showed strong inhibitory activity for aldose reductase (Paek *et al*., 2013). The inhibitory compounds from those fractions were identified as chlorogenic acid, rosmarinic acid, luteolin, and methyl rosmarinic acid (Paek *et al*., 2013). ROS are constantly produced and play a key role in the pathogenesis of a wide variety of acute and chronic neurodegenerative diseases. Hydrogen peroxide is one of the major ROS and excessive production is associated with pathological process of acute and chronic neuronal toxicity. The methanol extract of *P. frutescens* reduced cell damage and lipid peroxidation in C6 glial cells through the regulation of mRNA and protein expression of iNOS and COX-2 (Lee *et al*., 2016). Rosmarinic acid was the main component for neuro-protective effect.

Gastrointestinal discomfort is a common symptom in otherwise healthy adults. Approximately 20% of the population, particularly women suffer from gastrointestinal discomfort and this affects quality of life. However, those symptoms were significantly improved over time by *P. frutescens* water extract against placebo (Sybille *et al*., 2014).

Chronic high-fat diet feeding induced hepatic lipid overload and hepatocellular cholesterol metabolic imbalance. The perilla seed oil supplement rescued the HFD-induced steatosis and depressed hepatic inflammation (Chen *et al*., 2011). Perilla seed oil rich in α-linolenic aid can regulate the expression of multiple nuclear transcription factors, and it can be a potential dietary therapeutic tool (Chen *et al*., 2011). In another report, *P. frutescens* methanol extract promoted the induction of the ATP-binding cassette transporters and subsequently accelerated cholesterol efflux from the lipid-loaded macrophages (Park *et al*., 2015). α-asarone was isolated from methanol extract and characterized as a major component for those activity, but not β-asarone (Park *et al*, 2015).

House dust mite is a major causative factor for airway hypersensitiveness and asthma. Mite major allergen Der p 2 is known to trigger both pro-inflammatory and pro-allergic responses on respiratory epithelial cells. *P. frutescens* methanol extract diminished mRNA expression of pro-allergic cytokines as well as pro-inflammatory cytokines in BEAS-2B cells (Liu *et al*., 2013). And *P. frutescens* ethanol extract significantly suppressed Th2 responses and airway inflammation in allergic murine model of asthma (Chen *et al*., 2015b).

There are many previous reports about anti-inflammatory activities of *P. frutescens*: Inhibition of proinflammatory cytokine generation in lung inflammation by the leaves of *P. frutescens* (Lim *et al*., 2014); Inhibition of N-formyl-Met-Leu-Phe-induced phosphorylation of the Src family kinases and decrease of intracellular Ca^{2+} level by *P. frutescens* ethanol extract (Chen *et al*., 2015a).

The ethanol extract of *P. frutescens* leaves inhibited the growth, migration, and adhesion of human cancer cells (Kwak and Ju, 2015). The possible main components were luteolin, rosmarinic acid and isoegomaketone. And the methanol extract of *P. frutescens* leaves inhibited tumor proliferation of HCC via PI3K/AKT signal pathway (Wang *et al*., 2013). Isoegomaketone was the main component that showed anti-cancer activity.

2.2 Active constituents

P. frutescens contains several components including rosmarinic acid, luteolin, perillaldehyde, perillyl alcohol, perillic acid, and isoegomaketone. Recent studies demonstrated the pharmacological activities of those constituents of *P. frutescens* (Table 2.2).

Table 2.2. The constituents and their effects of *P. frutescens*

Constituents	Effects	Reference
Perillaldehyde	Activation of the Nrf2-Keap1 system	Masutani *et al*., 2009
	Promote the antioxidant activity of berries	Wang *et al*., 2008
Perillyl alcohol	Induce cell cycle arrest and cell death	Elegbede *et al*., 2003
	Inhibitory effects on HCT116 cells	Bardon *et al*., 2002
Perillic acid	Inhibitory effects on cancer cells	Bardon *et al*., 2002
Rosmarinic acid	Inhibit seasonal allergic rhinoconjunctivitis	Takano *et al*., 2004
	Anti-allergic effect	Oh *et al*., 2011
	Anticarcinogenic effects in murine two-stage skin model	Osakabe *et al*., 2004
	Inhibition of LPS-induced liver injury	Osakabe *et al*., 2002
Luteolin	Inhibit inflammation and allergic responses	Ueda *et al*., 2002
Isoegomaketone	Anti-inflammation and anti-cancer	Jin *et al*., 2010
		Cho *et al*., 2011

2.3 Extraction method

There have been many reports regarding extraction from perilla using organic solvents, supercritical carbon dioxide, and microwave-assisted techniques (Table 2.3). Generally, the water extraction method is used in the food industries, because it is an efficient and environmentally friendly technique for extracting various compounds from plants (Siti *et al*., 2016). Supercritical carbon dioxide (SC-CO_2) extraction is a novel and powerful technique for extraction lipophilic components (Guan *et al*., 2007). SC-CO_2 extraction has several advantages over the use of organic solvents, because CO2 is non-toxic, non-reactive, non-corrosive, and inexpensive.

Table 2.3. The several extraction methods from *P. frutescens*

Extraction	Region	Effect	Reference
Methanol	Leaf	Anti-microbial	Kang *et al*., 2011
	Leaf	Remove cholesterol	Park *et al*., 2015
	Leaf	Anti-cancer	Wang *et al*., 2013
	Leaf	Anti-allergic, Anti-inflammatory	Liu *et al*., 2013
	Leaf	Neuro-protective	Lee *et al*., 2016
	Leaf	Anti-diabetic	Paek *et al*., 2013
Water	Leaf	Gastrointestinal discomfort	Sybille *et al*., 2014
	Leaf	Anti-allergic, Anti-inflammatory	Chen *et al*., 2015
Ethanol	Leaf	Anti-cancer	Kwak and Ju, 2015
	Leaf	Anti-inflammation	Lim *et al*., 2014
		Anti-inflammation	Chen *et al*., 2015
Supercritical carbon dioxide	Seed	Anti-oxidant	Jung *et al*., 2012
	Seed	Anti-oxidant	Kim *et al*., 1998
Microwave	Leaf	Anti-oxidant	Shao *et al*., 2012

3. Pharmacological activities of isoegomaketone

Isoegomaketone (IK), an essential oil component in *P. frutescens*, has been shown to have several activities. IK is synthesized with perilla ketone directly from precursor egomaketone (Nishizawa *et al*., 1989). And perilla ketone is not converted from IK. In LPS-induced RAW264.7 cells, IK inhibited NO production through the heme oxygenase-1 induction and suppression of the interferon-β-STAT-1 pathway (Jin *et al*., 2010). To enhance anti-inflammatory activity of IK, its derivatives were synthesized as anti-inflammatory agents (Park *et al*., 2011). There are several reports about anti-cancer effect of IK: Induction of apoptosis in human DLD1 cells through caspase-dependent and –independent pathways (Cho *et al*., 2011); Induction of apoptosis in B16 melanoma cells mediated through ROS generation and mitochondrial-dependent, -independent pathway (Kwon *et al*., 2014a); Induction of apoptosis in SK-MEL-2 human melanoma cells through mitochondrial apoptotic pathway (Kwon *et al*., 2014b); Potentiating TRAIL-mediated apoptosis through up-regulation of death receptor 5 via a ROS-independent pathway (Lee *et al*., 2014); Inhibition tumor proliferation of HCC via PI3K/Akt signal pathway (Wang *et al*., 2013); Inhibition of the growth, migration, and adhesion of HCT116 and H1299 cells (Kwak and Ju, 2015).

4. Mouse models of rheumatoid arthritis

Rheumatoid arthritis (RA) is a chronic autoimmune disorder characterized by synovitis that leads to cartilage and bone erosion by invading fibrovascular tissue. The pathogenesis of RA is complex and involves genetic predispositions as well as environmental components (Imboden, 2009). The main cause to the pathogenesis is the activation of macrophages by autoreactive T cells, resulting in the releases of pro-inflammatory mediators such as tumor necrosis factor α (TNF-α), interleukin 1 (IL-1), and interleukin-6 (IL-6). The induction to articular disease onset is unknown and factors that define chronicity of the responses are poorly understood. Autoreactive T cells providing help to B cells or releasing several pro-inflammatory cytokines are a crucial factor in the initiation and maintenance of lesions in RA as well as mouse model (Cordova *et al*., 2013). However, T cells are not required for the induction of collagen antibody-induced arthritis (Nandakumar *et al*., 2004). Antibodies to citrullinated antigens that are implicated in the pathogenesis of RA have been shown to be important in mouse models, including collagen-induced arthritis (Kidd *et al*., 2008). Antibody- and complement-mediated effects are important drivers in RA as well as mouse models. Neutrophils are abundant in murine autoimmune arthritis and contribute to the pathogenesis through the release of cytotoxic

products and immunoregulatory mediators. Cartilage and bone injury is driven by the formation of an inflammatory pannus that classically invades the joint from the capsular angle. Macrophages infiltrating the synovium are central in the pathogenesis of RA, serving IL-1β and TNF-α. Mouse models are an important tool for investigating disease mechanisms *in vivo* and have been used for many years.

4.1 Collagen-induced arthritis (CIA)

CIA shares many similarities with human RA. Two characteristics of the CIA model such as breach of tolerance and generation of auto-antibodies toward self and collagen make CIA the good standard *in vivo* model for RA studies. DBA/1 mice are most widely used in the CIA model. Clinical signs of disease typically develop 21-25 days after the initial inoculation and presents as a polyarthritis, which is most prominent in the limbs and characterized by synovial inflammatory infiltration, cartilage and bone erosion similar to human RA. The development of CIA is associated with both B- and T-cells responses with the production of anti-collagen type II antibodies and collagen-specific T cells. Disease severity is expected to peak at approximately day 35, after which DBA/1 mice enter remission, marked by

increased concentration of serum IL-10 and a subsequent decrease in pro-inflammatory Th1 cytokines (Mauri *et al*., 1996).

4.2 Collagen antibody-induced arthritis (CAIA)

RA is associated with auto-antibody production against self-type II collagen, citrullinated proteins (ACPA) and IgG. This demonstrates a role for humoral immunity in the development of arthritis in which type II collagen is thought to be the predominant epitope (Rowley *et al*., 2008). In addition, anti-collagen antibody cocktails have been shown to induce the development of arthritis (Holmdahl *et al*., 1986). Although the clinical development of arthritis is similar to that in CIA and RA, CAIA is characterized by macrophage and polymorphonuclear inflammatory cell infiltrate (Santos *et al*., 1997), but is not associated with a T- and B-cell response. Furthermore, as disease develops within 48 h of antibody injection with 100% penetrance and is inducible regardless of the MHC class II haplotype, CAIA is well-suited for studying the development of arthritis in genetically modified strains of mice.

4.3 Zymosan-induced arthritis

Zymosan is a polysaccharide from the cell wall of Saccharomyces cerevisiae with repeating glucose units connected by β-1,3-glycosidic linkage. It binds to TLR2 in macrophages leading to the induction of pro-inflammatory cytokines, arachidonate mobilization, and protein phosphorylation and also activates complement. Injection of zymosan intra-articularly into the knee joints of mice results in a proliferative inflammatory arthritis with mononuclear cell infiltration, synovial hypertrophy and pannus formation with the peak of disease at about day 3 and inflammation subsiding by day 7 (Keystone *et al*., 1977). The main limitation of this model is the monoarthritic nature of the disease and the technical skill required for an intra-articular injection in mice.

5. Previous study

In an effort to assess whether radiation mutants (165 species) of *P. frutescens* var. *crispa* have enhanced anti-inflammatory activity when compared to wild type, the inhibitory activity for nitric oxide production in LPS-stimulated RAW264.7 cells was measured using ethanol extracts of mutants. As a result, one mutant (named “Antisperill) showed stronger inhibitory activity than wild type. The reason for enhanced anti-inflammatory property of the mutant was due to increase of IK content according to HPLC and NMR analysis

(Figure 2.2). Anti-inflammatory activities of IK were investigated in LPS-treated RAW264.7 cells (Jin *et al*., 2010). IK inhibited LPS-induced nitric oxide production by suppressing IFN-β-STAT-1 pathways as well as inducing of heme oxygenase-1 (Figure 2.3). However, the detailed mechanism for expression of HO-1 by IK treatment is not known yet.

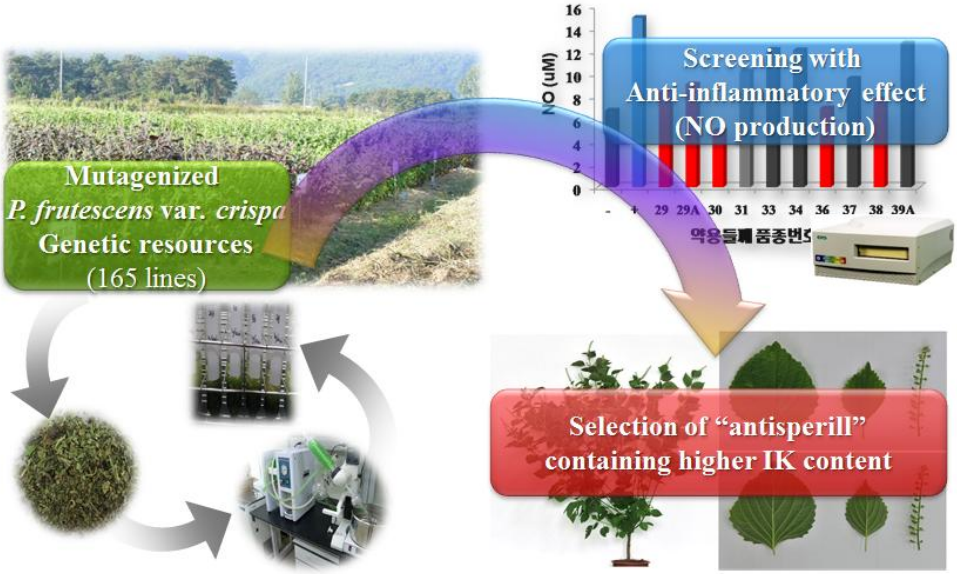

Figure 2.2. The selection process of "Antisperill", a radiation mutant *P. frutescens* var. *crispa* contained higher IK content.

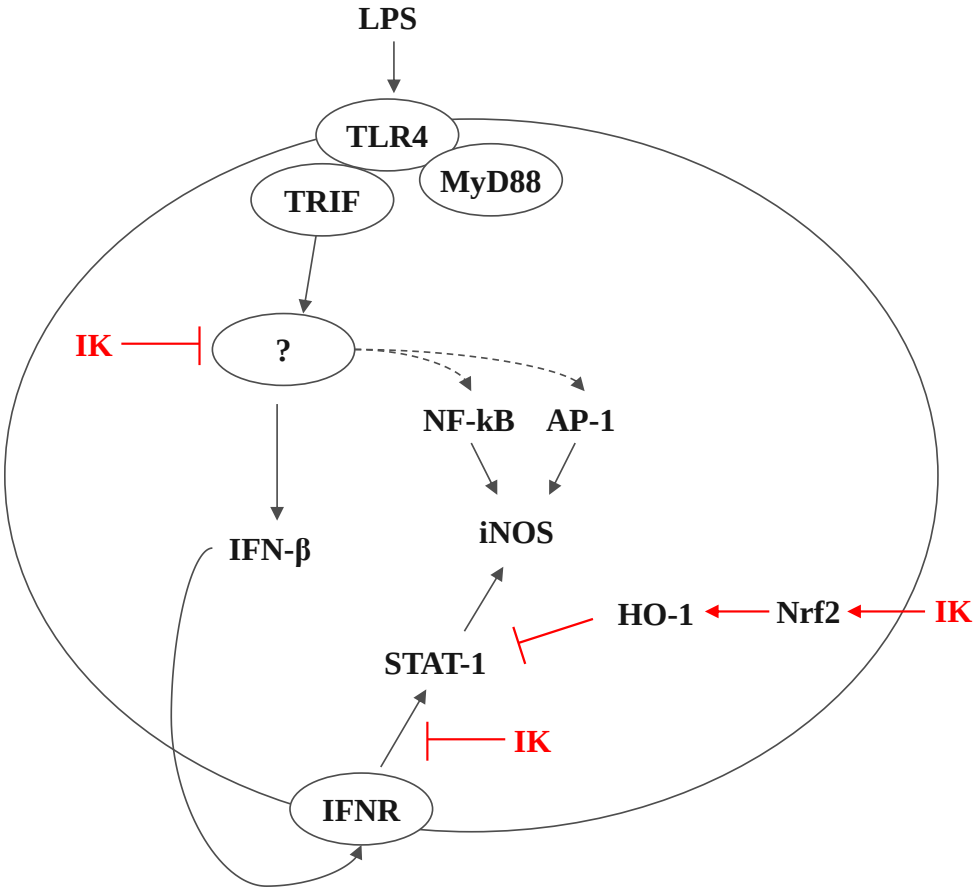

Figure 2.3. Putative model for the inhibition of NO production by IK in LPS-induced RAW264.7 cells.

III. Study 1

Isoegomaketone upregultes heme oxygenase-1 in RAW264.7 cells via ROS/p38 MAPK/Nrf2 pathway*

(*The part of the results was published in *Biomol. Ther.* 2016, 24(5):510-516)

1. Abstract

Isoegomaketone (IK) was isolated from *Perilla frutescens* var. *crispa*, which has been widely used as a food in Asian cuisine, and evaluated for its biological activity. We have already confirmed that IK induced the HO-1 expression via nuclear factor E2-related factor 2 (Nrf2) activation in RAW264.7 cells. In this study, we investigated the effect of IK on the mechanism of HO-1 expression. IK upregulated HO-1 mRNA and protein expression in a dose dependent manner. The level of HO-1 mRNA peaked at 4 h after 15 μM IK treatment. To investigate the mechanisms of HO-1 expression modulation by IK, we used pharmacological inhibitors for the protein kinase C (PKC) family, PI3K, and p38 MAPK. IK-induced HO-1 mRNA expression was only suppressed by SB203580, a specific inhibitor of p38 MAPK. ROS scavengers (N-acetyl-L-cysteine, NAC, and glutathione, GSH) also blocked the IK-induced ROS production and HO-1 expression. Furthermore, both NAC and SB203580 suppressed the IK-induced Nrf2 activation. In addition, ROS scavengers suppressed other oxidative enzymes such as catalase (CAT), glutathione S-transferase (GST), and NADH quinone oxidoreductase (NQO-1) in IK-treated RAW264.7 cells. Taken together, it can be concluded that IK induced the HO-1 expression through the ROS/p38 MAPK/Nrf2 pathway in RAW264.7 cells.

2. Introduction

Heme oxygenase-1 (HO-1), the inducible isoform of heme oxygenase that catalyzes the degradation of heme into biliverdin, iron, and carbon monoxide (CO), is a stress-responsive protein. HO-1 has anti-inflammatory, antioxidant, and antiproliferative effects (Gabunia *et al*., 2012; Yamada *et al*., 2000). HO-1 is an antioxidant enzyme induced by oxidative stress. However, recent studies have demonstrated that overexpression of HO-1 prior to stimulation with LPS markedly inhibited the production of subsequent inflammatory mediators such as nitric oxide (NO), interleukin-6 (IL-6), and monocyte chemoattractant protein-1 (MCP-1) (Park *et al*., 2009a; Tsoyi *et al*., 2008; Jin *et al*., 2010). Moreover, the deficiency of HO-1 resulted in severe inflammation in mice (True *et al*., 2007). Therefore, based on previous findings, the regulation of HO-1 expression may be a potential target for the treatment of inflammatory disease.

Perilla frutescens (L.) Britt. is an annual herbaceous plant belonging to the Lamiaceae family. Its leaves are used as food in Asian cuisines, and its seeds are used to make edible oil in Korea. It is also used in traditional Chinese medicine. The pharmacological activities of *P. frutescens* have been investigated in many studies (Ueda and Yamzaki, 1997; Brochers *et al*., 1997). Several compounds, such as rosmarinic acid, luteolin, apigenin,

fefulic acid, (+)-catechin, caffeic acid, and isoegomaketone, have been isolated from *P. frutescens*. Anti-inflammatory activities of rosmarinic acid (Huang *et al*., 2009), luteolin (Kim *et al*., 2005), and apigenin (Zhang *et al*., 2014) have been demonstrated in previous reports.

IK, an essential oil component in *P. frutescens*, has been shown to have numerous biological activities. It has been shown to have inhibitory activity on NO production in LPS-treated RAW264.7 cells (Jin *et al*., 2010), and IK induced apoptosis in several cancer cells through caspase-dependent and -independent pathways (Cho *et al*., 2011a; Kwon *et al*., 2014a). Furthermore, IK has the potential for increasing the effectiveness of prostate cancer therapy with TRAIL (Lee *et al*., 2014). Previously, our group has shown that IK induced the HO-1 expression in RAW264.7 cells (Jin *et al*., 2010), however, the detailed mechanism was yet to be elucidated. In this study, we investigated the mechanisms of HO-1 induction by IK in RAW264.7 cells.

3. Materials and Methods

3.1. Reagents

DMEM and fetal bovine serum (FBS) were purchased from Hyclone (Logan, UT, USA). LPS, phenylmethylsulfonyl fluoride, sodium nitrite, DMSO, Griess reagent, Rottlerin, GF102903X, and a protease inhibitor cocktail were purchased from Sigma-Aldrich (St. Louise, MO, USA). Goat anti-rabbit IgG HRP-conjugated antibody and Lipofectamine 2000 were purchased from Invitrogen (Carlsbad, CA, USA). The RNeasy kit was purchased from QIAGEN (Valencia, CA, USA). The EZ-Cytox Cell Viability assay kit was purchased from DAEIL lab (Seoul, Korea). The Advantage RT-for-PCR kit was purchased from Clontech (Mountain view, CA, USA). SYBR premix was purchased from Takara Bio Inc (Shiga, Japan). NP40 cell lysis buffer was purchase from Biosource (San Jose, CA, USA). SB203580 was purchased from Cell Signaling Technology (Danvers, MA, USA). LY294002 and Go6976 were purchased from Calbiochem (La Jolla, CA, USA). Rabbit polyclonal antibodies against β-tubulin, HO-1, laminB, and Nrf2 were purchased from Santa Cruz Biotechnology (Santa Cruz, CA, USA).

3.2. Isolation of IK

The radiation-induced mutant *P. frutescens* var. *crispa* was breeded by the Korea Atomic Energy Research Institute (Daejeon, Korea). The leaves of radiation mutant *P. frutescens* var. *crispa* were dried and then ground to powder (1.2kg). The powder was extracted with 80% methanol (10 L) at room temperature for 24 h and filtered through filter paper (No.4 Whatman international, UK). The methanol extracts (200 g) were suspended with 1 L distilled water. Following extraction, the solution was fractionated in the order of N-hexane, chloroform, ethyl acetate, and N-butanol (1L and three times respectively). N-hexane soluble fraction (15 g) was fractionated into 10 fractions (PH1-PH10) with N-hexane:ethyl acetate (1:0-1:1) using silica gel column chromatography. IK was isolated from PH4 fraction (200 mg) and analyzed using HPLC (YMC, Seongnam, Korea).

The leaves of the mutant cultivar of *P. frutescens* var. *crispa* were collected by the radiation breeding research team of the Korea Atomic Energy Research Institute (Park *et al*., 2009b). The leaves were air-dried, pulverized, and stored at 4℃ before extraction. Dried leaves (1.2 kg) of the mutant cultivar of *P. frutescens* var. *crispa* were extracted twice with 80% methanol (10 L) at room temperature for 24 h, and the supernatant was evaporated under vacuum using an evaporator. The methanol extract (200 g) was dissolved in distilled water and partitioned three times using n-hexane,

chloroform, ethyl acetate, and n-butanol. Evaporation of the solvent of the appropriate fraction under reduced pressure yielded the n-hexane extract (30 g), which was further fractionated on a reverse-phase (RP) silica gel column (YMC Gel ODS-A, 12 nm, S-150 μm; YMC Co.) and eluted using 35% methanol to give 10 fractions (PH1–PH10). PH4 (200 mg) was fractionated on a HPLC and eluted using n-hexane:ethyl acetate (10:1) to yield isoegomaketone (IK) as a yellow oil (60 mg) (Figure 3.1). The purity evaluation of IK was determined by analytical HPLC (0 min, acetonitrile−water, 45:55; 30 min, 55:45; flow rate 1 mL/min, detector UV 254 nm). The tR of IK was 23.112 min, and its purity was 99.178% (Figure 3.2). Its structure was identified as IK by comparison of its 1H-NMR data with the published values (Nam *et al*., 2016) (Figure 3.3). 1H-NMR (CDCl3, 500 MHz): δ 8.03 (1H, s, H-2), 7.44 (1H, d, J = 1.5 Hz, H-5), 7.00 (1H, dd, J = 15.5, 7.0 Hz, H-8), 6.81 (1H, d, J = 1.5 Hz, H-4), 6.47 (1H, dd, J = 15.5, 1.5 Hz, H-7), 2.52 (1H, m, H-9), 1.10 (3H, s, H-10), 1.09 (3H, s, H-11).

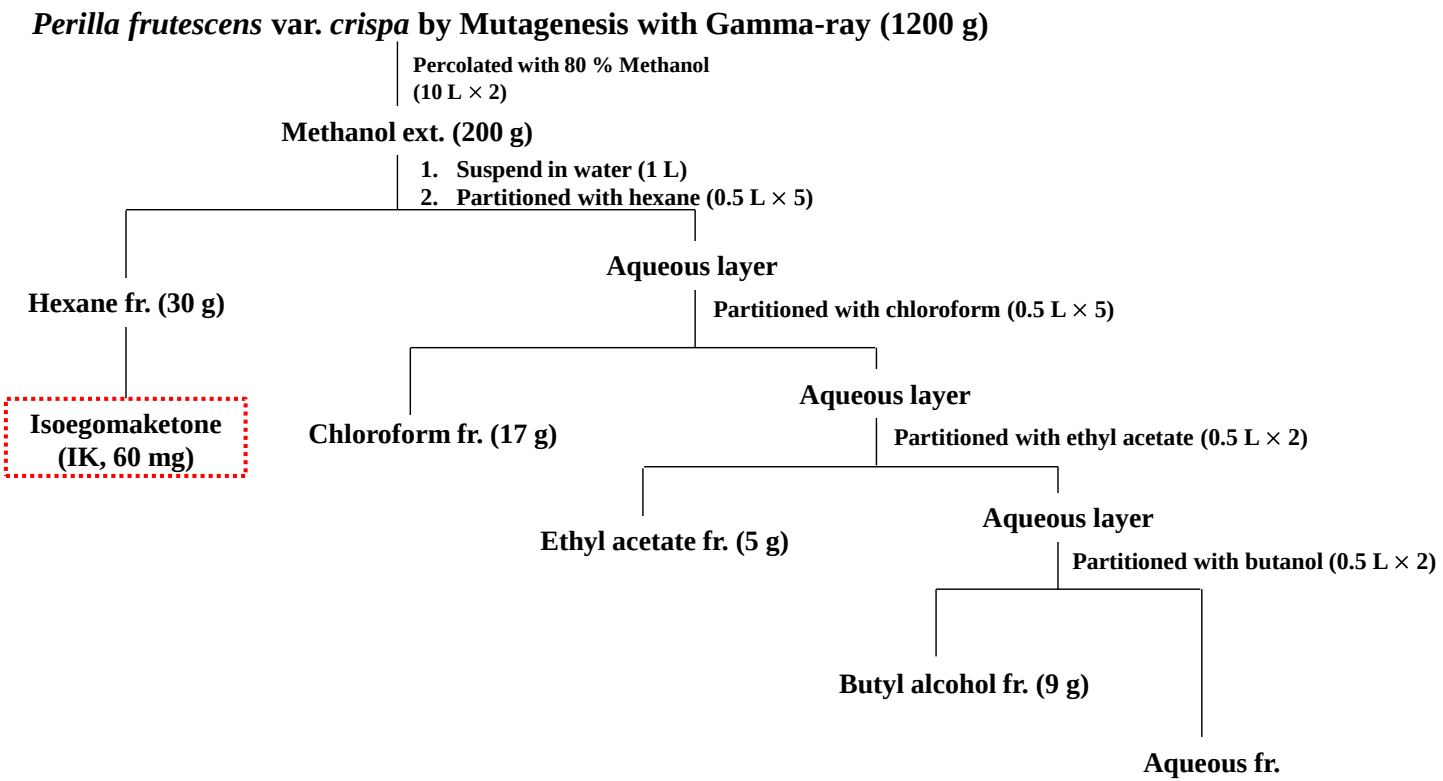

Figure 3.1. Isolation scheme for isoegomaeketone

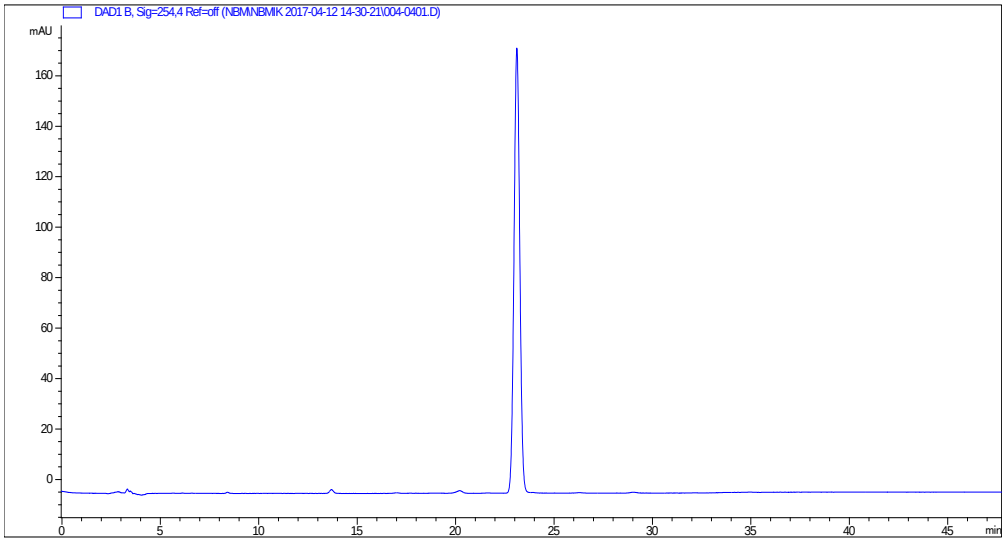

Time	Area	Height	Width	Area%	Symmetry
23.112	3572.6	176.3	0.3164	99.178	0.959

Figure 3.2. Purity of isoegomaketone measured by HPLC analysis.

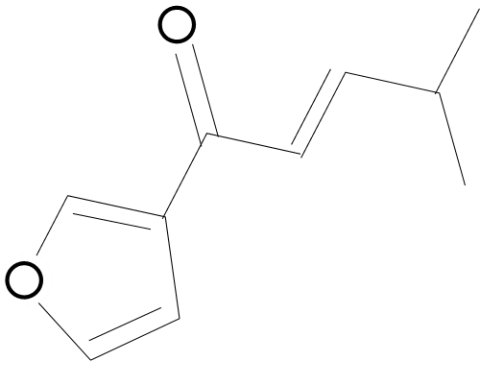

Figure 3.3. Chemical structure of isoegomaketone

3.3. Cell culture

RAW 264.7 macrophage cells were cultured in DMEM supplemented with 10% FBS, penicillin (100 U/mL) and streptomycin (100 μg/mL) and incubated at 37℃ with 5% carbon dioxide.

3.4. Cytotoxicity assay

To measure cell viability, the EZ-Cytox cell viability assay kit was used. The cells were cultured in a 96-well flat-bottom plate at a density of 2.0×10^5 cells/mL for 24 h. The cells were subsequently treated with various concentrations of kinase inhibitor for an additional 24 h. After the incubation period, EZ-Cytox 10 μL was added to each well and incubated for 4 h at 37℃ and 5% CO_2. The index of cell viability was determined by measuring formazan production at an absorbance of 480 nm, using an ELISA reader. The reference wavelength was 650 nm.

3.5. Determination of NO concentration

Nitrite in the cellular media was measured by the Griess method (Khan *et al*., 2009). The cells were cultured in a 96-well plate and treated with LPS (1 μg/mL) for 18 h. At the end of the culture period, the cellular media was collected for the determination of nitrite production. Equal volumes of Griess

reagent and cellular supernatant were mixed, and the absorbance was measured at 540 nm. The concentration of nitrite (μM) was calculated using a standard curve produced from known concentration of sodium nitrite dissolved in DMEM. The results are presented as the means ± SD of four replicates of one representative experiment.

3.6. Preparation of cell extracts and western analysis

Cells were washed once with cold PBS and harvested by pipetting. For whole-cell extract preparation, the cells were lysed on ice, in a NP40-based cell lysis buffer containing a protease inhibitor cocktail (Sigma, St. Louis, MO, USA) and phenylmethylsulfonyl fluoride (Sigma) for 30 min. Nuclear and cytosolic extracts were prepared using nuclear and cytosolic extraction reagents (Thermo Scientific, Rockford, IL, USA). The protein concentration of the cell lysate was determined using the Bio-Rad Protein Assay (Bio-Rad, Hercules, CA, USA). Fifty μg of protein was loaded and electrophoresed on a 10% SDS-polyacrylamide gel, following which it was transferred onto a nitrocellulose membrane (Hybond ECL Nitrocellulose, GE Healthcare, Chandler, AZ, USA). The membranes were washed once with a wash buffer (PBS with 0.05% Tween 20) and blocked with a blocking buffer (PBS with 5% skim milk and 0.05% Tween 20) for 1 h. After blocking, the membranes

were incubated with the rabbit anti-HO-1 or anti-β-tubulin primary antibody overnight at 4℃. Rabbit anti-HO-1 polyclonal antibody was diluted at 1:1000, and the rabbit anti-β-tubulin polyclonal antibody was diluted at 1:200 in blocking buffer. After incubation, the membranes were washed and subsequently incubated for 1 h at room temperature with the goat anti-rabbit IgG HRP-conjugated secondary antibody diluted to 1:5000 in blocking buffer. The membranes were washed and the protein bands were detected by a chemiluminescence system (GE Healthcare, Chandler, AZ, USA).

3.7. Quantitative real-time PCR

The cells were cultured in a 100-mm petri dish for 24 h (2×10^5 cell/mL). Total RNA was isolated using the RNeasy Kit according to the manufacturer's instructions. The Advantage RT-for-PCR kit was used for reverse transcription according to the manufacturer's protocol. A Chromo4 real-time PCR detection system (Bio-Rad) and iTaq^{TM} SYBR^{R} Green Supermix (Bio-Rad) were used for the RT-PCR amplification of HO-1 and β-actin using the following conditions: 50 cycles at 94℃ for 20 s, 60℃ for 20 s and 72℃ for 30 s. All the reactions were repeated independently at least three times to ensure the reproducibility of the results. Primers for HO-1 and

β-actin were purchased from Bioneer Corp (Daejeon, Korea). Primer sequences are shown in Table 3.1.

Table 3.1. Primers sequences for Real Time-PCR analysis

Target gene		5' to 3' direction
HO-1	**Forward**	**TTACCTTCCCGAACATCGAC**
	Reverse	**GCATAAATTCCCACTGCCAC**
Beta actin	**Forward**	**TGAGAGGGAAATCGTGCGTGAC**
	Reverse	**GCTCGTTGCCAATAGTGATGACC**

3.8. Statistical analysis

One-way analysis of variance (ANOVA) was used to determine overall differences among groups, followed by Fisher's LSD test for individual group comparisons. The results from all comparisons were considered significant at $P < 0.05$. Data were reported as mean ± SD. All data were analyzed using the SPSS 21.0 program (SPSS Inc., IL, USA).

4. Results

4.1. Effect of IK on HO-1 expression in RAW264.7 cell

Induction of HO-1 expression by IK was examined in RAW264.7 cells. As shown in Figure 3.1A, IK treatment markedly increased the expression of HO-1 mRNA in a dose-dependent manner. The maximum induction of HO-1 mRNA was at 4 h after treatment with 15 μM IK and the maximum induction level was approximately 60 fold greater than the level at 0 h timepoint (Figure 3.4B). IK also induced the HO-1 protein expression in a dose-dependent manner (Figure 3.4C). The maximum level of HO-1 protein expression was reached at 8 h after treatment with 15 μM IK. The induction of HO-1 protein went back to the basal level at 24 h (Figure 3.4D).

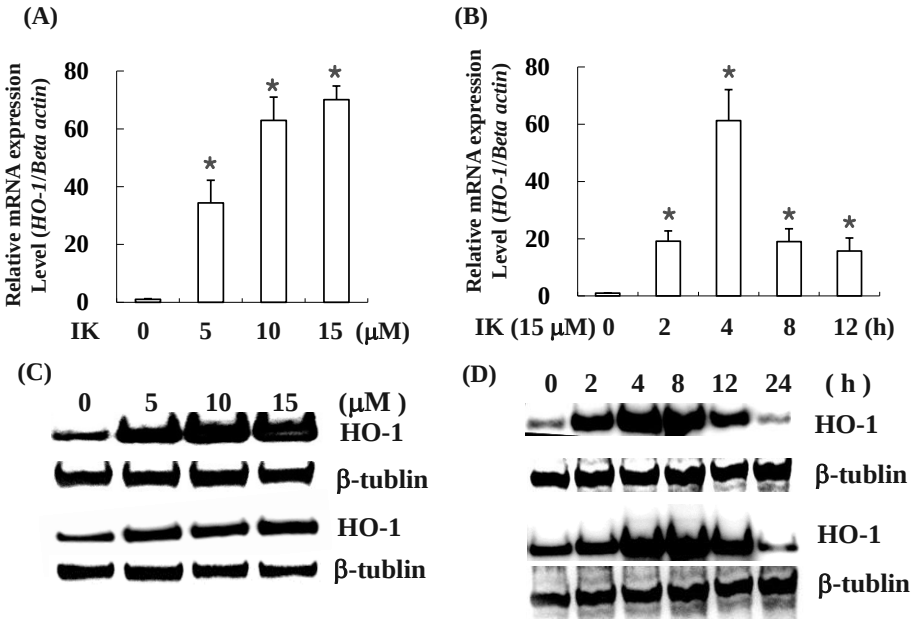

Figure 3.4. The expression of HO-1 by IK treatment in RAW264.7 cells. (A) The expression levels of HO-1 mRNA were measured by RT-PCR. IK was treated for 4 h with several concentrations (5, 10, 15 μM). (B) The expression levels of HO-1 mRNA were measured by RT-PCR. IK was treated for 2, 4, 8, and 12 h with 15 μM. Data shown are the means ± SD (n = 4). *p < 0.05 vs the control group. (C) A representative western blot of HO-1 protein expression. IK was treated for 4 h with several concentrations (5, 10, 15 μM). (D) A representative western blot of HO-1 protein expression. IK was treated for 2, 4, 8, and 12 h with 15 μM.

4.2. Effect of kinase inhibitors on HO-1 expression by IK treatment

Previous studies have reported that the expression of HO-1 was mediated through activation of PKC, PI3K, Nrf2, and p38 MAPK (Shih *et al*., 2011; Lee 2012 *et al*., 2012). Previously, we have shown that IK increased the translocation of Nrf2 into the nucleus without affecting Nrf2 expression in RAW264.7 cells (Jin *et al*., 2010). We further examined whether the induction of HO-1 by IK treatment is mediated through activation of other kinases using relative specific inhibitors. Before the experiment, we determined the non-toxic concentration of kinase inhibitors in RAW264.7 cells via the cell viability assay (Figure 3.5). Based on the cytotoxicity result, RAW264.7 cells were treated with 15 μM IK, along with various specific kinase inhibitors. As shown in Figure 3.6, only SB203580, a specific p38 MAPK inhibitor, treatment suppressed the HO-1 induction in IK-treated RAW264.7 cells, whereas treatment with the other kinase inhibitors such as LY294002, Rottlerin, GF102903, and Go6976 had no effect on HO-1 expression. Therefore, p38 MAPK seemed to play an important role in HO-1 induction by IK treatment.

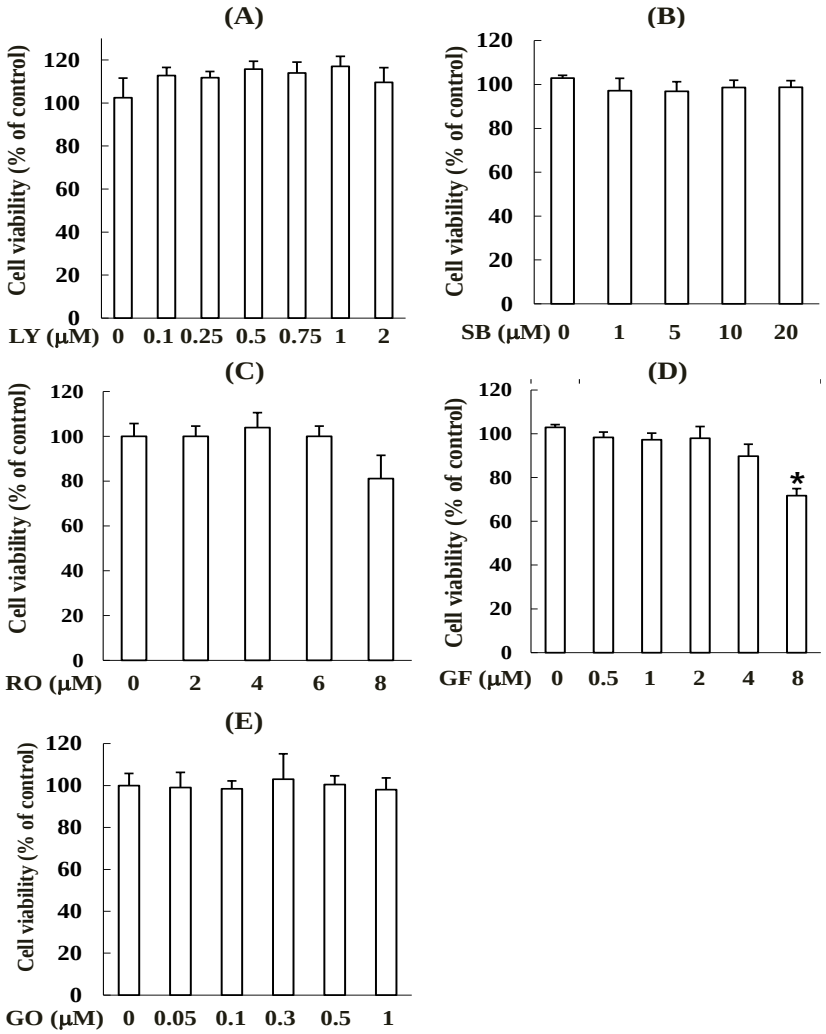

Figure 3.5. Effect of specific kinase inhibitors on cell viability. (A) Effect of LY, LY294002, on cell viability. (B) Effect of SB (SB203580), on cell viability. (C) Effect of RO (Rottlerin) on cell viability. (D) Effect of GF (GF109203X) on cell viability, (E) Effect of GO (Gö 6976) on cell viability. Cell viability was determined by the EZ-Cytox cell viability assay kit. Data shown are the means ± SD (n = 4). *p < 0.05 vs the control group.

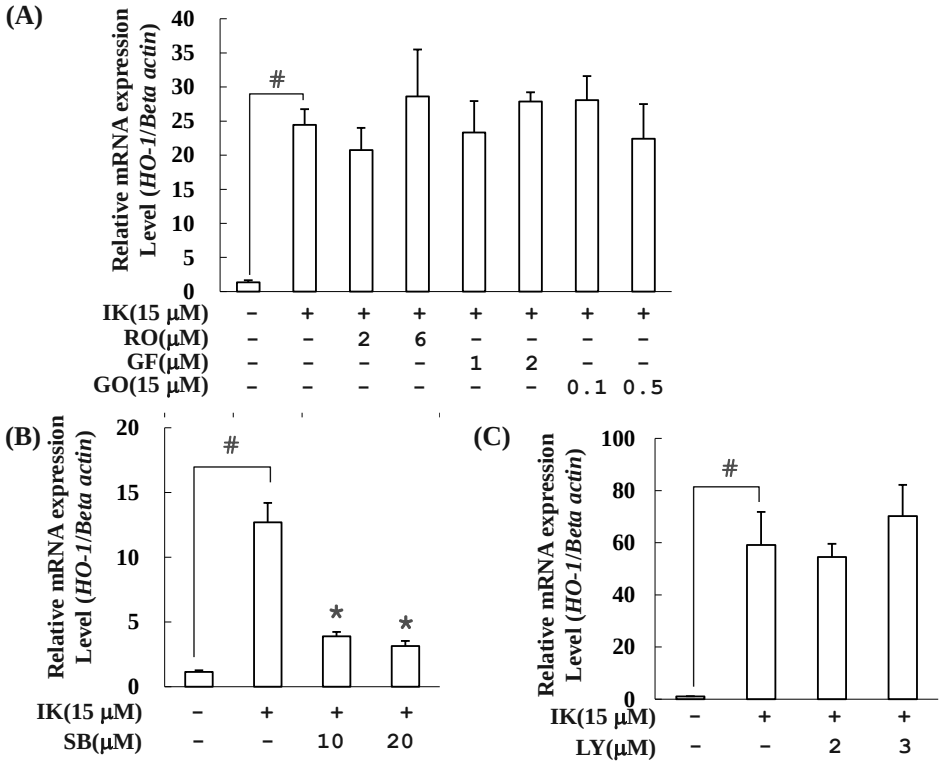

Figure 3.6. Effect of specific kinase inhibitors on HO-1 expression in IK-treated RAW274.7 cells. (A) Effect of RO, GF, and GO on IK-induced HO-1 mRNA expression. (B) Effect of SB on IK-induced HO-1 mRNA expression. (C) Effect of LY on IK-induced HO-1 mRNA expression. IK was added with and without various concentrations of kinase inhibitors for 4 h. Total RNA was isolated, then the expression of HO-1 mRNA was measured by quantitative real-time PCR. Data shown are the means ± SD ($n = 4$). $^{\#}p < 0.05$ vs the control cells, and $^{*}p < 0.05$ vs the cells treated with only IK. RO;Rottlerin, GF; GF102903, GO; Go6976, SB; SB203580, LY; LY294002.

4.3. Effect of ROS scavengers on HO-1 expression by IK treatment

In follow-up experiments, the upstream signaling pathway that stimulates HO-1 expression was investigated. Since reactive oxygen species (ROS) have been implicated in the activation of Nrf2 (Alam and Cook, 2003), the involvement of oxidative stress was examined. Addition of glutathione (GSH) or the glutathione donor N-acetyl-L-cysteine (NAC) suppressed the generation of reactive oxygen in cells. Cells were treated with GSH or NAC to test whether the expression of HO-1 mRNA by IK was mediated via ROS generation. As shown in Figure 3.7A, IK-induced expression of HO-1 mRNA was significantly reduced when NAC was added to the culture. The expression level of HO-1 protein was also reduced by GSH or NAC in IK-treated RAW264.7 cells (Figure 3.7B). Therefore, ROS generation might be involved in the IK-induced expression of HO-1 in RAW264.7 cells.

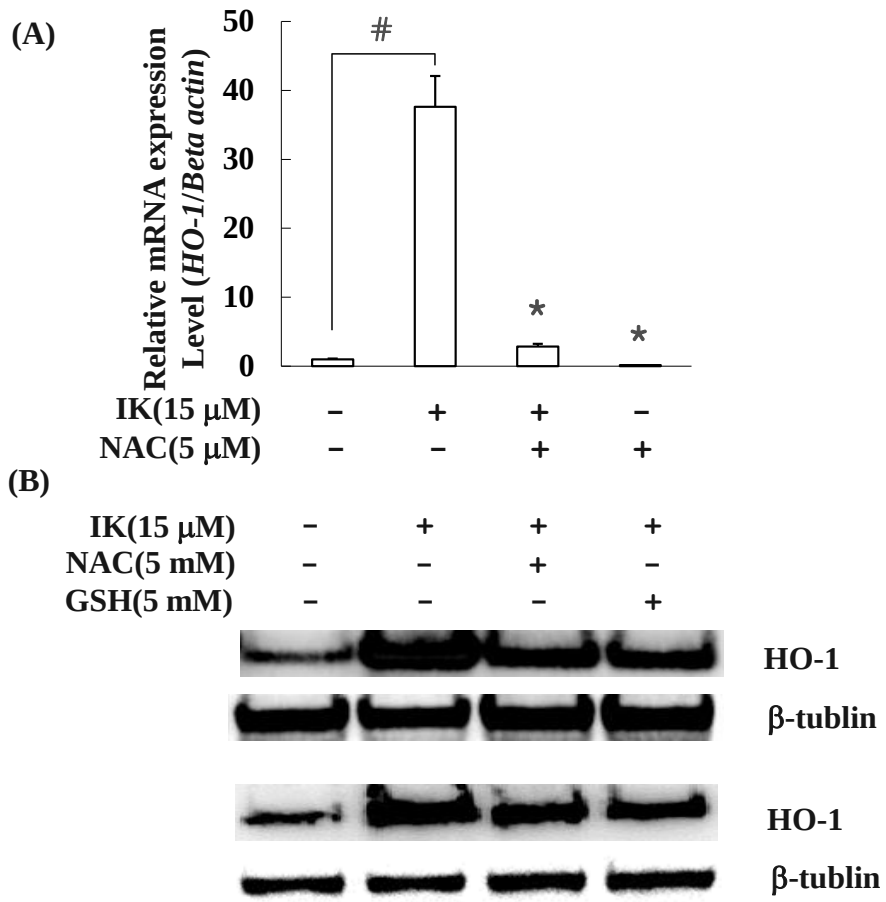

Figure 3.7. Effect of ROS scavengers on HO-1 expression in IK-treated RAW264.7 cells. (A) Total RNA was isolated, and the expression of HO-1 mRNA was measured by quantitative real-time PCR. Data shown are the means ± SD (n = 4). $^{\#}p < 0.05$ vs the control cells, and $*p < 0.05$ vs the cells treated with only IK. (B) A representative western blot of HO-1 protein expression.

4.4. Effect of ROS scavenger and p38 MAPK inhibitor on Nrf2 activation by IK treatment

Up to this point, we could not determine whether IK induces the HO-1 expression through two parallel pathways (p38 MAPK and ROS-Nrf2 pathway) or a single connected pathway, such as the ROS/p38 MAPK/Nrf2 pathway. To answer this question, we examined the effect of ROS scavenger (NAC) and specific p38 MAPK inhibitor (SB203580) on the subcellular localization of Nrf2 in IK-treated RAW264.7 cells. As shown in Figure 3.8, IK increased the Nrf2 protein levels in nuclear extracts. However, this increase was significantly reduced by NAC and SB203580 treatment, which suggested that IK induced the HO-1 expression through ROS/p38 MAPK/Nrf2 pathway.

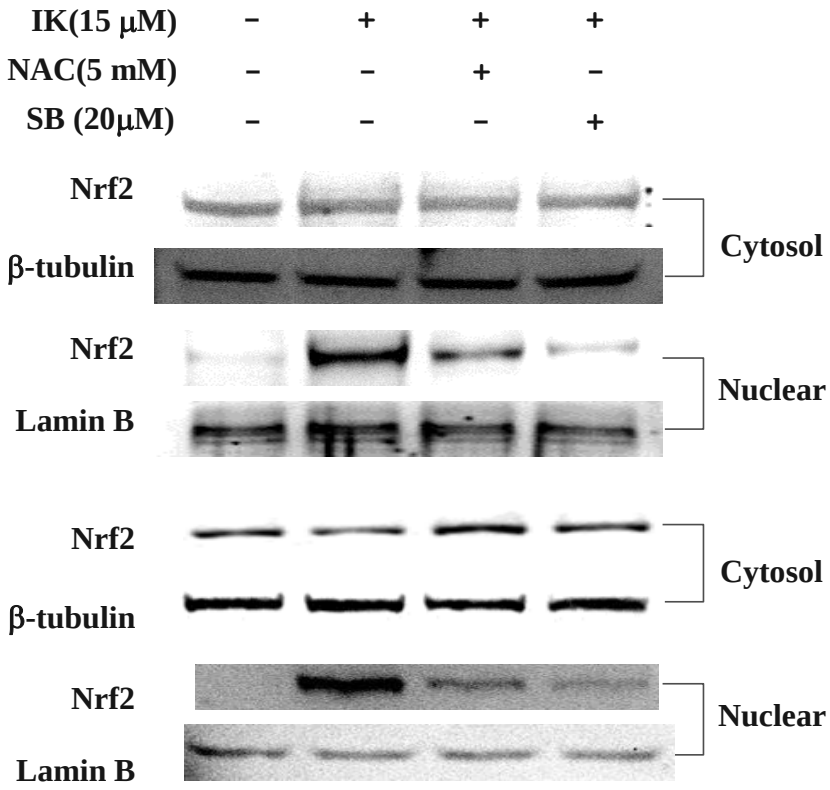

Figure 3.8. Effect of NAC and p38 MAPK inhibitor on Nrf2 activation in IK-treated RAW264.7 cells. RAW264.7 cells were treated with IK for 2 h with NAC and SB. Nuclear extracts (30 μg) and the cytosolic fraction (50 μg) were used for Western blot analysis. SB; SB203580.

4.5. Effect of NAC on NO production in LPS-treated RAW264.7 cells

Previous studies have shown that HO-1 expression mediates the NO production in LPS-treated RAW264.7 cells (Park *et al*., 2009a; Kim *et al*., 2014). Therefore, whether HO-1 expression by IK treatment is involved in inhibition of NO production was examined in LPS-treated RAW264.7 cells using NAC. Cells were treated with LPS and IK in the presence of NAC, and the resultant NO levels were measured. As shown in Figure 3.9, NAC treatment restored the IK-mediated inhibition of NO production by 33%, while NAC treatment alone had no effect on LPS-stimulated NO production. Therefore, HO-1 induction plays an important role in the inhibitory effect of IK on LPS-induced NO production.

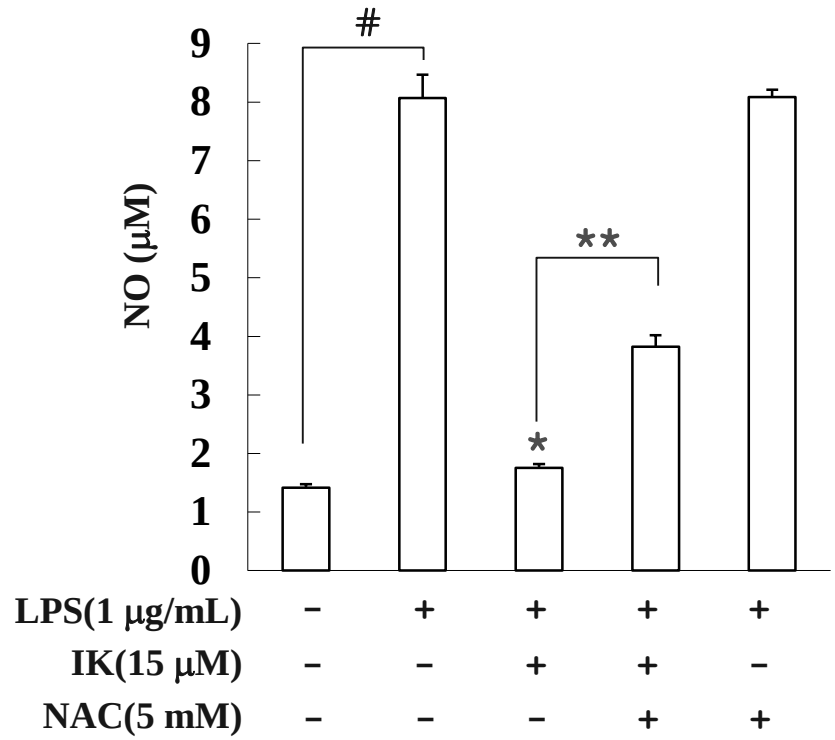

Figure 3.9. Effect of NAC on NO production in LPS-treated RAW264.7 cells. RAW264.7 cells were treated with IK for 2 h prior to LPS addition (1 μg/mL) and were incubated for an additional 18 h. Cellular media (100 μL) were mixed with equal volumes of Griess reagent. Nitrite level were measured as an indicator of NO production as described in the Materials and Methods. Data shown are the means ± SD (n = 4). $^{\#}p < 0.05$ vs the control cells, $*p < 0.05$ vs the cells treated with only LPS, and $**p < 0.05$ vs the cells treated with LPS and IK without NAC.

4.6. Effect of ROS scavengers on the production of antioxidant enzymes

Besides HO-1, the activation of Nrf2 is a major determinant of phase II enzyme induction, such as catalase (CAT), glutathione S-transferase (GST), and NADH quinone oxidoreductase (NQO-1) (Zhang *et al*., 2013). IK treatment induced the expression of HO-1 through ROS/Nrf2/p39 MAPK in RAW264.7 cells. Therefore, we examined whether IK could induce antioxidant enzymes CAT, GST, and NQO-1, and whether ROS scavengers could abolish the effects of IK on these enzymes. As shown in Figure 3.10, phase II enzymes were induced by IK treatment; however, the induction levels of these antioxidant enzymes were smaller than that of HO-1. The mRNA levels of CAT, GST, and NQO-1 in cells treated with IK were significantly reduced when cells were cultured in the presence of GSH or NAC.

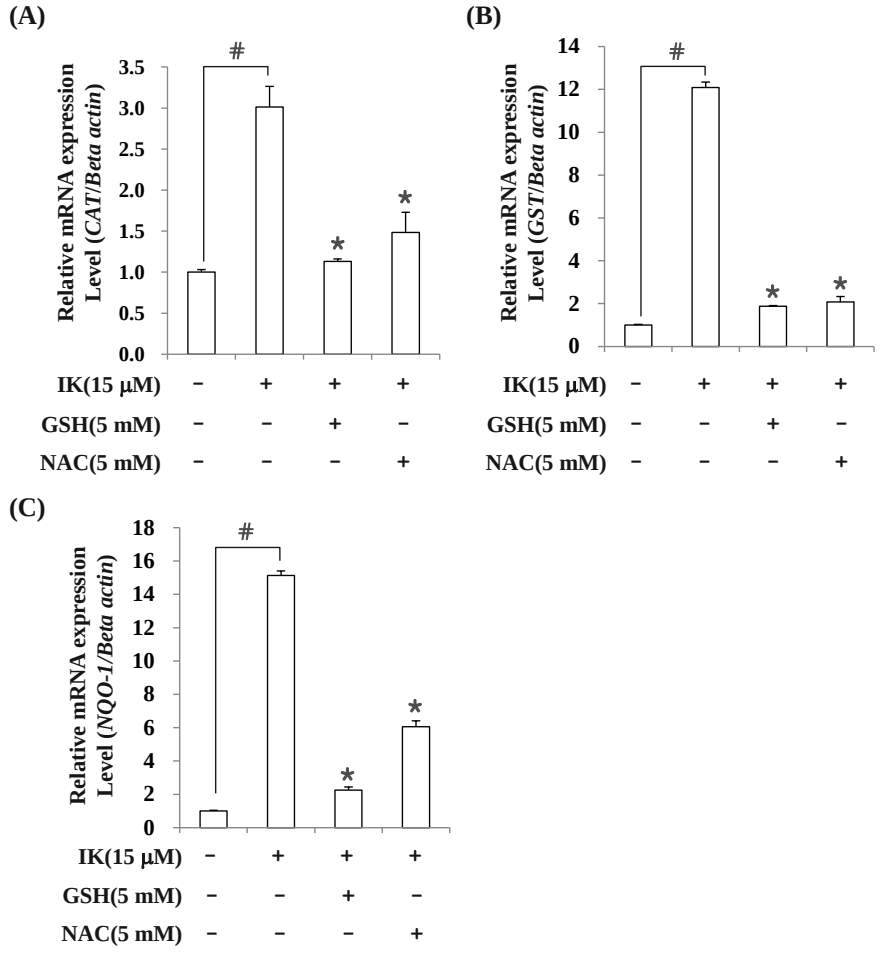

Figure 3.10. Effect of ROS scavengers on the production of antioxidant enzymes in IK-treated RAW264.7 cells. (A) Effect of GSH and NAC on IK-induced catalase (CAT) expression. (B) Effect of GSH and NAC on IK-induced glutathione S-transferase (GST) expression. (C) Effect of GSH and NAC on IK-induced NADH quinone oxidoreductase (NQO-1) expression. Total RNA was isolated, and the expression level of HO-1 mRNA was measured by quantitative real-time PCR. Data shown are the means ± SD (n = 4). $^{\#}p < 0.05$ vs the control cells, and $*p < 0.05$ vs the cells treated with only IK.

5. Discussion

Previously, isoegomaketone (IK) was isolated from *Perilla frutescens* var. *crispa* (Antisperill). *Perilla frutescens* var. *crispa* was mutated by gamma radiation (Park *et al*., 2009b) as mutant *P. frutescens* var. *crispa*., and contained about 10 times more IK than wild type species. IK is biosynthesized from egomaketone (EK), and this reaction is inhibited by gene *I* in *P. frutescens (*Nishizawa *et al*., 1989*)*. It is possible that gene *I* was affected by gamma radiation and consequently resulted in an increased IK content in the mutant. Recently, it was reported that IK induced the expression of HO-1 in RAW264.7 cells (Jin *et al*., 2010). However, the molecular mechanism underlying IK-induced HO-1 expression was not completely understood. In this study, the detailed mechanism of HO-1 expression by IK treatment in RAW264.7 cells was examined.

Quantitative real-time PCR of the cells with specific kinase inhibitors revealed that IK-induced HO-1 expression was mediated by activation of the p38 MAPK pathway. The western blot analysis of the cells treated with NAC and GSH suggested that IK-induced HO-1 expression was regulated through ROS generation. To our knowledge, our report is the first that describes the mechanism of HO-1 induction by IK in RAW264.7 cells.

HO-1 expression is induced in response to oxidative stress and

inflammatory stimuli in macrophages. HO-1 catalyzes the degradation of heme into equimolar amounts of carbon monoxide (CO), iron and biliverdin. Biliverdin is further converted to bilirubin, which is a potent endogenous anti-oxidant (Ryter *et al*., 2006). CO, one of the catabolic products of heme, exerts anti-inflammatory effects (Park *et al*., 2009a). Recent studies have demonstrated that HO-1 induction was mediated by the activation of PI3K, PKC, and p38 MAPK (Shih *et al*., 2011; Lee *et al*., 2012; Rojo *et al*., 2006). Signaling mechanisms of HO-1 expression may depend on cell types and inducers. Crotonaldehyde induces HO-1 expression in endothelial cells via PKC-δ and p38 MAPK activation (Lee *et al*., 2011). However, PKC-δ and p38 inhibitors did not affect the crotonaldehyde-induced HO-1 expression in RAW264.7 cells and A549 human lung epithelial cells. In this study, we investigated the contribution of PI3K, PKC, and p38 MAPK on IK-induced HO-1 expression using respective specific inhibitors. Among these inhibitors, only the specific p38 MAPK inhibitor attenuated HO-1 induction in IK-treated RAW264.7 cells. We have previously confirmed that IK increased the translocation of Nrf2 into the nucleus without affecting Nrf2 expression in RAW264.7 cells (Jin *et al*., 2010). The specific p38 MAPK inhibitor also suppressed the IK-induced translocation of Nrf2 into the nucleus. Therefore, our results show that the p38 pathway is required for IK-

stimulated expression of HO-1 and IK-induced translocation of Nrf2 into the nucleus. Until now, there have been no reports showing the activation of p38 pathway by IK.

Reactive oxygen species (ROS) have been implicated in the induction of HO-1 expression (Shih *et al*., 2011; Liu *et al*., 2011). Cigarette smoke extract upregulated the HO-1 induction via ROS production in mouse brain endothelial cells (Shih *et al*., 2011), and curcumin induced the HO-1 expression by generation of ROS in human hepatoma cells (McNally *et al*., 2007). According to these previous reports, ROS generation is upstream of p38 MAPK. HO-1 expression by IK also seemed to be dependent on oxidative stress. IK-mediated induction of HO-1 was markedly suppressed by co-treatment of GSH or NAC. Furthermore, IK-induced translocation of Nrf2 into the nucleus was inhibited by NAC. It has been reported that IK induced apoptosis in B16 melanoma cells was through ROS generation (Kwon *et al*., 2014a), in which ROS production by IK was measured by flow cytometry. However, the level of IK used for the treatment was 100 μM, which was high enough concentration to induce cytotoxicity in RAW264.7 cells (Jin *et al*., 2010). In this study, the level of IK was 15 μM, which was enough to induce ROS generation without toxicity. Even if NAC markedly suppressed the IK-mediated induction of HO-1, certain level of HO-1 protein

expression still remained, along with Nrf2 activation. Therefore, there may be another minor pathway involved, along with the ROS/p38 MAPK/Nrf2.

Upregulation of HO-1 is mediated by activation of Nrf2 (Otterbein and Choi, 2000). Under unstressed condition, Nrf2 remains inactive in the cytoplasm. Under oxidative stress, Nrf2 dissociates from Keap1, translocates into the nucleus and binds to the antioxidant response element (ARE) in the promoter region of phase II antioxidant enzymes such as HO-1, CAT, NQO-1, and GST (Kaspar *et al*., 2009). We observed that IK induces the translocation of Nrf2 into the nucleus in RAW264.7 cells (Jin *et al*., 2010). In the present study, we investigated and confirmed that IK also induced antioxidant enzymes other than HO-1, such as CAT, NQO-1, and GST. The expression levels of these enzymes were lesser than that of HO-1, and their expression was also blocked by the treatment with ROS scavengers. CAT and NQO-1 have been suggested to have anti-inflammatory activities (Turdi *et al*., 2012; Thapa *et al*., 2014). However, HO-1 is the most important enzyme for anti-inflammation among the phase II antioxidant enzymes. The expression level of HO-1 was much higher than that of CAT and NQO-1 in IK-treated RAW264.7 cell. Therefore, blocking HO-1 expression mainly resulted in decreased IK-mediated inhibition of NO production in LPS-treated RAW264.7 cells.

IV. Study 2

Isoegomaketone alleviates the development of collagen antibody-induced arthritis in male Balb/c mice*

(*The part of the results was accepted in *Molecules* 2017)

1. Abstract

In this study, we attempted to identify and assess the effects of isoegomaketone (IK) isolated from *Perilla frutescens* var. *crispa* on the development of rheumatoid arthritis (RA). RA was induced in male Balb/c mice by collagen antibody injection. Experimental animals were randomly divided into five groups: normal, CAIA, CAIA + IK (5 mg/kg/day), CAIA + IK (10 mg/kg/day), and CAIA + apigenin (16 mg/kg/day) and respective treatments were administered via oral gavage once per day for 4 days. Mice treated with IK (10 mg/kg/day) developed less severe arthritis than the control CAIA mice. Arthritic score, paw volume, and paw thickness were less significant compared to the control CAIA mice at day 7 (73%, 15%, and 14% lower, respectively). Furthermore, histopathological examination of ankle for inflammation showed that infiltration of inflammatory cells and edema formation were reduced by IK treatment. Similarly, neutrophil to lymphocyte ratio (NLR) in whole blood was lower in mice treated with IK (10 mg/kg/day) by 85% when compared to CAIA mice. Taken together, treatment with IK delays the onset of the arthritis and alleviates the manifestations of arthritis in CAIA mice.

2. Introduction

Rheumatoid arthritis (RA) is a systemic autoimmune disease in which chronic joint inflammation leads to cartilage destruction and bone erosion (Scott *et al*., 2010). In addition, about 1% of US population is affected by RA, and RA increases the risk for cardiovascular disease, lymphoma, and death (Yang *et al*., 2013). Typically, RA is treated with steroidal/nonsteroidal anti-inflammatory drugs (NSAID) or biological modulators such as tumor necrosis factor alpha (TNF-α) inhibitors and interleutkin-1 (IL-1) receptor antagonists (Smolen *et al*., 2014). Acetaminophen, a kind of NSAID, is most frequently implemented and taken in very high doses (4 g/day) (Dragos *et al*., 2017). However, the use of standard drugs in RA is known to produce a variety of side effects: Infusion hypersensitivity reactions with the use of TNF-α inhibitors (Matucci *et al*., 2016); gastrointestinal ulcerations and hemorrhagic events triggered by NSAID (McAlindon *et al*., 2014); higher risk of infection due to the use of biological drugs (Cabral *et al*., 2016); etc. Therefore, the need for new cure in RA is still high.

Because RA arises from complex etiology, different animal models are implemented to assess the efficacy of new therapies. Collagen-induced arthritis (CIA) is widely used to study RA and shares many histopathological features of the human arthritis (Cho *et al*., 2007). However, the susceptibility

for CIA is low in Balb/c mice, and long period of time is required for the induction of arthritis. Collagen antibody-induced arthritis (CAIA) represents a relevant model for studying the efferent phase of RA, where leukocytes are attracted and respond to the focal immune complex in the joint (Nandakumar *et al*, 2003). In the case of CAIA, induction is rapid and results in a steady and controlled disease progression that exhibits histological similarities to the CIA model.

Previously, our group showed that IK reduced NO production and iNOS protein levels in LPS-treated Balb/c mice (Jin *et al*., 2010). Although there is strong evidence to suggest that that IK has anti-inflammatory properties, the efficacy of IK as a treatment option for inflammatory disease (such as RA) has not been explored or tested. Therefore, the purpose of the present study was to observe and evaluate the effect of IK on RA in CAIA animal model.

3. Materials and Methods

3.1. Animals

Animals were maintained in accordance with the guidelines of the Guide for the Care and Use of Laboratory Animals (Institute of Laboratory Animal Resources, KAERI(Korea Atomic Energy Research Institute)-IACUC-2016-017). Male Balb/c mice (4 weeks) were purchased from Orient Bio Inc. (Seongnam, Korea) and allowed to acclimate for 1 week prior to the beginning of the study. Mice were maintained in a room which controlled light/dark cycle (12h/12h), temperature (about 23 ± 2℃), and humidity (55 ± 10%).

3.2. Sample preparation

IK and apigenin (API) was diffused into sterile phosphate-buffered saline (PBS, pH 7.4) containing 0.5% Tween 20 by sonication.

3.3. Collagen antibody-induced arthritis

Mice were randomly divided into 5 groups; (1) PBS (n = 6), (2) CAIA (n = 6), (3) CAIA plus IK (5 mg/kg, n = 6), (4) CAIA plus IK (10 mg/kg, n = 6), (5) CAIA plus API (16 mg/kg, n = 6). A cocktail of four monoclonal antibodies to type II collagen (ArthritoMab; MD Bioscience, Saint Paul, MN,

USA; 2 mg/100 μL) was injected intravenously at day 0. Mice in PBS group were injected with equal volume of sterile PBS. At day 3, all animals except PBS group were intraperitoneally injected with LPS (Escherichia coli 055:B5; MD Biosciences; 50 μg/200 μL endotoxin-free water). And treatments (PBS, IK, and API) were administered by oral gavage once a day from day 3 through day 6. Mice were examined for the development of arthritis for 4 days after LPS injection (Figure 4.1).

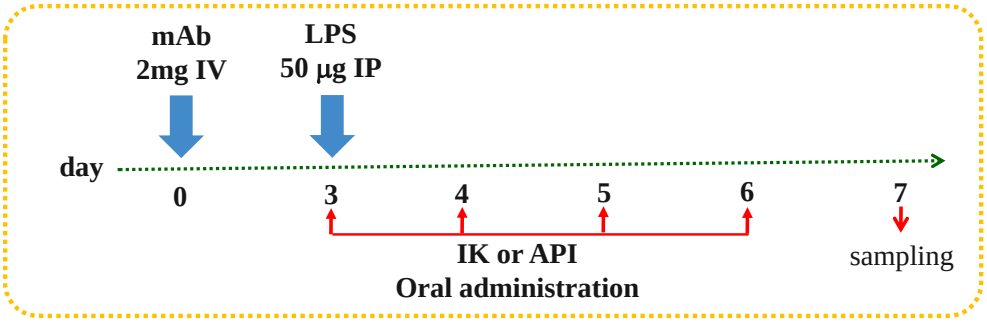

Figure 4.1. The scheme of induction of CAIA and sample treatment

3.4. Assessment of clinical signs of inflammation

Paw volumes were measured using a Digital Plethysmometer (LE7500, Panlab, Spain) every day after LPS injection. The hind leg was soaked in the buffer calibrated with 1 mL standard sinker. The increased volume was measured. The average volume of both hind legs was used. Paw thickness was measured using a digital caliper (Mitutoyo, Andover, UK) every day after LPS injection. The average thickness of both hind legs was used. Arthritic score was done blindly by using a system based on the number of inflamed joints in front and hind paws, inflammation being defined by swelling and redness at the scale from 0 (no redness and swelling) to 3 (severe swelling with joint rigidity or deformity; maximal score for four paws, 12).

3.5. Histopathological assessment

Hind feet were removed after euthanization and fixed using 4.5% buffered formalin. Hind feet were decalcified in buffered formalin containing 5.5% EDTA. Upon decalcification, paws were embedded in paraffin wax blocks, sectioned, and stained with hematoxylin and eosin for microscopic evaluation, which was performed by an expert blinded to the treatments received. Each section was screened for infiltration of neutrophils to

synovium and every joint was scored as follows: 0, normal; 1, minimal; 2, mild; 3, moderate; and 4, marked.

3.6. Analysis of neutrophil and lymphocyte

Whole blood samples were collected by cardiac puncture. The blood was placed in Vacutainer TM tubes containing EDTA (BD science, Franklin Lakes, NJ, USA). Anti-coagulated blood was used for the determination of the blood cell population analysis including neutrophil and lymphocytes in a HEMAVET 950 (Drew Scientific Inc., Miami Lakes, FL, USA).

3.7. Statistical analysis

One-way analysis of variance (ANOVA) was used to determine overall differences among groups, followed by Fisher's LSD test for individual group comparisons. The results from all comparisons were considered significant at $P < 0.05$. Data were reported as mean ± SD. All data were analyzed using the SPSS 21.0 program (SPSS Inc., IL, USA).

4. Results

4.1. Effect of IK treatment on the development of RA in CAIA model

First, in whether IK treatment by oral administration could serve to obviate inception of the disease in Balb/c mice with CAIA was investigated. IK-treated mice developed less severe arthritis in a dose-dependent manner (Figure 5.1). Both redness and swelling of joints were induced in CAIA group, but those arthritic symptoms were significantly attenuated in IK-treated group (10 mg/kg). Furthermore, IK-treated group (10 mg/kg) showed less severe redness and swelling than the API-treated group. API is one of the bioactive components in plant flavones containing anti-inflammatory activities (Li *et al*., 2016). Histopathological examinations also indicated that IK treatment reduced synovial hyperplasia, as well as the infiltration of inflammatory cells in the joint space (Figure 4.2). Mean histopathological arthritic score of CAIA-group, IK-treated group (10 mg/kg) and API-treated group were 3.67 ± 0.52, 1.17 ± 0.41, and 2.33 ± 0.82, respectively (Table 4.1 and Figure 4.3).

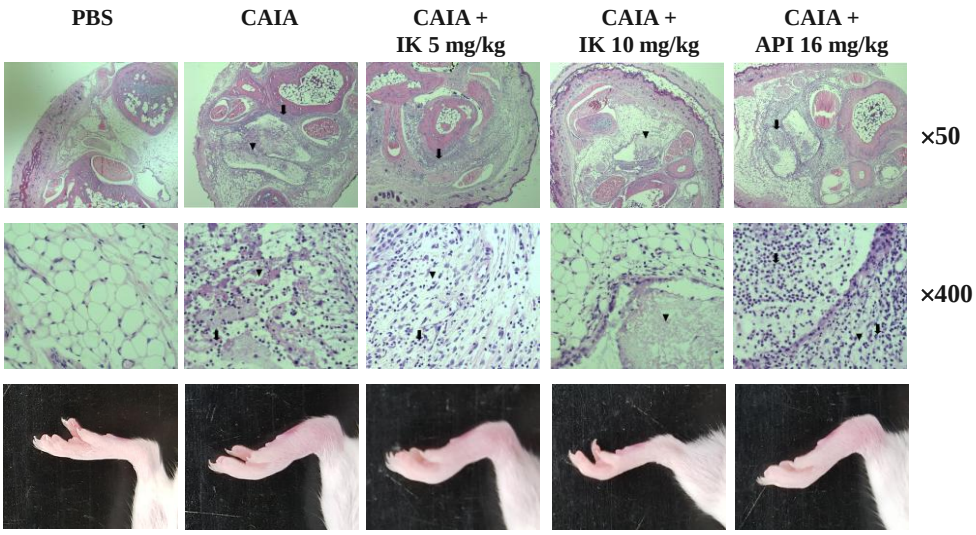

Figure 4.2. Image of representative microscopic features of knee joint and mice joint. IK and API were administered via oral gavage once per day for 4 days. Arrow indicates infiltration of neutrophils and arrowhead indicates the necrosis.

Table 4.1. Histopathological scores of the groups

Organ	Group		PBS	CAIA	CAIA + IK 5 mg/kg	CAIA + IK 10 mg/kg	CAIA + API 16 mg/kg
Ankle joint	-Inflammation	-	6	0	0	0	0
		±	0	0	0	5	1
		+	0	0	2	1	2
		++	0	2	3	0	3
		+++	0	4	1	0	0

Grade- -: normal, ±: minimal, +: mild, ++: moderate, +++: marked

No. of examined: 6/group

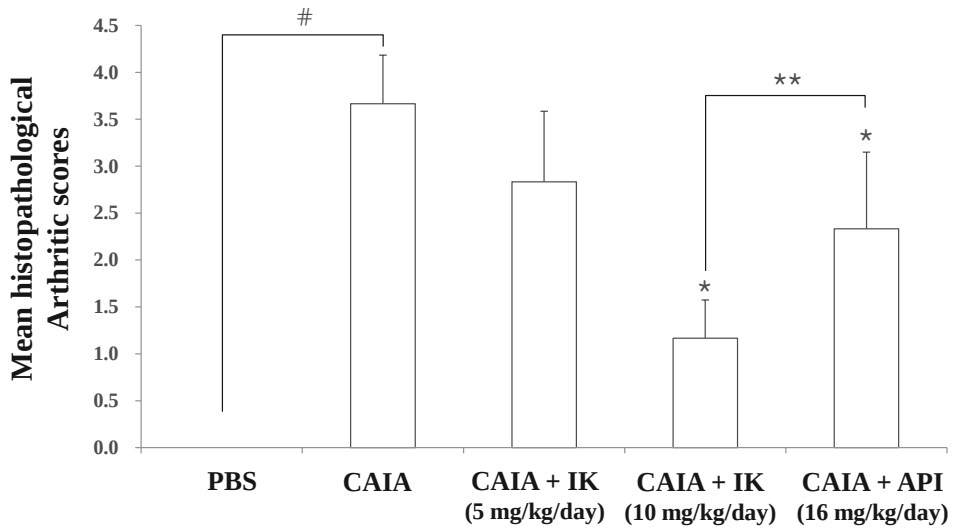

Figure 4.3. Effect of IK and API on mean histopathological arthritis scores in CAIA mice. Results were expressed as a score (means ± SD) of six mice. $^{\#}p<0.05$ vs. PBS-group, $^{*}p<0.05$ vs. CAIA-group, and $^{**}p<0.05$ vs. CAIA + IK (10 mg/kg/day)-group. Every joint was scored as follows: 0, normal; 1, minimal; 2, mild; 3, moderate; and 4, marked.

4.2. Effect of IK treatment on paw volume in CAIA model

In an effort to assess any potential effect of IK on the progression of RA in CAIA model, male Balb/c mice were provided with the PBS with or without IK from day 3 through day 6. CAIA group showed a significant increase in the paw volume at the days 5, 6, and 7 (27.6%, 27.6% and 29.8%, respectively) compared to the PBS group (Figure 4.4). Paw volume was significantly lower in the IK-treated group (10 mg/kg), when compared with the control CAIA group on days 6 and 7 (17.4% and 13.7%, respectively). Therefore, oral administration of IK seems to attenuate the increase of paw volume in CAIA model. Furthermore, paw volume of IK-treated group (10 mg/kg) was lower compared with API-treated group at days 6 and 7 (7.0% and 5.0%, respectively). However, IK-treatment at 5 mg/kg didn't result in any appreciable difference in paw volume, when the treated group was compared with the control CAIA group.

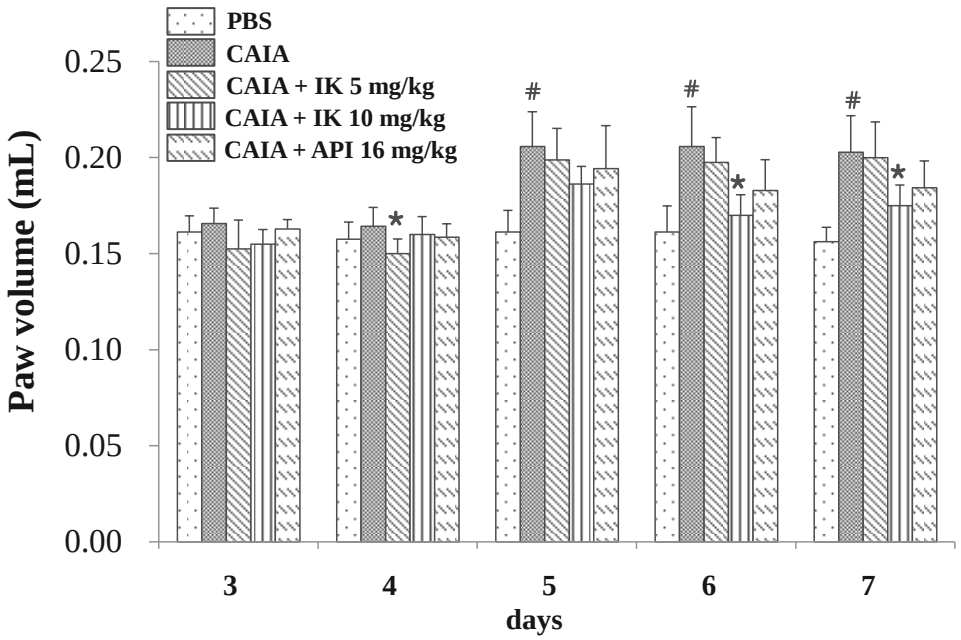

Figure 4.4. Effect of IK and API on paw volume in CAIA mice. Paw volume were measured using a Digital Plethysmometer every day after LPS injection and oral administration of treatments. The average volume of both hind legs were used. Data are presented as means ± SD (n = 6). $^{\#}p<0.05$ vs. PBS-group and $^{*}p<0.05$ vs. CAIA-group.

4.3. Effect of IK treatment on paw thickness in CAIA model

In an effort to assess whether IK had any palpable effect on the progression of RA in CAIA model, paw thickness also was measured by digital caliper. CAIA group showed a significant increase in the paw thickness at days 6 and 7 (15.5% and 18.4%, respectively) compared to the PBS group (Figure 4.5). Paw thickness was significantly lower in the IK-treated group (10 mg/kg) compared with the control CAIA group at days 6 and 7 (15.8% and 14.2%, respectively). Therefore, oral administration of IK seemed to attenuate the increase of paw thickness in CAIA model. Furthermore, paw thickness of IK-treated group (10 mg/kg) was lower compared with API-treated group at days 6 and 7 (6.1% and 3.7%, respectively). However, IK-treatment at 5 mg/kg didn’t result in significant difference in paw thickness compared with the control CAIA group.

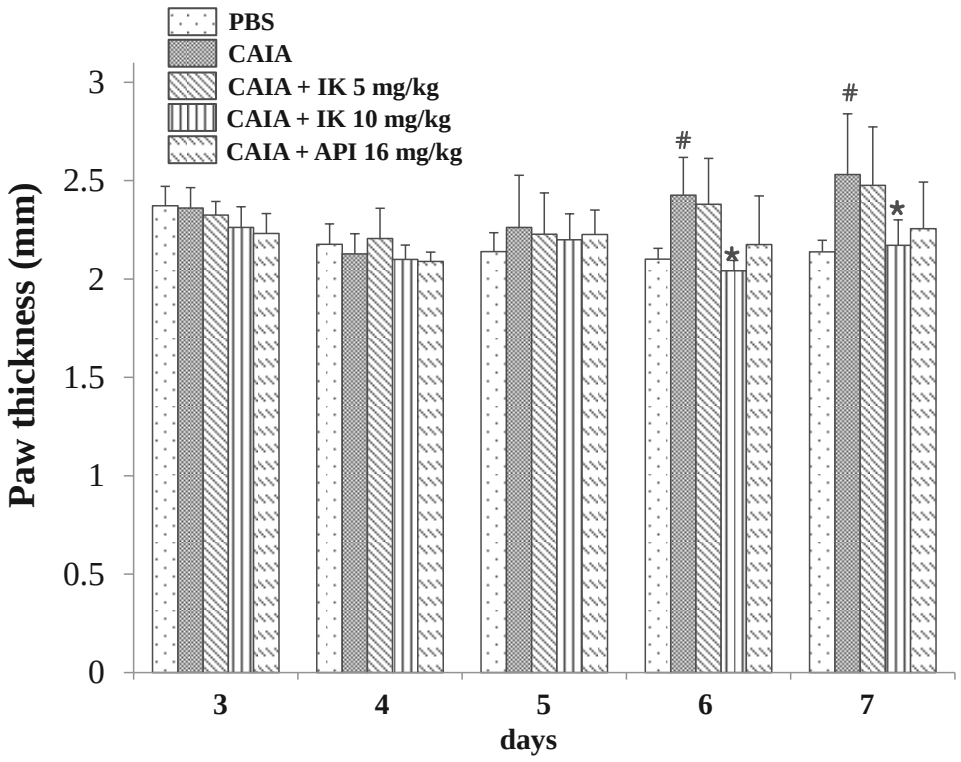

Figure 4.5. Effect of IK and API on paw thickness in CAIA mice. Paw thickness was measured using a digital caliper every day after LPS injection and oral administration of treatments. The average thickness of both hind legs was used. Data are presented as means ± SD (n = 6). $^{\#}p<0.05$ vs. PBS-group and $^{*}p<0.05$ vs. CAIA-group.

4.4. Effect of IK treatment on arthritic score in CAIA model

Arthritic score was measured (blindly) by four different people in an effort to further determine whether IK suppressed RA progression in CAIA model. CAIA group showed a significant increase in arthritic score from days 4 through 7 compared with the PBS group (Figure 4.6). The normal group didn't show any redness and swelling of joints until day 7, however, the control CAIA group showed arthritic symptoms in all joints from days 4 through 7. Those arthritic signs were significantly attenuated in IK-treated group (10 mg/kg) from days 5 through 7. Oral administration of IK alleviated the arthritic symptoms such as redness and swelling of joints in CAIA model. Furthermore, IK-treated group (10 mg/kg) showed delayed onset of the signs when the IK-treated group was compared with API-treated group. However, IK-treatment at 5 mg/kg didn't show significant benefit with regard to the arthritic score, when compared to the control CAIA group.

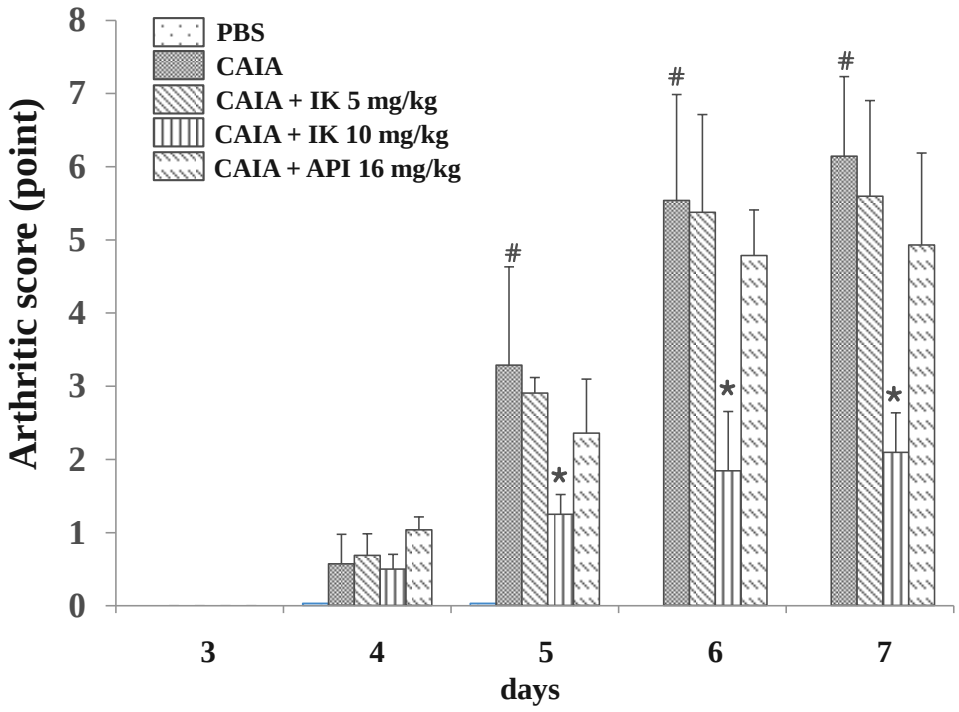

Figure 4.6. Effect of IK and API on arthritic score in CAIA mice. Arthritic score was done blindly by using a system based on the number of inflamed joints in front and hind paws, inflammation being defined by swelling and redness at the scale from 0 (no redness and swelling) to 3 (severe swelling with joint rigidity or deformity; maximal score for four paws, 12). Data are presented as means ± SD (n = 6). $^{\#}p<0.05$ vs. PBS-group and $^{*}p<0.05$ vs. CAIA-group.

4.5. Effect of IK treatment on blood cell population in CAIA model

The neutrophil-to-lymphocyte ratio (NLR) is defined as “the proportion of absolute neutrophil count to lymphocyte count in whole blood cells”. It is generally accepted that NLR is a useful marker for the evaluation of inflammatory activity in chronic inflammatory diseases such as ulcerative colitis (Torun *et al*., 2012), prostate cancer (Yin *et al*., 2016), and RA (Mercan *et al*., 2015). To further investigate whether IK affects blood cell population in CAIA model, NLR was measured from the whole blood sample. CAIA group showed a significant increase in NLR at day 7 compared to the PBS group (Figure 4.7). NLR level was lower in IK-treated group (10 mg/kg) than the control CAIA group by 51.9%. Furthermore, IK-treated group (10 mg/kg) showed lower NLR levels compared with the API-treated group. However, IK-treated group (5 mg/kg) didn’t show significant result compared with the CAIA group in NLR levels.

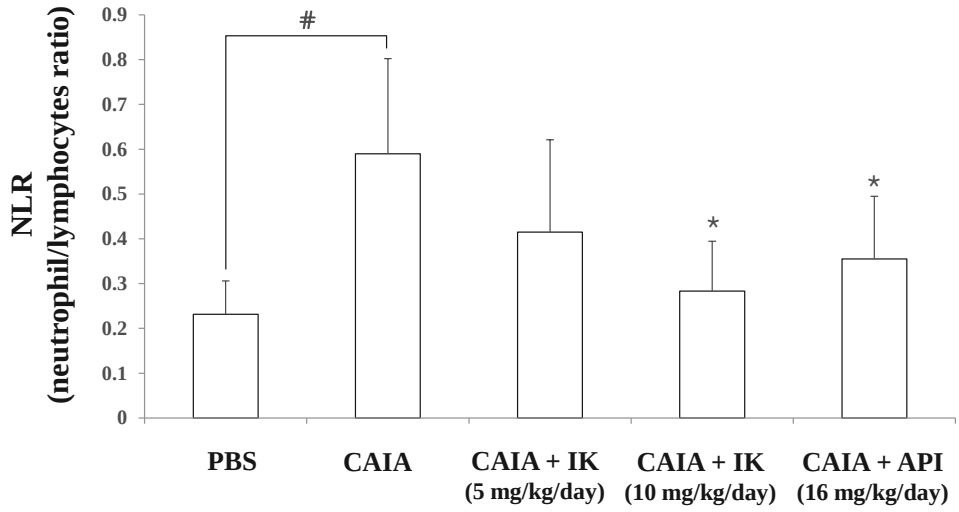

Figure 4.7. Effect of IK and API on neutrophil-to-lymphocyte ratio in CAIA mice. Whole blood samples were collected by cardiac puncture. Data are presented as means ± SD (n = 6). $^{\#}p<0.05$ vs. PBS-group and $^{*}p<0.05$ vs. CAIA-group.

5. Discussion

In the present study, we evaluated the anti-arthritic effect of IK and compared with the effect of apigenin (API) on the development of CAIA model. The treatment with IK attenuated the infiltration of immune cells into joint synovium, paw edema, arthritic score, and NLR levels. Furthermore, IK treatment showed more effective anti-arthritic activity compared with API. At day 7 of CAIA, marked infiltration of inflammatory cells into the synovium and cartilage damage were observed. Immune complex in CAIA activates metalloproteinases that cleave collagen and, in turn, induces cartilage matrix loss. From day 3, paw edema manifest as volume and thickness increased in CAIA group. However, introduction of IK therapy markedly reduced clinical arthritic scores and the incidence of clinically evident signs and symptoms and additionally, the therapy seems to have blocked synovial inflammation and erosive joint destruction. The results indicate that IK treatment not only obviates the onset of CAIA, but may also decrease the signs and symptoms, the severity, of the disease.

RA is a chronic inflammatory autoimmune disease and normally treated by pharmacologic and non-pharmacologic therapies. The pharmacological treatment of RA aims to prevent further development of the disease by introducing anti-rheumatoid drugs in the early phase of the disease (Donahue

et al., 2008). However, significant side effects emanate from these treatments (in the later stages of the disease). Many previous studies suggest that nutrient supplementation has the potential for improving RA. These benefits are achieved by attenuating symptoms, and slowing the progression of the RA pathology, as well as obviating potential negative side effects arising from pharmacologic therapy (Rennie *et al*., 2003). The efficacy of nutrient supplementation is based on phytochemicals such as polyphenol, flavonoid, tannin, anthocyanin, and glycoside.

API, used as positive control in this study, is a dietary flavonoid found in fruits, vegetables, and herbs. Many studies have been reported that API has anti-arthritic properties: Suppression of the collagenase activity involved in RA (Lee *et al*., 2007); protection against CIA (Li *et al*., 2016); induction of apoptosis in rheumatoid fibroblast-like synoviocytes by ROS and activation of ERK1/2 (Shin *et al*., 2009). Unlike previous study (Li *et al*., 2016) which API was administered intraperitoneally (20 mg/kg), API was administered by oral gavage (16 mg/kg) in this study. Curcumin is the major curcuminoid of turmeric (*Curcuma longa*). It has been shown to inhibit acute and chronic joint inflammation (Funk *et al*., 2006), as well as suppress the nuclear factor kappa B (NF-κB) which is pivotal regulator in arthritic patient (Roshak *et al*., 2002). Epigallocatechin-3-gallate (EGCG) is the major active component of

green tea (*Camellia sinensis*) and is believed to ameliorate the signs and symptoms of collagen-induced arthritis in mice (Haqqi *et al*., 1999) and inhibit the IL-1β-induced iNOS and COX-2 in human chondrocytes derived from arthritic cartilage (Ahmed *et al*., 2002). Gallic acid is a natural polyphenolic acid found in gall nuts, sumac, oak bark, tea leaves, and grapes. Several findings suggest figuring out the anti-arthritic activity of gallic acid: inhibition the expression of several pro-inflammatory genes in TNF-α treated fibroblast from patients with rheumatoid arthritis (Chung *et al*., 2010); induction caspase-3 dependent apoptosis of rheumatoid arthritis fibroblast-like synoviocytes (Yoon *et al*., 2013). Resveratrol is a polyphenol present in grape skin, seed, and red wine. This substance has been shown to prevent synovial hyperplasia of human rheumatoid arthritis synovial cells (Shakibaei *et al*., 2008) and modulates collagen-induced arthritis by inhibiting Th17 and B-cell function (Leonarda *et al*., 2003).

IK is an essential oil component in *P. frutescens*. In previous reports, we already examined various pharmacological activities of IK: anti-inflammatory activities in RAW264.7 cells (Jin *et al*., 2010); anti-cancer activities in human DLD1 cells (Cho *et al*., 2011a); anti-obesity activities in 3T3-L1 cells and C57BL/6J mice (So *et al*., 2015); and anti-oxidant activities in RAW264.7 cells (Study 1). To our knowledge, this is the first

report to the effects that that IK has real, actual, material and palpable anti-arthritic effect in CAIA animal model. The results of this study encourage the therapeutic use of IK or *P. frutescens* var. *crispa* in the chronic inflammatory situation like RA.

Because RA is caused by complex etiology, different animal models are utilized to evaluate the efficacy of any new therapy. CIA has been widely used to study RA and shares many histopathological features of the human counterpart (Cho *et al*., 2007). However, the susceptibility for CIA is low in Balb/c mice and induction needs long period. CAIA is a relevant model for studying the efferent phase of RA, where leukocytes are attracted and respond to the immune complex in the joint (Nandakumar *et al*, 2003). And male mice generally developed stronger arthritic symptoms and had a higher incidence of arthritis development (Beckmann *et al*., 2016). For these reasons, we induced RA in male Balb/c mice using CAIA for investigating anti-arthritic activity of IK.

V. Study 3:
Comparison of the anti-inflammatory activities of supercritical carbon dioxide versus ethanol extracts from leaves of radiation mutant *Perilla frutescens* var. *crispa**

(*The part of the results was published in *Molecules* 2017, 22:311)

1. Abstract

In this study, we aimed to compare supercritical carbon dioxide extraction and ethanol extraction for isoegomaketone (IK) content in perilla leaf extracts and to identify the optimal method for offering radiation mutant *P. frutescens* var. *crispa* to functional food. We measured the IK concentration using HPLC from the extracts and production of inflammatory mediators in lipopolysaccharide (LPS)-stimulated RAW 264.7 cells treated with extracts. The IK concentration was 5-fold higher in perilla leaf extracts prepared by supercritical carbon dioxide extraction (SFE) compared with that in perilla leaf extracts prepared by ethanol extraction (EE). When the extracts were treated in LPS-induced RAW 264.7 cells at 25 μg/mL, the SFE inhibited the expression of inflammatory mediators such as nitric oxide (NO), monocyte chemoattractant protein-1 (MCP-1), interleutkin-6 (IL-6), interferon-β (IFN-β), and inducible nitric oxide synthase (iNOS) to a much greater extent compared with EE. Taken together, supercritical carbon dioxide extraction is considered optimal process for obtaining high concentration of IK and anti-inflammatory activities in leaf extracts from the radiation mutant *P. frutescens* var. *crispa.*

2. Introduction

Perilla frutescens (L.) Britt. is an annual herbaceous plant in the Lamiaceae family, which has been widely cultivated in India, China, Japan, and Korea. Its leaves are used in Asian cuisines, and its seeds are used to for extraction of edible oil in Korea. It is also commonly used in traditional Chinese medicine. *P. frutescens* contains several components including rosmarinic acid, luteolin, apigenin, ferulic acid, (+)-catechin, triterpenoids, and caffeic acid (Peng *et al*., 2005; Woo *et al*., 2014). Recent studies demonstrated the pharmacological activities of extracts from *P. frutescens*. Ethanol extracts from *P. frutesens* leaves were shown to possess anti-cancer (Kwak and Ju, 2015), anti-inflammatory (Lee and Han, 2012), and anti-bacterial (Kim *et al*., 2011) activities. In addition, methanol extracts from *P. frutescens* leaves showed anti-allergy, anti-inflammatory (Liu *et al*., 2013), and anti-cancer (Wang *et al*., 2013) activities. Water extracts from *P. frutescens* leaves improved gastrointestinal discomfort (Sybille *et al*., 2014) and suppressed tumor necrosis factor-alpha production in mice (Ueda and Yamazaki, 1997).

Previously, we identified a radiation mutant *P. frutescens* var. *crispa* with an approximately 10-fold greater isoegomaketone (IK) level than that of the wild-type (Park *et al*., 2009b). IK, an essential oil component in *P. frutescens*, exhibits several biological activities. It has been shown to suppress NO

production in LPS-treated RAW264.7 cells (Jin *et al*., 2010) and to induce apoptosis in several cancer cells through both caspase-dependent and caspase-independent pathways (Cho *et al*., 2011a; Kwon *et al*., 2014a).

Supercritical carbon dioxide (SC-CO_2) extraction is a novel and powerful technique for extracting lipophilic components (Guan *et al*., 2007; Sookwong *et al*., 2016). SC-CO_2 extraction has several advantages over the use of organic solvents, because CO_2 is non-toxic, non-reactive, non-corrosive, and inexpensive. SC-CO_2 extraction of *P. frutescens* seed has been performed previously (Jung *et al*., 2012; Kim *et al*., 1998), but SC-CO_2 extraction method has not been used for the extraction of IK from *P. frutescens* leaves. In the present study, we identified the optimal extraction method from the leaves of radiation mutant *P. frutescens* var. *crispa* for applying to functional food by comparing SFE with EE.

3. Materials and Methods

3.1. Materials

Leaves of the radiation mutant *P. frutescens* var. *crispa* were harvested at Advanced Radiation Technology Institute (Jeongeup, Korea). DMEM and fetal bovine serum (FBS) were purchased from Hyclone (Logan, UT, USA). LPS, phenylmethylsulfonyl fluoride, sodium nitrite, DMSO, Griess reagent, and protease inhibitor cocktail were purchased from Sigma-Aldrich (St. Louis, MO, USA). Goat anti-rabbit IgG HRP-conjugated antibody was purchased from Invitrogen (Carlsbad, CA, USA). The RNeasy kit was purchased from QIAGEN (Valencia, CA, USA). The EZ-Cytox Cell Viability assay kit was purchased from Daeil Lab Services (Seoul, Korea). The Advantage RT-for-PCR kit was purchased from Clontech (Mountain view, CA, USA). SYBR Premix was purchased from Takara Bio Inc (Shiga, Japan). NP40 cell lysis buffer was purchased from Biosource (San Jose, CA, USA). Rabbit polyclonal antibodies against β-tubulin and iNOS were purchased from Santa Cruz Biotechnology (Santa Cruz, CA, USA).

3.2. Cell culture

RAW 264.7 cells were cultured in DMEM supplemented with 10% FBS, penicillin (100 U/mL), and streptomycin (100 μg/mL) and incubated at 37°C in an atmosphere of 5% CO_2.

3.3. Ethanol extraction

The dried leaves of *P. frutescens* var. *crispa* (10 g) were extracted with ethanol (100 mL) in a shaking incubator for 6 h at 60℃ and filtered through filter paper (Whatman No. 4). Ethanol was of analytical grade (≥95.0%) and obtained from Duksan Co. (Seoul, Korea). The moisture content in dried sample was found to be 5.3 ± 1.4%. The solvent was evaporated in vacuo to afford the ethanol extract (0.9 g). Ethanol extraction was repeated three times.

3.4. SC-CO_2 extraction

A laboratory-scale supercritical fluid extraction system (Ilshin Autoclave Co., Daejeon, Korea) was used for SC-CO_2 extraction of perilla leaves. The dried perilla leaves were ground using a milling machine, and the powder (180 g) was transferred to an extraction column. The moisture content in the powder sample was found to be 5.3 ± 1.4%.The powder sample was held in place within the extraction column by glass wool mounted on both ends of the extractor. After the extractor reached the predetermined temperature (50℃)

and pressure (400 bar), the sample was allowed to stand for 10 min for temperature (50℃) and pressure (400 bar) equilibration. Then, the extraction was performed by passing the CO_2 (99.9%) through the column at a flow rate of 60 mL/min at 50℃ and 400 bar for 3 h. The extracted oil was separated by pressure reduction and collected in the trap. The collected oils were stored in a refrigerator at 4℃. SC-CO_2 extraction was repeated two times

3.5. HPLC analysis

HPLC analysis was conducted using the Agilent Technologies model 1100 instrument (Agilent Technologies, Santa Clara, CA, USA). The samples were analyzed by reverse phase (C18) HPLC analysis (YMC-Triart C18, 4.6 × 250 mm I.D, S-5 μm, flow rate 1 mL/min, UV detection: 254 nm) using acetonitrile:water (44:55 to 55:45, 30 min) as the gradient solvent. Solvents used in HPLC analysis were of analytical grade (≥99.9%) and obtained from Sigma Chemical Co. (St. Louis, MO, USA).

3.6. Cytotoxicity assay

To measure cell viability, we used the EZ-Cytox cell viability assay kit (Daeil Lab Service, Seoul, Korea). The cells were cultured in a 96-well flat-bottom plate at a density of 2.0×10^5 cells/mL for 24 h. The cells were

subsequently treated with various concentrations of the extracts for an additional 24 h. After the incubation period, 10 μL EZ-Cytox were added to each well and incubated for 4 h at 37℃ and 5% CO_2. Cell viability was determined by measuring formazan production using an ELISA reader at an absorbance of 480 nm with a reference wavelength of 650 nm.

3.7. Determination of NO concentration

Nitrite in the cellular media was measured by the Griess method (Khan *et al*., 2009). The cells were cultured in a 96-well plate and treated with LPS (1 μg/mL) for 18 h. The medium was collected at the end of the culture period for determination of nitrite production. Equal volumes of Griess reagent and cellular supernatant were mixed, and the absorbance was measured at 540 nm. The concentration of nitrite (μM) was calculated using a standard curve generated from known concentrations of sodium nitrite dissolved in DMEM. The results are presented as the means ± SD of four replicates in one representative experiment.

3.8. Preparation of cell extracts and western blot analysis

Cells were washed once with cold PBS and harvested by pipetting. For whole-cell extract preparation, the cells were lysed in NP40-based cell lysis

buffer containing protease inhibitor cocktail (Sigma, St. Louis, MO, USA) and phenylmethylsulfonyl fluoride (Sigma) for 30 min on ice. The protein concentration of the cell lysate was determined using the Bio-Rad Protein Assay (Bio-Rad, Hercules, CA, USA). Aliquots of 50 μg protein were loaded and electrophoresed on 10% SDS-polyacrylamide gels and then transferred to nitrocellulose membranes (Hybond ECL Nitrocellulose; GE Healthcare, Chandler, AZ, USA). The membranes were washed once with wash buffer consisting of PBS with 0.05% Tween 20 and blocked with blocking buffer consisting of PBS with 5% skim milk and 0.05% Tween 20 for 1 h. After blocking, the membranes were incubated with rabbit anti-HO-1 or anti-β-tubulin primary antibody overnight at 4℃. Rabbit anti-iNOS polyclonal antibody was diluted 1:1000, and rabbit anti-β-tubulin polyclonal antibody was diluted 1:200 in blocking buffer. After incubation, the membranes were washed and subsequently incubated for 1 h at room temperature with goat anti-rabbit IgG HRP-conjugated secondary antibody diluted 1:5000 in blocking buffer. The membranes were washed and the protein bands detected by chemiluminescence analysis (GE Healthcare).

3.9. Quantitative real-time PCR

The cells (2×10^5 cell/mL) were cultured in a 100-mm petri dish for 24 h. Total RNA was isolated using the RNeasy Kit according to the manufacturer's instructions. The Advantage RT-for-PCR kit was used for reverse transcription according to the manufacturer's protocol. The Chromo4 real-time PCR detection system (Bio-Rad) and iTaqTM SYBRR Green Supermix (Bio-Rad) were used for RT-PCR amplification of HO-1 and β-actin under the following conditions: 50 cycles of 94℃ for 20 s, 60℃ for 20 s and 72℃ for 30 s. All of the reactions were repeated independently at least three times to ensure reproducibility of the results. Primers were purchased from Bioneer Corp (Daejeon, Korea). Primer sequences are shown in Table 4.1.

Table 5.1. Primers sequences for Real Time-PCR analysis

Target gene		5' to 3' direction
iNOS	Forward	TGAGAGGGAAATCGTGCGTGAC
	Reverse	GCTCGTTGCCAATAGTGATGACC
IL6	Forward	GTTCTCTGGGAAATCGTGGAA
	Reverse	GCAAGTGCATCATCGTTGTTC
MCP1	Forward	GCATCTGCCCTAAGGTCTTCA
	Reverse	AAGTGCTTGAGGTGGTTGTGG
Beta actin	Forward	TCCTACACCACACCAAACTGTGTGC
	Reverse	CTCCAATCTCTGCCTATCCGTCTC

3.10. Measurement of MCP-1, IFN-β, and IL-6 by ELISA

The levels of MCP-1, IFN-β, and IL-6 in the culture medium were measured using an ELISA kits (R&D Systems, Minneapolis, MN, USA) according to the manufacturers' protocols.

3.11. Statistical analysis

One-way analysis of variance (ANOVA) was used to determine overall differences among groups, followed by Fisher's LSD test for individual group comparisons. The results from all comparisons were considered significant at $P < 0.05$. Data were reported as mean ± SD. All data were analyzed using the SPSS 21.0 program (SPSS Inc., IL, USA).

4. Results

4.1. Yield and composition of SFE and EE

In this study, we obtained extracts from the radiation mutant *P. frutescens* var. *crispa* leaves using supercritical carbon dioxide extraction and ethanol extraction methods. To our knowledge, this is the first study to apply the SC-CO_2 extraction technique for perilla leaves. Generally, temperature and pressure influence the yield from SC-CO_2 extraction. In the case of perilla seed, when the pressure was above 340 bar, the yield was saturated with 3 kg CO_2 regardless of temperature and pressure (Kim *et al*., 1998). And the solubility of perilla oil at 400 bar in SC-CO_2 was constant at all temperatures (Kim *et al*., 1998). To obtain maximum SC-CO_2 extraction yield from perilla leaves, we used sufficient CO_2 at 400 bar. The extraction yields of SFE and EE were 5.0 ± 0.2% and 9.0 ± 0.2%, respectively (Table 5.2). Figure 5.1 shows the compositions of the two extracts. SFE contained three main oil components, including isoegomaketone (IK) and perilla ketone (PK), but EE contained numerous components, including polar and nonpolar substances. These differences in composition are due to the difference in solubility between ethanol and CO_2. IK content was 6.3 ± 0.2 mg/g and 63.8 ± 2.6 mg/g in EE and SFE, respectively. And PK content was 13.3 ± 0.3 mg/g and 146.9 ± 5.6 mg/g in EE and SFE, respectively. IK and PK contents were

approximately 5-fold higher in SFE compared with EE, given that extraction yield of SFE was 2-fold lower than that of EE. While the extraction yield from SC-CO_2 extraction method was lower than that from ethanol extraction method, SC-CO_2 extraction was more effective in obtaining an extract with higher IK content from the radiation mutant *P. frutescens* var. *crispa* leaves.

Table 5.2. Extraction yield and HPLC data of samples extracted with ethanol and SC-CO_2 from *P. frutescens* var. *crispa* leaves

Extraction Method	Extraction Yield (%)	Concentration (mg/g)	
		Isoegomaketone (IK)	Perillaketone (PK)
Ethanol	10	6.3	13.3
SC-CO_2	5	63.8	146.9

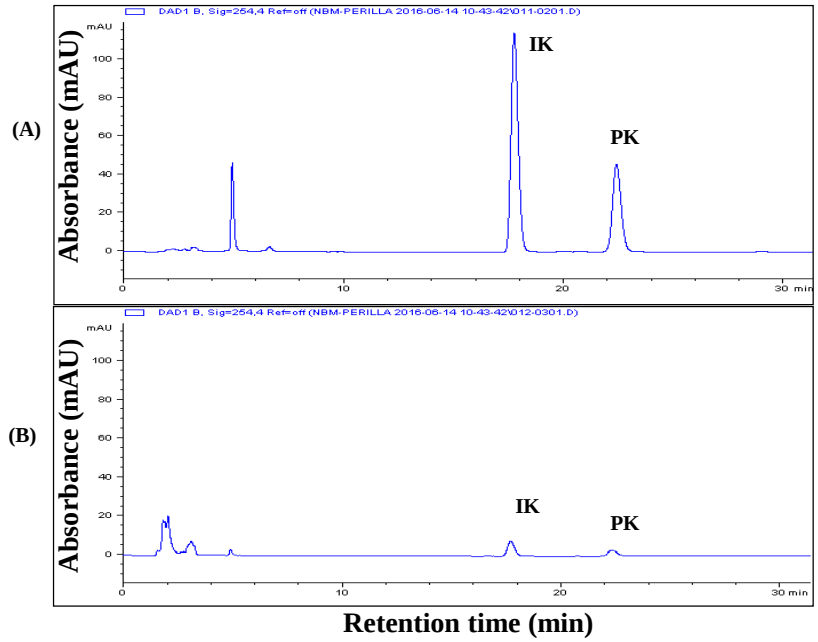

Figure 5.1. HPLC chromatograms. (A) SFE (50℃, 400 bar, 3h, and CO_2 flow rate of 60 mL/min) and (B) EE (shaking incubation for 6 h at 60℃) at 254 nm.

4.2. Effect of SFE and EE on cell viability

To determine the cytotoxicity of SFE and EE, RAW 264.7 cells were treated with two extracts at concentrations of 5, 10, and 25 μg/mL for 24 h. As shown in Figure 5.2, neither extracts affected cell viability at the concentration lower than 25 μg/mL. Therefore, we performed all the experiments using treatment with extracts lower than 25 μg/mL.

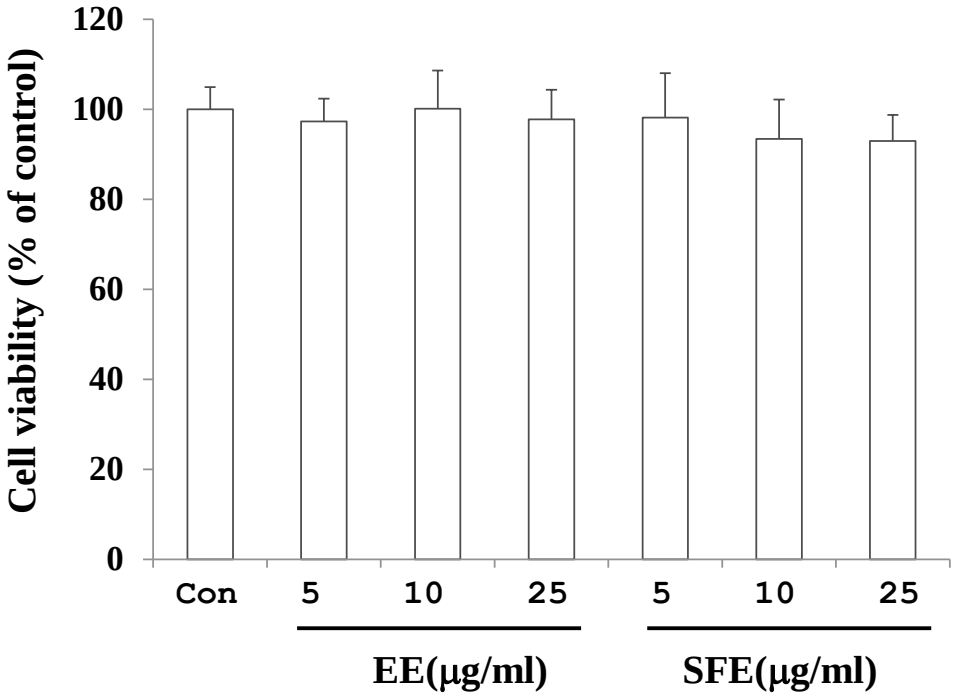

Figure 5.2. Effects of SFE and EE on cell viability. Cell viability was determined using the EZ-Cytox cell viability assay kit. The cells were treated with various concentrations of SFE and EE for 24 h. After the incubation period, 10 μL of the kit solution were added to each well and incubated for an additional 4 h. Data are presented as means ± SD (n = 3).

4.3. Effect of SFE and EE on LPS-stimulated NO production in RAW264.7 cells

We first compared the anti-inflammatory effects of SFE and EE on nitric oxide (NO) production in LPS-treated RAW 264.7 cells. NO is a potentially toxic gas produced from the amino acid l-arginine via nitric oxide synthase (NOS) activity. Appropriate levels of NO are important for organ protection, but excessive NO production is associated with many diseases, including cancer, arthritis, and diabetes (Ruan, 2002; Tylor *et al*., 1997). RAW 264.7 cells were treated with SFE and EE for 2 h before the stimulation with 1 μg/mL LPS for 18 h. NO production increased significantly after incubation with LPS (Figure 5.3A). Both extracts decreased the levels of LPS-stimulated NO production in a dose dependent manner. However, SFE exerted 5-fold greater inhibitory activity on NO production compared with EE (Figure 5.3A). To determine whether suppression of NO production by SFE and EE was due to inhibition of iNOS expression, we measured protein and mRNA levels of iNOS. Western blot analyses showed that LPS-induced increase in iNOS levels were attenuated by treatment with SFE in a dose-dependent manner (Figure 5.3B). Furthermore, RT-PCR analyses showed that iNOS mRNA level was increased by LPS stimulation and this increase was significantly reduced by SFE treatment in a dose dependent manner

(Figure 5.3C). While EE also decreased iNOS mRNA levels, its magnitude of inhibition was much lower than that of SFE. These results indicate that IK plays an important role in the anti-inflammatory activity of SFE and has greater anti-inflammatory activity than the polar components in EE.

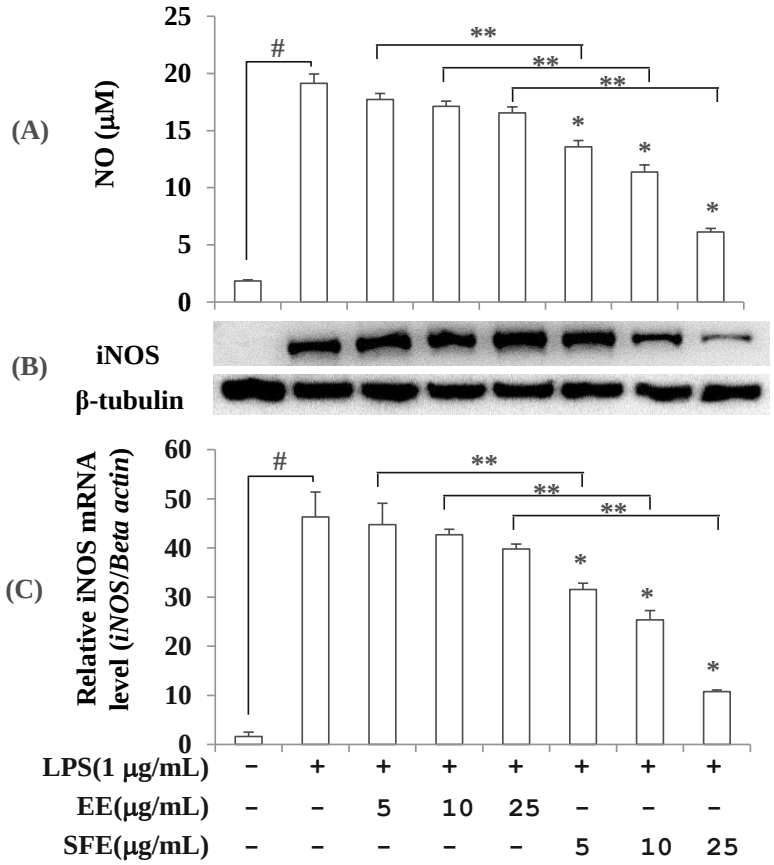

Figure 5.3. Effects of SFE and EE on NO production and iNOS expression levels in RAW 264.7 cells. (A) Cellular media (100 μl) were mixed with equal volumes of Griess reagent. Nitrite levels were measured as an indicator of NO production as described in the Materials and Methods section. Data are presented as means ± SD (n = 4). (B) A representative western blot of iNOS protein expression. (C) Total RNA was isolated and used to measure the expression level of iNOS mRNA by quantitative real-time PCR. Data are presented as means ± SD (n = 3). $^{\#}p<0.05$ vs. the negative control, $*p<0.05$ vs. LPS alone-treated group, and $**p<0.05$ vs. the EE-treated group.

4.4. Effect of SFE and EE on production of inflammatory mediators in LPS-stimulated RAW264.7 cells

To determine the effects of SFE and EE treatment on the production of inflammatory mediators, RAW 264.7 cells were treated with SFE and EE for 2 h before the stimulation with 1 μg/mL LPS for 4 h and the levels of monocyte chemoattractant protein-1 (MCP-1), interferon-β (IFN-β), and interleukin-6 (IL-6) were measured. As shown in Figure 5.4, both SFE and EE treatments suppressed the production of MCP-1, IFN-β, and IL-6 in LPS-stimulated RAW 264.7 cells. However, SFE showed about 3-4 fold stronger inhibitory activity on the production of all inflammatory mediators compared with EE. Furthermore, SFE treatment lowered IL-6 and MCP-1 mRNA levels to a greater extent than EE (Figure 5.5).

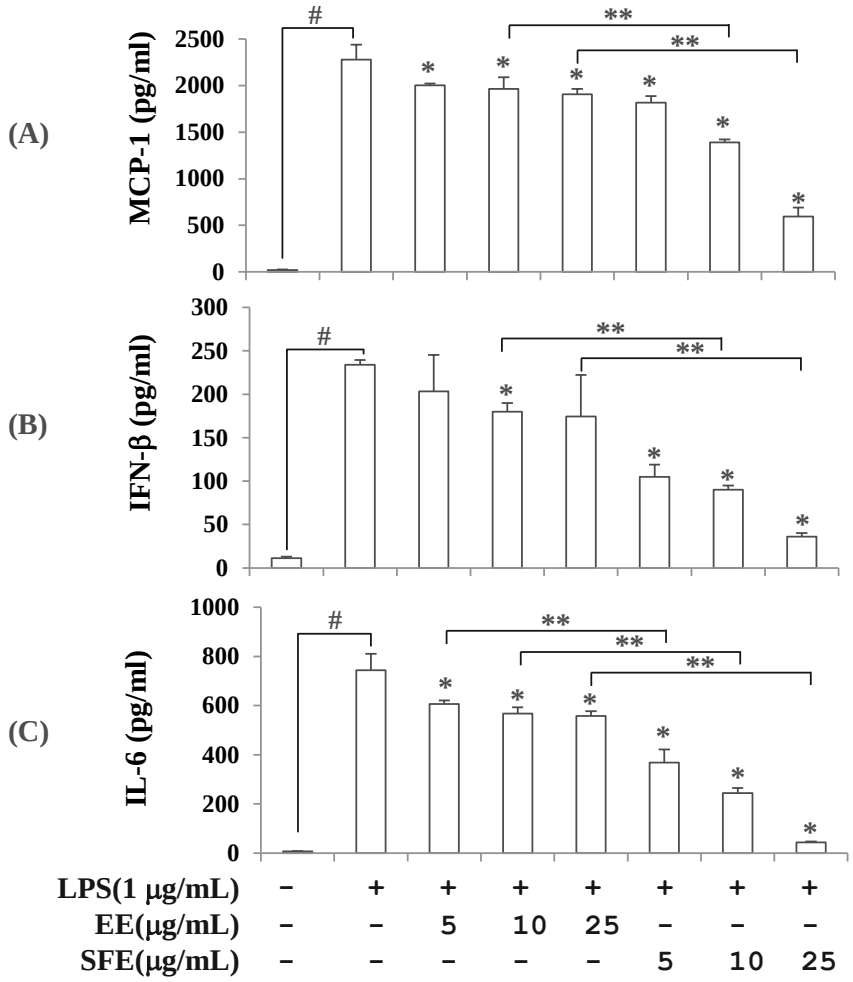

Figure 5.4. Effects of SFE and EE on the production of inflammatory mediators in RAW 264.7 cells. RAW 264.7 cells were treated with each extract for 2 h prior to addition of LPS (1 μg/mL) and further incubated for 4 h. MCP-1 (A), IFN-β (B), and IL-6 (C) levels were measured in the cellular medium using an ELISA kit. Data are presented as means ± SD (n = 3). $^{\#}p<0.05$ vs. the negative control, $^{*}p<0.05$ vs. LPS alone-treated group, and $^{**}p<0.05$ vs. the EE-treated group.

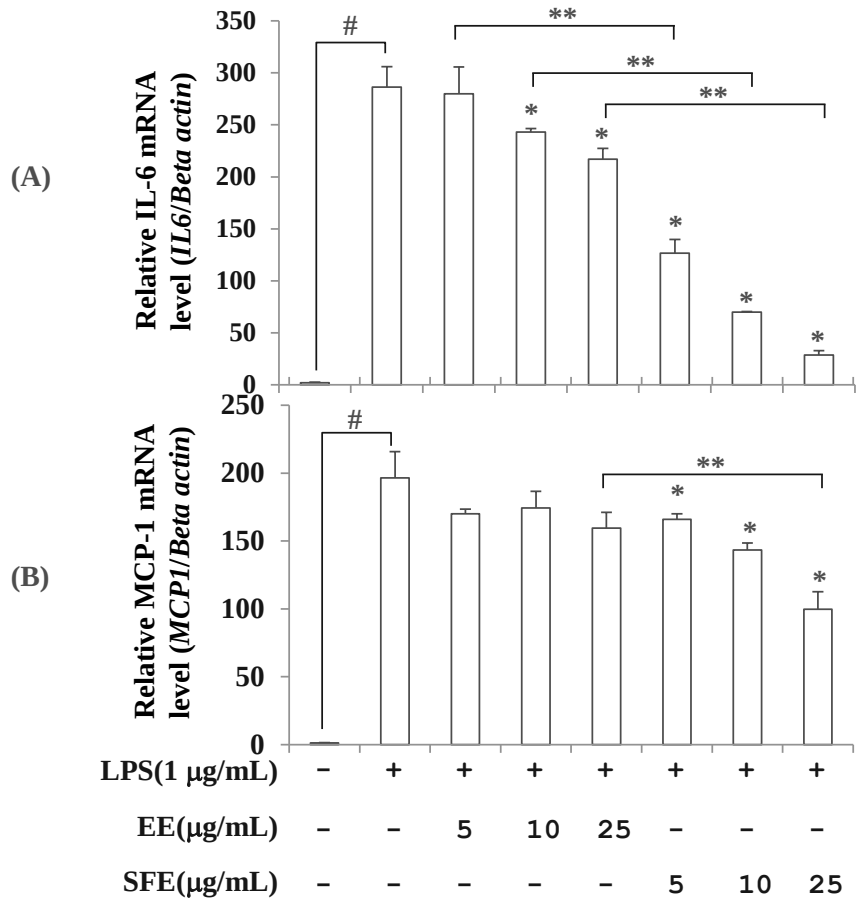

Figure 5.5. Effects of SFE and EE on IL-6 and MCP-1 expression levels in RAW 264.7 cells. Total RNA was isolated and used to measure the expression levels of IL-6 (A) and MCP-1 (B) mRNA by quantitative real-time PCR. Data are presented as means ± SD (n = 3). $^{\#}p<0.05$ vs. the negative control, $*p<0.05$ vs. LPS alone-treated group, and $**p<0.05$ vs. the EE-treated group.

5. Discussion

Previously, a mutant *P. frutescens* var. *crispa* obtained by mutagenesis using gamma rays (Jin *et al*., 2010), which had much higher anti-inflammatory activity than the wild-type control, was identified. After HPLC analysis and assay-based purification of the mutant, we showed that the enhanced anti-inflammatory activity was due to a 10-fold increase in IK content in the leaves compared with wild-type (Park *et al*., 2009b). There have been many reports regarding extraction from perilla using organic solvents (Kwak and Ju, 2015; Lee and Han, 2012; Kim *et al*., 2011; Liu *et al*., 2013; Wang *et al*., 2013; Sybille *et al*., 2014; Ueda and Yamazaki, 1997), SC-CO_2 (Jung *et al*., 2012; Kim *et al*., 1998), and microwave-assisted techniques (Shao *et al*., 2012). In this study, we focused on the SC-CO_2 method because the mutant *P. frutescens* var. *crispa* has a high content of IK and SC-CO_2 method had never been used for obtaining extract from perilla leaves. Perilla oil is present mostly in the seeds; therefore, the SC-CO_2 technique has been used previously only on seeds and not on leaves. However, IK content was approximately 5-fold higher in leaves compared with seeds from the mutant *P. frutescens* var. *crispa* (data not shown). Generally, water extraction method is used in the food industries, because it is an efficient and environmentally friendly technique for extracting various compounds from

plants (Siti *et al*., 2016). And extracts prepared by water extraction method can be applied to various forms of food processing. However, it was not an effective method for extracting IK from perilla leaves. The extract from mutant perilla leaves using water extraction method did not contain IK. Extraction of IK from mutant perilla leaves had been accomplished by employing organic solvents such as methanol, ethanol, or hexane. However, when organic solvents are used for extraction, an additional process to evaporate these solvents from extracts is required. IN addition, there is increasing public concern for the possibility of toxic solvent residues remaining in the final product. For the above reasons, we used SC-CO_2 method to extract IK from mutant perilla leaves.

In this study, we obtained extracts from the radiation mutant *P. frutescens* var. *crispa* leaves using supercritical carbon dioxide extraction and ethanol extraction. The extraction yields of SFE and EE were 5.0 ± 0.2% and 9.0 ± 0.2%, respectively. IK and PK contents were approximately 5-fold higher in SFE compared with EE, given that extraction yield of SFE was 2-fold lower than that of EE. Although the extraction yield from SC-CO_2 extraction method was lower than that from ethanol extraction method, SC-CO_2 extraction was more effective in obtaining an extract with higher IK content from the radiation mutant *P. frutescens* var. *crispa* leaves.

Furthermore, SFE showed much higher inhibitory activity on the production of all inflammatory mediators, such as NO, MCP-1, IFN-β, and IL-6, than did EE. The better anti-inflammatory activity of SFE can be explained by the higher IK content.

IK, an essential oil present in *P. frutescens*, exhibits several biological activities, including anti-inflammatory (Jin *et al*., 2010) and anti-cancer effects (Cho *et al*., 2011a; Kwon *et al*., 2014a). While SFE had a higher IK content, EE contained several anti-inflammatory polar compounds, such as pomolic acid, tormentic acid, corosolic acid (Banno *et al*., 2004), and rosmarinic acid methyl ester (So *et al*., 2016). However, the concentration of these compounds in EE was too low to exert anti-inflammatory activities in LPS-stimulated RAW 264.7 cells. The superior anti-inflammatory activities of SFE seemed to result from the higher IK content. Furthermore, we tried to adopt SFE and EE into food processing. Unlike SFE, EE had disadvantage due to the mixture of both polar and nonpolar ingredients. Therefore, SC-CO_2 is a much more effective method of acquiring extract from mutant perilla leaves for the future development of functional foods.

VI. Study 4

Anti-arthritic activities of the supercritical carbon dioxide extract from radiation mutant *Perilla frutescens* var. *crispa* in collagen antibody-induced arthritis

1. Abstract

In this study, we determined the anti-arthritic effects of the radiation mutant *Perilla frutescens* var. *crispa* leaf extract (SFE-M) and wild type leaf extract (SFE-W), both prepared by supercritical carbon dioxide (SC-CO_2) extraction, on the development of collagen antibody-induced arthritis (CAIA) in Balb/c mice. Experimental animals were randomly divided into four groups: normal, CAIA, CAIA + SFE-M (100 mg/kg/day), and CAIA + SFE-W (100 mg/kg/day) and respective treatments were administered via oral gavage once per day for 4 days. Mice treated with SFE-M developed less severe arthritis than the control CAIA mice. They showed significantly improved arthritic score, paw volume, and paw thickness compared to the control CAIA mice from days 3 through 7. Furthermore, histopathological examination of ankle for inflammation showed that infiltration of inflammatory cells and edema formation were reduced by SFE-M treatment. Similarly, neutrophil to lymphocyte ratio (NLR) in whole blood was lower in mice treated with SFE-M by 37% compared to the control CAIA mice. However, SFE-W didn't show any significant result compared to the control CAIA group. Taken together, SFE-M treatment delays the onset of the arthritis and alleviates the manifestations of arthritis in CAIA mice.

2. Introduction

Perilla frutescens (L.) Britt. is an annual herbaceous plant in the Lamiaceae family. Its leaves are used as food in Asian cuisines, and its seeds are used to make edible oil in Korea. In traditional medicine practices, *P. frutescens* is also used to treat a variety of illnesses including cough, phlegm, back pain, and diabetes (Han *et al*., 1994; Kim *et al*., 2007). In previous studies, extracts from *P. frutescens* var. *crispa* were acquired using various methods to examine the pharmacological activities: the ethanol extract (Lee and Han, 2012) and the supercritical carbon dioxide (SC-CO_2) extract showed anti-inflammatory effects; the water and ethanol extracts had antioxidant effects (Cho *et al*., 2011b); the methanol extract exerted a preventative action against Alzheimer's disease (Choi *et al*., 2004).

SC-CO_2 extraction is a novel and powerful technique for extracting lipophilic components (Guan *et al*., 2007; Sookwong *et al*., 2016). SC-CO_2 extraction has several advantages over the use of organic solvents, because CO_2 is non-toxic, non-reactive, non-corrosive, and inexpensive. SC-CO_2 extraction of *P. frutescens* has been performed previously using seeds (Jung *et al*., 2012; Kim *et al*., 1998).

Rheumatoid arthritis (RA) is a systemic autoimmune disease in which chronic joint inflammation leads to cartilage destruction and bone erosion

(Scott *et al*., 2010). Typically, RA is treated by pharmacologic and non-pharmacologic therapies. The pharmacological treatment of RA aims to prevent further development of the disease using anti-rheumatic drugs in the early course of the disease (Donahue *et al*., 2008). However, the use of standard drugs in RA caused significant side effects from these treatments in the later stages of the disease. Therefore, the renewed interest in botanical origin remedies which lack severe side effects and have millennia-proven efficacy is growing (Umar *et al*., 2014). These remedies maybe have a beneficial effect not only on the symptoms but also on the development of the disease (Akhtar *et al*., 2011).

Mutation induction and selection of mutants have been powerful tools for plant breeding as well as for physiological and molecular studies for the past 80 years. X-ray, γ (gamma) ray irradiation, and chemical treatments have been used for mutation breeding in a wide range of plants (Nakano *et al*., 2010). Over the past 40 years, the use of γ rays in mutation induction has become particularly prevalent, while the use of X-rays has been significantly reduced. Gamma rays are a type of ionizing radiation which interacts with atoms to induce free radicals in cells which damage or modify important components of plant cells such as chromosome.

In the previous report, the radiation mutant *P. frutescens* var. *crispa*, which has enhanced anti-inflammatory activities compared to wild type, was found (Park *et al*., 2009b). Furthermore, the extract from radiation mutant *P. frutescens* var. *crispa* (SFE-M) prepared by SC-CO_2 extraction had a higher anti-inflammatory activities compared to the extract from wild type (SFE-W) in RAW264.7 cells (Park *et al*., 2016). Although there is strong evidence that SFE-M has anti-inflammatory effect, whether SFE-M can exert a treatment effect on inflammatory disease such as RA has not been investigated. Therefore, the present study was undertaken to determine the effect of SFE-M on RA in CAIA animal model.

3. Materials and Methods

3.1. Animals

Animals were maintained in accordance with the guidelines of the Guide for the Care and Use of Laboratory Animals (Institute of Laboratory Animal Resources, KAERI(Korea Atomic Energy Research Institute)-IACUC-2017-016). Male Balb/c mice (4 weeks) were purchased from Orient Bio Inc. (Seongnam, Korea) and allowed to acclimate for 1 week prior to the beginning of the study. Mice were maintained in a room which controlled light/dark cycle (12h/12h), temperature (about 23 ± 2℃), and humidity (55 ± 10%).

3.2. SC-CO_2 extraction

A laboratory-scale supercritical fluid extraction system (Ilshin Autoclave Co., Daejeon, Korea) was used for SC-CO_2 extraction of perilla leaves (radiation mutant and wild type). The dried perilla leaves were ground using a milling machine, and the powder (180 g) was transferred to an extraction column. The moisture content in the powder sample was found to be 5.3 ± 1.4%. The powder sample was held in place within the extraction column by glass wool mounted on both ends of the extractor. After the extractor reached the predetermined temperature (50℃) and pressure (400 bar), the sample was

allowed to stand for 10 min for temperature (50℃) and pressure (400 bar) equilibration. Then, the extraction was performed by passing the CO_2 (99.9%) through the column at a flow rate of 60 mL/min at 50℃ and 400 bar for 3 h. The extracted oil was separated by pressure reduction and collected in the trap. The collected oils were stored in a refrigerator at 4℃. SC-CO_2 extraction was repeated two times

3.3. HPLC analysis

HPLC analysis was conducted using the Agilent Technologies model 1100 instrument (Agilent Technologies, Santa Clara, CA, USA). The samples were analyzed by reverse phase (C18) HPLC analysis (YMC-Triart C18, 4.6 × 250 mm I.D, S-5 μm, flow rate 1 mL/min, UV detection: 254 nm) using acetonitrile:water (44:55 to 55:45, 30 min) as the gradient solvent. Solvents used in HPLC analysis were of analytical grade (≥99.9%) and obtained from Sigma Chemical Co. (St. Louis, MO, USA).

3.4. Sample preparation and treatment

SFE-M and SFE-W were suspended into corn oil with concentration of 20 mg/mL and were treated with 100 μL per mouse by oral administration. Mice were fasted at 7 p.m. and were fed at 10 a.m. after oral administration from

day 2 to day 6.

3.5. Collagen antibody-induced arthritis

Mice were randomly divided into 5 groups; (1) Corn oil only (n = 6), (2) CAIA (n = 6), (3) CAIA plus SFE-M (100 mg/kg, n = 6), (4) CAIA plus SFE-W (100 mg/kg, n = 6). A cocktail of four monoclonal antibodies to type II collagen (ArthritoMab; MD Bioscience, Saint Paul, MN, USA; 2 mg/100 μl) was injected intravenously at day 0. Mice in corn oil group were injected with equal volume of corn oil. At day 3, all animals except corn oil group were intraperitoneally injected with LPS (*Escherichia coli* 055:B5; MD Biosciences; 50 μg/200 μl endotoxin-free water). And treatments (corn oil, SFE-M, SFE-W) were administered by oral gavage once a day from day 3 to day 6. Mice were examined for the development of arthritis for 4 days after LPS injection (Figure 6.1).

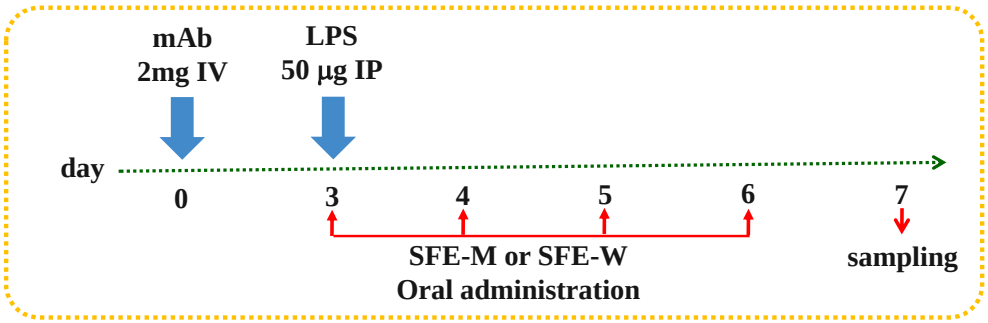

Figure 6.1. The scheme of induction of CAIA and sample treatment

3.6. Assessment of clinical signs of inflammation

Paw volumes were measured using a Digital Plethysmometer (LE7500, Panlab, Spain) every day after LPS injection. The hind leg was soaked in the buffer calibrated with 1 mL standard sinker. The increased volume was measured. The average volume of both hind legs was used. Paw thickness was measured using a digital caliper (Mitutoyo, Andover, UK) every day after LPS injection. The average thickness of both hind legs was used. Arthritic score was done blindly by using a system based on the number of inflamed joints in front and hind paws, inflammation being defined by swelling and redness at the scale from 0 (no redness and swelling) to 3 (severe swelling with joint rigidity or deformity; maximal score for four paws, 12).

3.7. Histopathological assessment

Hind feet were removed after euthanization and fixed using 4.5% buffered formalin. Hind feet were decalcified in buffered formalin containing 5.5% EDTA. Upon decalcification, paws were embedded in paraffin wax blocks, sectioned, and stained with hematoxylin and eosin for microscopic evaluation, which was performed by an expert blinded to the treatments received. Each section was screened for infiltration of neutrophils to

synovium and every joint was scored as follows: 0, normal; 1, minimal; 2, mild; 3, moderate; and 4, marked.

3.8. Analysis of neutrophil and lymphocyte

Whole blood samples were collected by cardiac puncture. The blood was placed in Vacutainer TM tubes containing EDTA (BD science, Franklin Lakes, NJ, USA). Anti-coagulated blood was used for the determination of blood cell population analysis including neutrophil and lymphocytes in a HEMAVET 950 (Drew Scientific Inc., Miami Lakes, FL, USA).

3.9. Statistical analysis

One-way analysis of variance (ANOVA) was used to determine overall differences among groups, followed by Fisher's LSD test for individual group comparisons. The results from all comparisons were considered significant at $P < 0.05$. Data were reported as mean ± SD. All data were analyzed using the SPSS 21.0 program (SPSS Inc., IL, USA).

4. Results

4.1. Composition of SFE-M and SFE-W

In this study, leaf extracts from radiation mutant *P. frutescens* var. *crispa* and wild type were acquired using SC-CO_2 method. Figure 6.2 shows the compositions of the two extracts. IK content was approximately 7-fold higher in SFE-M compared with SFE-W. IK content was 76.0 ± 0.7 mg/g and 10.8 ± 0.3 mg/g in SFE-M and SFE-W, respectively.

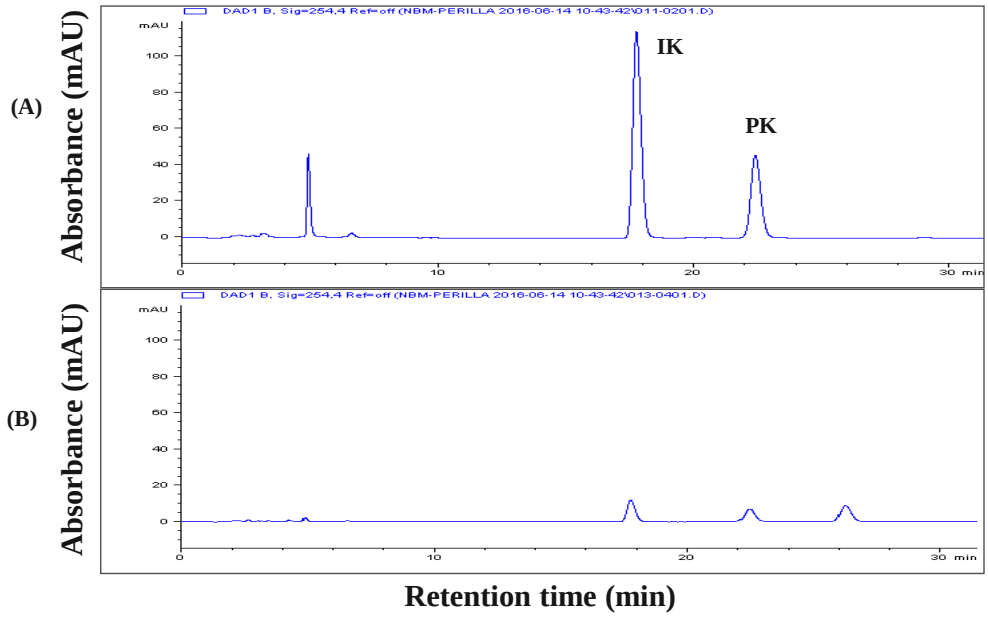

Figure 6.2. HPLC chromatograms. (A) SFE-M and (B) SFE-W

4.2. Effect of SFE-W and SFE-M treatment on the development of RA in CAIA model

At first, whether SFE-W treatment by oral administration prevented initiation of disease in Balb/c mice with CAIA was investigated. SFE-M-treated mice developed less severe arthritis (Figure 6.3). Both redness and swelling of joints were induced in the control CAIA group, but those arthritic symptoms were significantly attenuated in SFE-M-treated group (100 mg/kg). Histopathological examinations also indicated that SFE-M treatment reduced synovial hyperplasia and the infiltration of inflammatory cells in the joint space (Figure 6.3). Mean histophathological arthritic score of CAIA-group, SFE-M-treated group, and SFE-W-treated group were 2.33 ± 0.82, 0.00 ± 0.00, 1.00 ± 0.89, respectively (Table 6.1 and Figure 6.4). The weight of mice was reduced from days 3 through 6 in all CAIA-induced groups except the corn oil group (Figure 6.5).

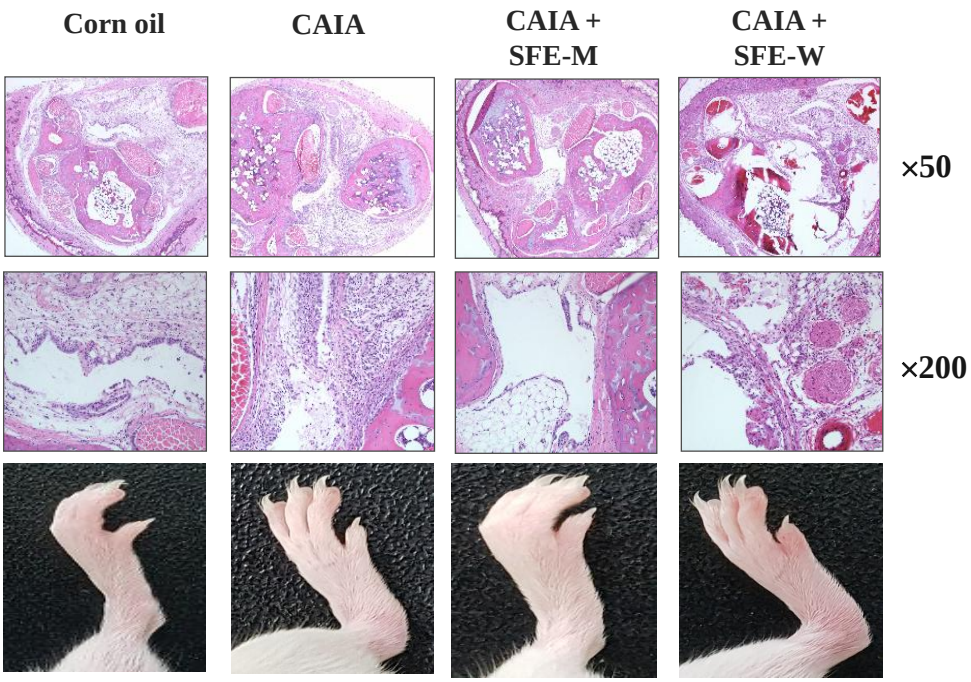

Figure 6.3. Image of representative microscopic features of knee joint and mice joint. Samples were treated with a concentration of 100 mg/kg. SFE-M and SFE-W were administered via oral gavage once per day for 4 days.

Table 6.1. Histopathological scores of the groups

Organ	Group		Corn oil	CAIA	CAIA + SFE-M	CAIA + SFE-W
Ankle joint	-Inflammation	-	6	0	6	2
		±	0	1	0	2
		+	0	2	0	2
		++	0	3	0	0
		+++	0	0	0	0

Grade- -: normal, ±: minimal, +: mild, ++: moderate, +++: marked

No. of examined: 6/group

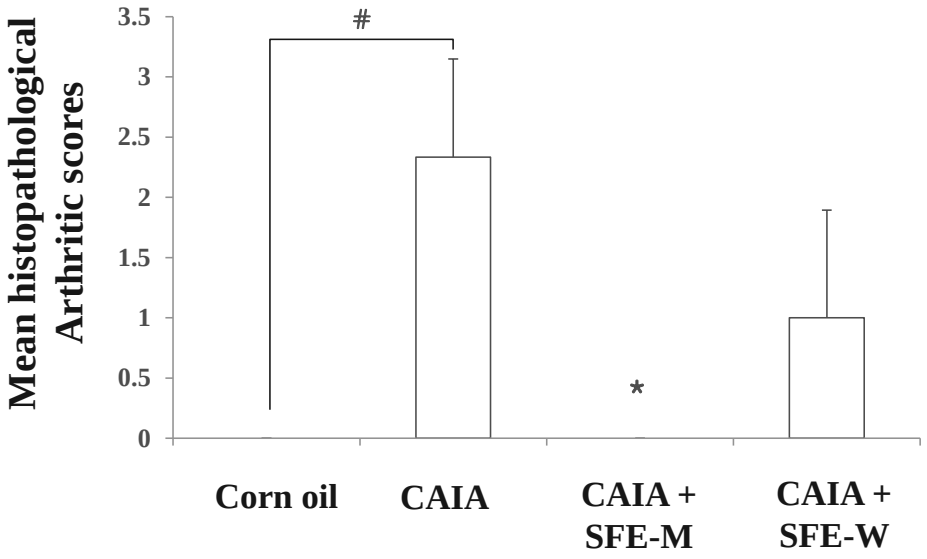

Figure 6.4. Effect of SFE-M and SFE-W on mean histopathological arthritis score in CAIA mice. Samples were treated with a concentration of 100 mg/kg. Results were expressed as a score (means ± SD) of six mice. $^{\#}p<0.05$ vs. Corn oil-group and $*p<0.05$ vs. CAIA-group. Every joint was scored as follows: 0, normal; 1, minimal; 2, mild; 3, moderate; and 4, marked.

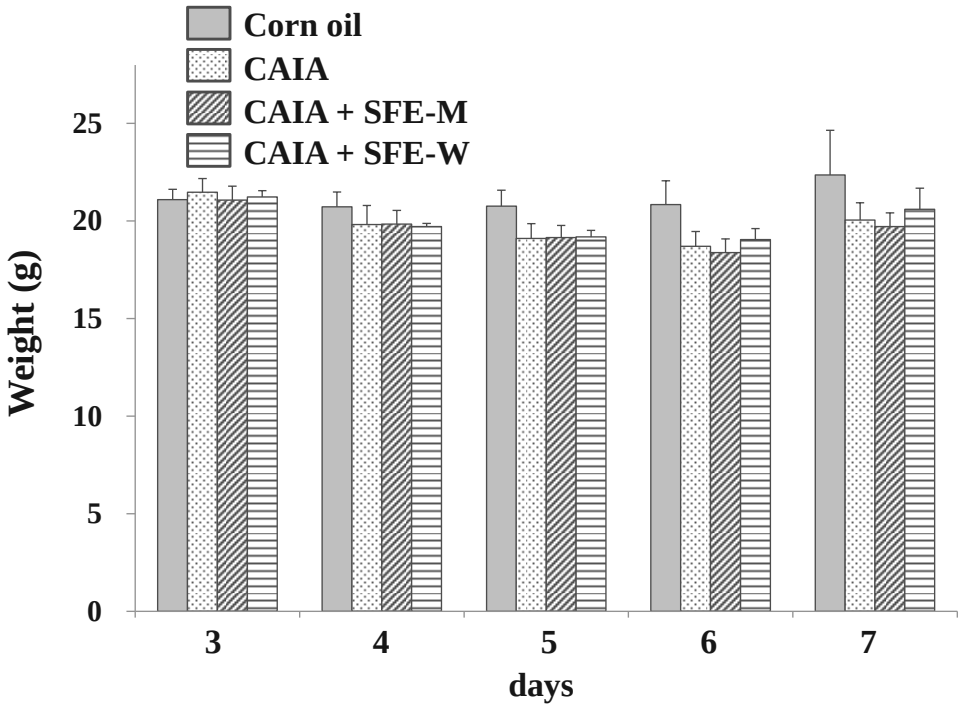

Figure 6.5. Effect of SFE-M and SFE-W on weight in CAIA mice. Samples were treated with a concentration of 100 mg/kg. Results were expressed as a score (means ± SD) of six mice.

4.3. Effect of SFE-W and SFE-M treatment on paw volume in CAIA model

To evaluate whether SFE-W and SFE-M had an effect on the progression of RA in CAIA model, male Balb/c mice were provided with the corn oil with or without SFE-M and SFE-W from day 3 through day 6. CAIA group showed a significant increase in the paw volume at the days 5, 6, and 7 (17.3%, 14.4% and 20.7%, respectively) compared to the corn oil group (Figure 6.6). Paw volume was significantly lower in SFE-M-treated group compared with the control CAIA group at days 5, 6, and 7 (17.4%, 22.8%, and 22.4%, respectively). Therefore, oral administration of SFE-M seems to attenuate the increase of paw volume in CAIA model. However, SFE-M treatment didn't result in significant difference in paw volume compared with the control CAIA group.

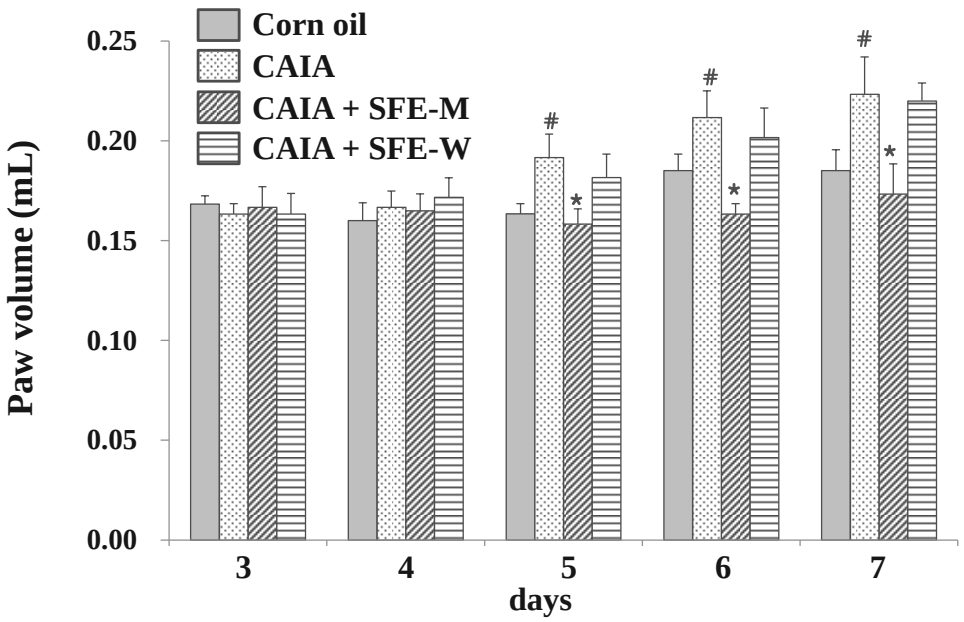

Figure 6.6. Effect of SFE-M and SFE-W on paw volume in CAIA mice. Samples were treated with a concentration of 100 mg/kg. Paw volume were measured using a Digital Plethysmometer every day after LPS injection and oral administration of treatments. The average volume of both hind legs were used. Data are presented as means ± SD (n = 6). $^{\#}p<0.05$ vs. Corn oil-group and $^{*}p<0.05$ vs. CAIA-group.

4.4. Effect of SFE-W and SFE-M treatment on paw thickness in CAIA model

To evaluate whether SFE-W and SFE-M had an effect on the progression of RA in CAIA model, paw thickness was measured by digital caliper. CAIA group showed a significant increase in the paw thickness at days 6 and 7 (12.5% and 7.8%, respectively) compared to the corn oil group (Figure 6.7). Paw thickness was significantly lower in SFE-M-treated group compared with the control CAIA group at days 5, 6 and 7 (4.7%, 15.3%, and 15.9%, respectively). Therefore, oral administration of SFE-M seems to attenuate the increase of paw thickness in CAIA model. However, SFE-W-treatment didn't result in significant difference in paw thickness compared with the control CAIA group.

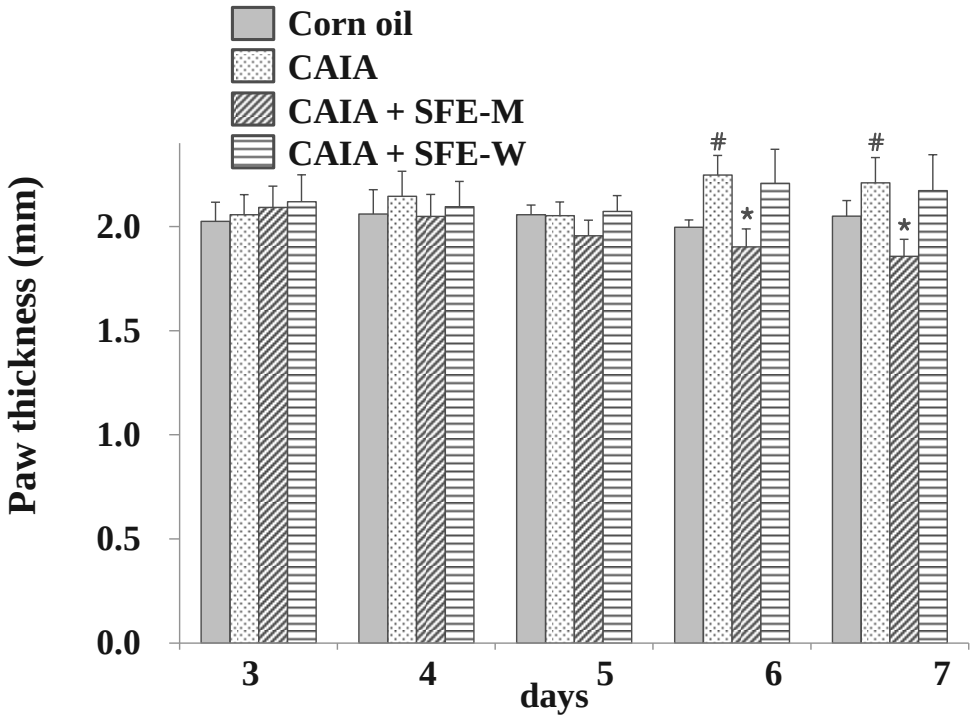

Figure 6.7. Effect of SFE-M and SFE-W on paw thickness in CAIA mice. Samples were treated with a concentration of 100 mg/kg. Paw thickness was measured using a digital caliper every day after LPS injection and oral administration of treatments. The average thickness of both hind legs was used. Data are presented as means ± SD (n = 6). $^{\#}p<0.05$ vs. Corn oil-group and $^{*}p<0.05$ vs. CAIA-group.

4.5. Effect of SFE-M and SFE-W treatment on arthritic score in CAIA model

Arthritic score was measured blindly by three persons to further determine whether SFE-M and SFE-W suppressed RA progression in CAIA model. CAIA group showed a significant increase in arthritic score from days 4 through 7 compared with the corn oil group (Figure 6.8). The corn oil group didn't show any redness and swelling of joints until day 7, however the control CAIA group showed arthritic symptoms in all joints from days 4 through 7. Those arthritic symptoms were significantly attenuated in SFE-M-treated group form days 4 through 7. Therefore, oral administration of SFE-M seems to alleviate the arthritic symptoms such as redness and swelling of joints in CAIA model. However, SFE-W-treatment didn't result in significant difference in arthritic score compared with the control CAIA group.

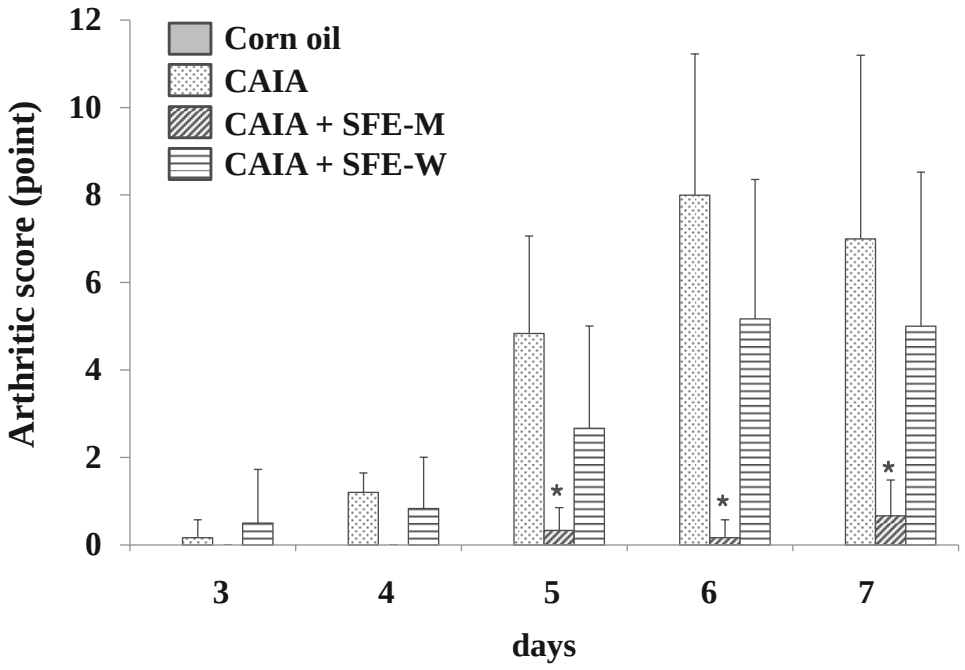

Figure 6.8. Effect of SFE-M and SFE-W on arthritic score in CAIA mice. Samples were treated with a concentration of 100 mg/kg. Arthritic score was done blindly by using a system based on the number of inflamed joints in front and hind paws, inflammation being defined by swelling and redness at the scale from 0 (no redness and swelling) to 3 (severe swelling with joint rigidity or deformity; maximal score for four paws, 12). Data are presented as means ± SD (n = 6). *p<0.05 vs. CAIA-group.

4.6. Effect of SFE-M and SFE-W treatment on blood cell population in CAIA model

Neutrophil-to-lymphocyte ratio (NLR) is the proportion of absolute neutrophil count to lymphocyte count in whole blood cells. It has been widely accepted that NLR is a useful marker for the evaluation of inflammatory activity in chronic inflammatory diseases such as ulcerative colitis (Torun *et al*., 2012), prostate cancer (Yin *et al*., 2016), and RA (Mercan *et al*., 2015). To further determine whether SFE-M and SFE-W affects blood cell population in CAIA model, NLR was measured from whole blood sample. CAIA group showed a significant increase in NLR at 7 day compared with the corn oil group (Figure 6.9). NLR level was lower in SFE-M-treated group compared with the control CAIA group by 37%. However, SFE-W-treatment didn’t result in significant difference in NLR levels compared with the control CAIA group.

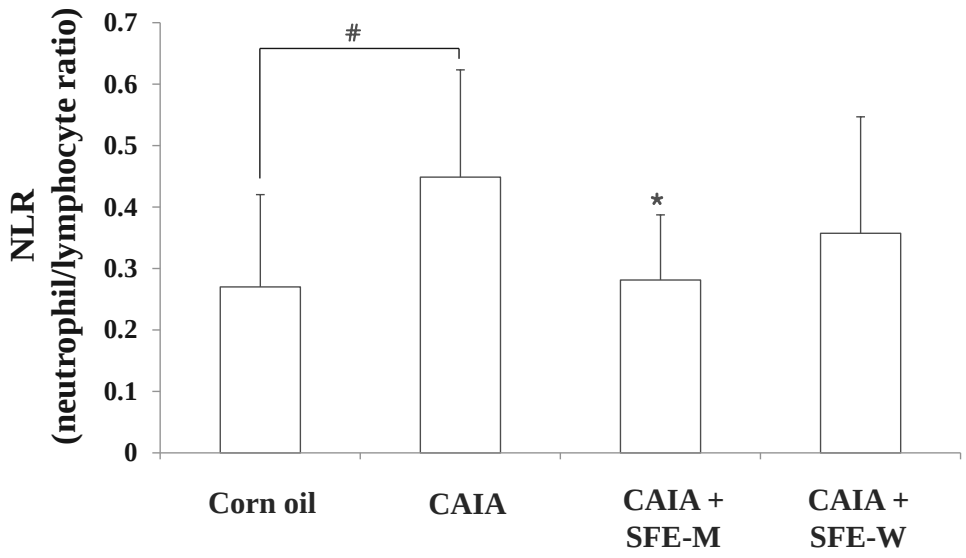

Figure 6.9. Effect of SFE-M and SFE-W on neutrophil-to-lymphocyte ratio in CAIA mice. Samples were treated with a concentration of 100 mg/Kg. Whole blood samples were collected by cardiac puncture. Data are presented as means ± SD (n = 6). $^{\#}p<0.05$ vs. Corn oil-group and $^{*}p<0.05$ vs. CAIA-group.

5. Discussion

In the present study, the anti-arthritic effect of the extract from radiation mutant *P. frutescens* var. *crispa* prepared by supercritical carbon dioxide extraction (SFE-M) on the development of arthritis in CAIA model was investigated. The efficacy of SFE-M was compared with supercritical carbon dioxide extract of wild type (SFE-W). The treatment with SFE-M alleviated the infiltration of immune cells into joint synovium, paw edema, arthritic score, and NLR levels. The treatment with SFE-W didn't affect to the development of arthritis. In a previous report, SFE-M had higher anti-inflammatory activities than SFE-W in LPS-induced RAW264.7 cells (Park *et al*., 2016). The enhanced anti-inflammatory activities of SFE-M seemed to be due to the increase of isoegomaketone (IK) content about 7 times compared with SFE-W (Park *et al*., 2016). Like the preceding study, SFE-M was more effective on delaying the onset of arthritis in CAIA model compared with SFE-W.

Radiation-induced mutants have been extensively studied and utilized in mutation breeding after discovering that X ray can induce mutations in Drosophila (Muller, 1927) and barley (Stadler, 1928). Later, it was found that ionizing radiation causes DNA damage is a major contributing factor to mutations (Sachs *et al*., 2000). Radiation-induced mutation breeding was

focus on the crop improvement (Sangsiri C *et al*., 2005), enhancing resistance to abiotic and biotic stresses (Cho *et al*., 2012), and development of new flower varieties (Kim *et al*., 2015). However, there are no reports about increasing functional metabolites in radiation-induced plant mutants. This study carries an important meaning in that it contributes to enhancing therapeutic possibility for radiation-induced plant mutants by increasing functional phytochemical contents. One of the biggest problem in the investigation for functional food or phytomedicine using natural resources is that natural resources usually contain very small amount of functional components. In this study, possibility for selection of new resources contained higher functional constituents from radiation-induced plant mutants was confirmed. Radiation-induced mutant *P. frutescens* var. *crispa* used in this study was acquired using gamma rays. It contained about 7 times more IK than wild type species. IK is biosynthesized from egomaketone (EK), and this reaction is inhibited by gene *I* in *P. frutescens* (Nishizawa *et al*., 1989). Therefore, we guess gene *I* was affected by gamma radiation and consequently had lower activity compared with wild type. The correlation between gene variation and changing IK content is currently being studied.

Rheumatoid arthritis (RA) is a systemic autoimmune disease in which chronic joint inflammation leads to cartilage destruction and bone erosion

(Scott *et al*., 2010). Generally, the use of standard drugs in RA caused numerous side effects (Matucci *et al*., 2016; McAlindon *et al*., 2014; Cabral *et al*., 2016). In these days, the renewed interest in medicines of botanical origin, which lack severe side effects and have millennia-proven efficacy, is growing (Umar *et al*., 2014). These remedies maybe have a beneficial effect not only on the symptoms but also on the development of the disease (Akhtar *et al*., 2011). There are many reports about anti-arthritic medicinal plants, which have been tested in animal and human studies: *Arnica montana* (Sharma *et al*., 2016), *Boswellia* spp. (Umar *et al*., 2014); *Curcuma* spp. (Kamarudin *et al,* 2012); *Equisetum arvense* (Farinon *et al*., 2014); *Harpagophytum procumbens* (Lanhers *et al*., 1992); and *Salix* spp.; *Sesamum indicum* (Sotnikova *et al*., 2009). Radiation-induced mutant *P. frutescens* var. *crispa* used in this study has higher anti-inflammatory activities and its extract prepared by supercritical carbon dioxide extraction also has a good potential as anti-arthritic medicinal plant source. To our knowledge, this is the first report that describes the radiation-induced plant mutants containing higher anti-arthritic properties compared to wild-type.

VII. Overall Discussion

In this thesis, isoegomaketone (IK) isolated from radiation mutant *P. frutescens* var. *crispa* showed anti-inflammatory properties due to the induction of heme oxygenase-1 (HO-1) via ROS/p38 MAPK/Nrf2 pathway in RAW264.7 cells. Recent studies have demonstrated that HO-1 induction was mediated by the activation of PI3K, PKC, and p38 MAPK (Shih *et al*., 2011; Lee *et al*., 2012; Rojo *et al*., 2006). According to the experiments using respective specific inhibitors, IK-induced HO-1 expression was suppressed only by p38 MAPK specific inhibitor. Although IK-induced ROS production was not measured in RAW264.7 cells, the relation between ROS and IK-induced HO-1 expression was confirmed using radical scavengers such as NAC and GSH. In addition, IK treatment palpably reduced clinical signs and symptoms of rheumatoid arthritis in collagen antibody-induced arthritis (CAIA) animal model. IK treatment showed more effective anti-arthritic activity compared with apigenin (API), a positive control, in mean histopathological score and arthritic score. Even if CAIA model characterized by macrophage and inflammatory cell infiltration is not associated with T and B cell response (Nandakumar *et al*., 2004) over collagen-induced arthritis (CIA) model, it include important features of human RA, such as inflammatory synovitis, formation of pannus (an

aggressive fibrovascular tissue that invades the joint), cartilage degradation, and bone remodeling (Caplazi *et al*., 2015).

Because application of IK itself as a functional food could be problematic, it is necessary to develop the methods to acquire extracts from *P. frutescens* var. *crispa* with high IK content and confirm the efficacy of the extract. Before investigating anti-arthritic effect using extracts, the optimal extraction method for higher IK content from *P. frutescens* var. *crispa* should be set up. Usually, water and ethanol extraction method is implemented for food processing. However, those are not suitable for acquiring extracts containing higher IK content because of hydrophobicity of IK. For this reason, the extracts were obtained from radiation mutant *P. frutescens* var. *crispa* using supercritical carbon dioxide extraction (SC-CO_2) method. The extracts acquired by SC-CO_2 method from radiation mutant *P. frutescens* var. *crispa* (SFE-M) included five times higher IK content than the extracts obtained by ethanol extraction method. And the elevated IK content of extracts actually had effect on anti-inflammatory activity in LPS-stimulated RAW264.7 cells. Furthermore, the treatment with SFE-M alleviated the infiltration of immune cells into joint synovium, paw edema, arthritic score, and NLR levels in CAIA animal model. 100 mg SFE-M contained about 6.38 mg IK. However, SFE-M treatment (100 mg/kg) showed more effective anti-arthritic activity

compared with IK treatment (10 mg/kg) in CAIA animal model. This probably due to other ingredients contained in the extracts except IK.

Radiation-induced mutation breeding was focused on the crop improvement (Sangsiri C *et al*., 2005), enhancing resistance to abiotic and biotic stresses (Cho *et al*., 2012), and development of new flower varieties (Kim *et al*., 2015). However, there are no reports about increasing functional metabolites in radiation-induced plant mutants. This study carries an important meaning in that it contributes to enhancing therapeutic possibility for radiation mutant resources comparing to previous studies that mainly concentrate on a higher production yield and climate change response. One of the biggest problem in the investigation for functional food or phytomedicine using natural resources is that natural resources usually contain very small amount of functional components. However, one advantage of using radiation mutant resource is that new resources containing higher functional constituents can be selected like radiation mutant *P. frutescens* var. *crispa* used in this study. Recently, ICT (information and communication technology)-based technology was applied and utilized in plant breeding, but it cannot be connected with metabolites until now. If this problem can be solved somehow, the potential value of radiation mutant resources is expected to increase.

Korea is now becoming aging society rapidly, which suggests that the number of patients with aging-associated diseases such as Alzheimer's disease, metabolic disease, and arthritis can be increasing. Rheumatoid arthritis (RA) and Osteoarthritis (OA) are common arthritis in adults, and leading causes of disability. In Korea, the prevalence of RA was decreased from 0.74% at 2011 to 0.68% at 2014. On the other hand, that of OA was increased from 7.96% at 2011 to 8.75% at 2014 (Moon, 2016). Annual direct medical costs per patient tended to increase in both RA and OA, but rate of increase was greater in RA. Korea relies mostly on imports for functional health ingredient for arthritis. New Zealand green lipped mussel oil is a typical example. Therefore, development of functional food or phytomedicine using domestic resources could contribute to alleviation of economic burden associated with several diseases. Radiation mutant *P. frutescens* var. *crispa* may have potential for giving a good example of domestic resources for person with mild arthritis.

References

Ahloowalia B, and Maluszynski M (2001) Induced mutations- a new paradigm in plant breeding. *Euphyutica* **118**: 167−173

Ahmed S, Rahman A, Hasnain A, Lalonde M, Goldberg VM, and Haqqi TM (2002) Green tea polyphenol epigallocatechin-3-gallate inhibits the IL-1 beta-induced activity and expression of cyclooxygenase-2 and nitric oxide synthase-2 in human chondrocytes. *Free Radic. Biol. Med.* **33**: 1097−1105

Akhtar N, Miller MJ, and Haqqi TM (2011) Effect of a Herbal-Leucine mix on the IL-1β-induced cartilage degradation and inflammatory gene expression in human chondrocytes. *BMC Complement. Altern. Med.* **11**: 66

Alam J, and Cook JL (2003) Transcriptional regulation of the heme oxygenase-1 gene via the stress response element pathway. *Curr. Pharm. Des.* **9**: 2499−2511

Banno N, Akihisa T, Tokuda H, Yasukawa K, Higashihara H, Ukiya M, Watanabe K, Kimura Y, Hasegawa J, and Nishino H (2004) Triterpene acids from the leaves of Perilla frutescens and their anti-inflammatory and anti-tumor-promoting effects. *Biosci. Biotechnol. Biochem.* **68**: 85–90

Bardon S, Foussard V, Fournel S, and Loubat A (2002) Monoterpenes inhibit proliferation of human colon cancer cells by modulating cell cycle-related protein expression. *Cancer Lett.* **181**: 187−194

Beckmann J, Dittmann N, Schütz I, Klein J, and Lips KS (2016) Effect of M3 muscarinic acetylcholine receptor deficiency on collagen antibody-induced arthritis. *Arthritis Res. Ther.* **18**: 17

Brochers AT, Hackman RM, Keen CL, Stern JS, and Gershwin ME (1997) Complementary medicine: a riview of immunomodulatory effects of Chinese herbal medicines. *Am. J. Clin. Nutr.* **66**: 1303−1312

Cabral VP, Andrade CA, Passos SR, Martins MF, and Hokerberg YH (2016) Severe infection in patients with rheumatoid arthritis taking anakinra, rituximab, or abatacept: A systematic review of observational studies. *Rev. Bras. Reumatol.* **56**: 543−550

Caplazi P, Baca M, Barck K, Carano RAD, DeVoss J, Lee WP, Bolon B, and Diehl L. (2015) Mouse models of rheumatoid arthritis. *Vet. Pathol.* **52**: 819−826

Chen CY, Leu YL, Fang Y, Lin CF, Kuo LM, Sung WC, Tsai YF, Chung PJ, Lee MC, Kuo YT, Yang HW, and Hwang TL (2015a) Anti-inflammatory effects of Perilla frutescens in activated human neutrophils through two independent pathways: Src family kinases and calcium. *Sci. Rep.* **5**: 18204

Chen ML, Wu CH, Hung LS, and Lin BF (2015b) Ethanol extract of Perilla frutescens suppresses allergen-specific Th1 respnoses and alleviates airway inflammation and hyperreactivtiy in ovalbumin-sensitized murine model of asthma. *Evid. Based Complement. Altern. Med.* **2015**: 324265

Chen T, Yuan F, Wang H, Tian Y, He L, Shao Y, Li N, and Liu Z (2016) Perilla oil supplementation ameliorates high-fat/high-cholesterol diet induced nonalcoholic fatty liver disease in rats via enhanced fecal cholesterol and bile acid excretion. *BioMed. Res. Int.* **2016**: 2384561

Cho BO, Jin CH, Park YD, Ryu HW, Byun MW, Seo KI, and Jeong IY (2011a) Isoegomaketone induces apoptosis through caspase-dependent and caspase-independent pathways in human DLD1 cells. *Biosci. Biotechnol. Biochem.* **75**: 1306−1311

Cho BO, Park HY, Ryu HW, Jin CH, Choi DS, Kim DS, Lim ST, Seo KI, Byun MW, and Jeong IY (2011b) Protective effect of Perilla frutescens cv. Chookyoupjaso mutant water extract against oxidative injury in vitro and in vivo. *Food Sci. Biotechnol.* **20**: 1705−1711

Cho HY, Hwang SG, Kim DS, and Jang CS. (2012) Genome-wide transcriptome analysis of rice genes responsive to chilling stress. *Can. J. Plant Sci.* **92**: 447−460

Cho YG, Cho ML, Min SY, and Kim HY (2007) Type II collagen autoimmunity in a mouse model of human rheumatoid arthritis. *Autoimmun. Rev.* **7**: 65−70

Choi WH, Um MY, Ahn JY, Kim SR, Kang MH, and Ha TY (2004) Acetylcholinesterase inhibitory activity and protective effect against cytotoxicity of perilla seed methanol extract. *Kor. J. Food Sci. Technol*. **36**: 1026−1031 (in Korean)

Chung SJ, Kim TY, Kwon YJ, Park YB, Lee SK, and Park MC (2010) Gallic acid diminishes cellular proliferation and pro-inflammatory gene expressions in fibroblast like synoviocytes from patients with rheumatoid arthritis. *Arthritis Rheum*. **62**:27

Cordova KN, Willis VC, Haskins K, and Holers VM (2013) A citrullinated fibrinogen-specific T cell line enhances autoimmune arthritis in a mouse model of rheumatoid arthritis. *J. Immunol*. **190**: 1457−1465

Donahue K, Gartlehner G, and Jonas D (2008) Systematic review: comparative effectiveness and harms of disease-modifying medications for rheumatoid arthritis. *Ann. Intern. Med.* **148**: 124−134

Dragos D, Gilca M, Gaman L, Vlad A, Iosif L, Stoian I, and Lupescu O (2017) Phytomedicine in joint disorders. *Nutrients* **9**: 70

Elegbede JA, Flores R, and Wang RC (2003) Perillyl alcohol and Perillaldehyde induced cell cycle arrest and cell deaths in BroTo and A549 cells cultured in vitro. *Life Sci.* **73**: 2831−2840

Farinon M, Lora PS, Francescato LN, Bassani VL, Henriques AT, Xavier RM, and de Oliveira PG (2013) Effect of aqueous extract of giant horsetail (Equisetum giganteum L.) in antigen-induced arthritis. *Open Rheumatol. J.* **7**: 129−133

Funk JL, Oyarzo JN, Frye JB, Chen G, Lantz RC, Jolad SD, Sólyom AM, and Timmermann BN (2006) Turmeric extracts containing curcuminoids prevent experimental rheumatoid arthritis. *J. Nat. Prod.* **69**: 351−355

Gabunia K, Ellison SP, Singh H, Datta P, Kelemen SE, Rizzo V, and Autieri MV (2012) Interleukin-19 (IL-19) induces heme oxygenase-1 (HO-1) expression and decreases reactive oxygen species in human vascular smooth muscle cells. *J. Biol. Chem.* **287**: 2477−2484

Gong Z, Yamazaki M, Sugiyama M, Tanaka Y, and Saito K (1997) Cloning and molecular analysis of structural genes involved in anthocyanin biosynthesis and expressed in a forma-specific manner in Perilla frutescens. *Plant Mol. Biol.* **35**: 915−927

Green RE, Cornell SJ, Scharlemann JP, and Balmford A (2005) Farming and the fate of wild nature. *Science* **307**: 550−555

Guan W, Li S, Yan R, Tang S, and Quan C (2007) Comparison of essential oil of clove buds extracted with supercritical carbon dioxide and other three traditional extraction methods. *Food Chem.* **101**: 1558−1564

Han DS, Chung BH, Yoo HG, Kim YO, and Baek SH (1994) Studies on the cytotoxicity and antitumor activitiy of Perilla frutescens. *Kor. J. Pharm.* **25**: 249−257

Haqqi TM, Anthony DD, Gupta S, Ahmad N, Lee MS, Kumar GK, and Mukhtar H (1999) Prevention of collagen-induced arthritis in mice by a polyphenolic fraction from green tea. *Proc. Natl. Acad. Sci. USA* **96**: 4524−4529

Holmdahl R, Rubin K, Klareskog L, Larsson E, and Wigzell H (1986) Characterization of the antibody response in mice with type II collagen-induced arthritis, using monoclonal anti-type II collagen antibodies. *Arhritis Rheum*. **29**: 400−410

Huang N, Hauck C, Yum MY, Rizshsky L, Widrlechner MP, McCoy JA, Murphy PA, Dixon PM, Nikolau BJ, and Birt DF (2009) Rosmarinic acid in *Prunella vulgaris* ethanol extract inhibits LPS-induced prostaglandin E2 and nitric oxide in RAW264.7 mouse macrophage. *J. Agric. Food Chem.* **25**: 10579−10589

Hwang JE, Ahn JW, Kwon SJ, Kim JB, Kim SH, Kang SY, and Kim DS (2014) Selection and molecular characterization of a high tocopherol accumulation rice mutant line induced by gamma irradiation. *Mol. Biol. Rep.* **41**: 7671−7682

Imboden JB (2009) The immunopathogenesis of rheumatoid arthritis. *Annu. Rev. Pathol.* **4**: 417−434

Jin CH, Lee HJ, Park YD, Choi DS, Kim DS, Kang SY, Seo KI, and Jeong IY (2010) Isoegomaketone inhibits lipopolysaccharide-induced nitric oxide production in RAW264.7 macrophages through the heme oxygenase-1 induction and inhibition of the interferon-β-STAT-1 pathway. J. Agric. Food Chem. 58: 860−867

Jiang X, Qu Q, Li M, Miao S, Li X, and Cai W (2014) Horsetail mixture on rheumatoid arthritis and its regulation of TNF-α and IL-10. *Pak. J. Pharm. Sci.* **27**: 2019−2023

Jung DM, Yoon SH, and Jung MY (2012) Chemical properties and oxidative stability of perilla oils obtained from roasted perilla seeds as affected by extraction methods. *J. Food Sci.* **77**: C1249−1255

Kamarudin TA, Othman F, Mohd Ramli ES, Md Isa N, and Das S (2012) Protective effect of curcumin on experimentally induced arthritic rats: Detailed histopathological study of the joints and white blood cell count. *EXCLI J.* **11**: 226−236

Kang CG, Hah DS, Kim CH, Kim YH, Kim EK, and Kim JS (2011) Evaluation of antimicrobial activity of the methanol extracts from 8 traditional medicinal plants. *Toxicol. Re*. **27**: 31−36

Kaspar JW, Niture SK, and Jaiswal AK (2009) Nrf2:INrf2 (Keap1) signaling in oxidative stress. *Free Radic. Biol. Med.* **47**: 1304−1309

Keystone EC, Schorlemmer HU, Pope C, and Allison AC (1977) Zymosan-induced arthritis: a model of chronic proliferative arthritis following activation of the alternative pathway of complement. *Arthritis Rheum.* **20**: 1396−1401

Khan MS, Priyadarshini M, and Bano B (2009) Preventive effect of curcumin and quercetin against nitric oxide mediated modification of goat lung cystatin. *J. Agric. Food Chem.* **57**: 6055−6059

Kharkwal MC and Shu QY (2009) The role of induced mutations in world food security. In: Induced plant mutations in the genomics era. Proceeding of the International Joint FAO/IAEA Symp IAEA, Vienna. 33−38

Kidd BA, Ho PP, Sharpe O, Zhao X, Tomooka BH, Kanter JL, Steinman L, and Robinson WH (2008) Epitope spreading to citrullinated antigens in mouse models of autoimmune arthritis and demyelination. *Arthritis Res. Ther.* **10**: R119

Kim DH, Kim YC, and Choi UK (2011) Optimization of antibacterial activity of Perilla frutescens var. acuta Leaf against Staphylococcus aureus using evolutionary operation factorial design technique. *Int. J. Mol. Sci.* **12**: 2395–2407

Kim IH, Kim MH, Kim YE, and Lee YC (1998) Oxidative stability and extraction of perilla seed oil with supercritical carbon dioxide. *Food Sci. Biotech.* **7**: 177−180

Kim JS, and Jobin C (2005) The flavonoid luteolin prevents lipopolysaccharide-induced NF-κB signaling and gene expression by blocking IκB kinase activity in intestinal epithelial cells and bone-marrow derived dendritic cells. *Immunology* **115**: 375−387

Kim JY, Kim JS, Jung CS, Jin CB, and Ryu JH (2007). Inhibitory activity of nitric oxide synthase and peroxynitrite scavenging activity of extracts of Perilla frutescens. *Kor. J. Pharm.* **38**: 1−24

Kim MJ, Kadayat T, Kim DE, Lee ES, and Park PH (2014) TI-I-174, a synthetic chalcone derivative, suppresses nitric oxide production in murine macrophages via heme oxygenase-1 induction and inhibition of AP-1. *Biomol. Ther.* **22**: 390−399

Kim YS, Kim SH, Sung SY, Kim DS, Kim JB, Jo YD, and Kang SY. (2015) Genetic relationships among diverse spray- and standard-type Chrysanthemum varieties and their derived radio-mutants determined using AFLPs. *Hortic. Environ. Biotechnol.* **56**: 498−505

Kwak YE, and Ju JH (2015) Inhibitory activities of Perilla frutescens britton leaf extract against the growth, migration, and adhesion of human cancer cells. *Nutr. Res. Pract.* **9**: 11−16

Kwon SJ, Lee JH, Moon KD, Jeong IY, Ahn DU, Lee MK, and Seo KI (2014a) Induction of apoptosis by isoegomaketone from Perilla frutescens L. in B16 melanoma cells is mediated through ROS generation and mitochondrial-dependent, -independent pathway. *Food Chem. Toxicol.* **65**: 97−104

Kwon SJ, Lee JH, Moon KD, Jeong IY, Yee ST, Lee MK, and Seo KI (2014b) Isoegomaketone induced apoptosis in SK-MEL-2 human melanoma cells through mitochondrial apoptotic pathway via activating the PI3K/Akt pathway. *Int. J. Oncol.* **45**: 1969−1976

Lanhers M, Fleurentin J, Mortier F, and Al E (1992) Antiinflammatory and analgesic effects of an aqueous extract of Harpagophytoum procumbens. *Planta Med.* **58**: 117−123

Lee AY, Wu TT, Hwang BR, Lee JM, Lee MH, Lee SH, and Cho EJ (2016) The neuro-protective effect of the methanolic extract of Perilla frutescens var. japonica and rosmarinic acid against H2O2-induced oxidative stress in C6 glial cells. *Biomol. Ther*. **24**: 338–345

Lee HA, and Han JS (2012) Anti-inflammatory effect of Perilla frutescens (L.) Britton var. frutescens extract in LPS-stimulated RAW 264.7 macrophage. *Prev. Nutr. Food Sci.* **17**: 109–115

Lee JH, Zhou HY, Cho SY, Kim YS, Lee YS, and Jeong CS (2007) Anti-inflammatory mechanisms of apigenin: inhibition of cyclooxygenase-2 expression, adhesion of monocytes to human umblilical vein endothelial cells, and expression of cellular adhesion molecules. *Arch. Pharm. Res.* **30**: 1318−1327

Lee JH, Cho HD, Jeong IY, Lee MK, and Seo KI (2014) Sensitization of tumor necrosis factor-related apoptosis-inducing ligand (TRAIL)-resistant primary prostate cancer cells by isoegomaketone form *Perilla frutescens*. *J. Nat. Prod.* **77**: 2438−2443

Lee KJ, Hwang JE, Velusamy V, Ha BK, Kim JB, Kim SH, Ahn JW, Kang SY, and Kim DS (2014) Selection and molecular characterization of a lipoxygenase-free soybean mutant line induced by gamma irradiation. *Theor. Appl. Genet*. **127**: 2405−2413

Lee SE, Jeong SI, Kim GD, Yang H, and Park CS (2011) Upregulation of heme oxygenase-1 as an adaptive mechanism for protection against crotonaldehyde in human umbilical vein endothelial cells. *Toxicol. Lett.* **201**: 240−248

Lee SE, Yang H, Jeong SI, Jin YH, Park CS, and Park YS (2012) Induction of heme oxygenase-1 inhibits cell death in crotonaldehyde-stimulated HepG2 cells via the PKC-δ-p38-Nrf2 pathway. *PLoS One* **7**: e41676

Lee YI, Kim JK, Lee IS, and Kim DS (1999) Variation of leaf flavor components in progenies of Perilla mutants induced by gamma ray. *Korea J. Breed.* **31**: 114−118 (in Korean)

Leonard SS, Xia C, Jiang BH, Stinefelt B, Klandorf H, Harris GK, and Shi X (2003) Resveratrol scavenges reactive oxygen species and effects radical-induced cellular responses. *Biochem. Biophys. Res. Commun.* **309**: 1017−1026

Li X, Han Y, Zhou Q, Jie H, He Y, Han J, He J, Jing Y, and Sun E (2016) Apigenin, a potent suppressor of dendritic cell maturation and migration, protects against collagen-induced arthritis. *J. Cell. Mol. Med.* **20**: 170−180

Lim HJ, Woo KW, Lee KR, Lee SK, and Kim HP (2014) Inhibition of proinflammatory cytokine generation in lung inflammation by the leaves of Perilla frutescens and its constituents. *Biomol. Ther.* **22**: 62−67

Liu JY, Chen YC, Lin CH, and Kao SH (2013) Perilla frutescens leaf extract inhibits mite major allergen Der p 2-induced gene expression of pro-allergic and pro-inflammatory cytokines in human bronchial epithelial cell BEAS-2B. *PLoS One* **8**: e77458

Liu XM, Peyton KJ, Shebib AR, Wang H, and Durante W (2011) Compound C stimulates heme oxygenase-1 gene expression via the Nrf2-ARE pathway to preserve human endotherial cell survival. *Biochem. Pharmacol.* **82**: 371−379

Masutani H, Otsuki R, and Yamaguchi Y (2009) Fragrant unsaturated aldehydes elicit activation of the keap1/Nrf2 system leading to the upregulation of thioredoxin expression and protection against oxidative stress. *Antioxid. Redox Signal.* **11**: 949−962

Matucci A, Cammelli D, Cantini F, Goletti D, Marino V, Milano GM, Scarpa R, Tocci G, Maggi E, and Vultaggio A (2016) Influence of anti-TNF immunogenicity on safety in rheumatic disease: A narrative review. *Expert Opin. Drug Saf.* **15**: 3−10

Mauri C, Williams RO, Walmsley M, and Feldmann M (1996) Relationship between Th1/Th2 cytokine patterns and the arthritogenic response in collagen-induced arthritis. *Eur. J. Immunol.* **26**: 1511−1518

McAlindon TE, Bannuru RR, Sullivan MC, Arden NK, Berenbaum F, Bierma-Zeinstra SM, Hawker GA, Henrotin Y, Hunter DJ, and Kawaguch H (2014) OARSI guidelines for the non-surgical management of knee osteoarthritis. *Osteroarthr. Cartil.* **22**: 363−388

McNally SJ, Harrison EM, Ross JA, Garden OJ, and Wiqmore SJ (2007) Curcumin induces heme oxygenase 1 through generation of reactive oxygen species, p38 activation and phosphatase inhibition. *Int. J. Mol. Med.* **19**: 165−172

Mercan R, Bitik B, Tufan A, Bozbulut UB, Atas N, Ozturk AO, Haznedaroglu S., and Goker B (2016) The association between neutrophil/lymphocyte ratio and disease activity in rheumatoid arthritis and ankylosing spondylitis. *J. Clin. Lab. Anal.* **30**: 597−601

Moon KW (2016) AB1016 The change of prevalence of rheumatoid arthritis and osteoarthritis in Korea between 2011 to 2014. *Ann. Rheum. Dis.* **75:** Issue suppl2

Muller HJ (1927) Artificial transmutation of the gene. *Science* **66**: 84−87

Nam BM, Lee SY, Kim JB, Kang SY and Jin CH. (2016). Simultaneous determination of isoegomaketone and perillaketone in *Perilla frutescens* (L.) Britton Leaves by HPLC-DAD. *Kor. J. Pharmacogn.* **47:** 79−83.

Nandakumar KS, Backlund J, Vestberg M, and Holmdahl R (2004) Collagen type II (CII)-specific antibodies induce arthritis in the absence of T or B cells but the arthritis progression in enhanced by CII-reactive T cells. *Arthritis Res. Ther*. **6**:R544−R550

Nandakumar KS, Svensson L, and Holmdahl R. (2003) Collagen type II-specific monoclonal antibody-induced arthritis in mice: description of the disease and the influence of age, sex, and genes. *Am. J. Pathol.* **163**: 1827−1837

Nakano M, Amano J, and Watanabe Y (2010) Morphological variation in Tricyrtis hirta plants regenerated from heavy ion beam-irradiated embryogenic calluses. *Plant Biotech.* **27**: 155−160

Nishizawa A, Hoda G, and Tabata M. (1989) Determination of final steps in biosynthesis of essential oil components in *Perilla frutescens*. *Planta Med.* **55**: 251−253

Oh HA, Park CS, Ahn HJ, Park YS, and Kim HM (2011) Effect of Perilla frutescens var. acuta Kudo and rosmarinic acid on allergic inflammatory reactions. *Exp. Biol. Med.* **236**: 99−106

Osakabe N, Yasuda A, and Natsume M (2002) Rosmarinic acid, a major polyphenolic component of Perilla frutescens, reduces lipopolysaccharide (LPS)-induced liver injury in D-galactosamine (D-GalN)-senstitized mice. *Free Radic. Biol. Med.* **33**: 798−806

Osakabe N, Yasuda A, Natsume M, and Yoshikawa T (2004) Rosmarinic acid inhibits epidermal inflammatory responses: anti-carcinogenic effect of Perilla frutescens extract in the murine two-stage skin model. *Carcinogenesis* **25**: 549−557

Otterbein LE, and Choi AM (2000) Heme oxygenase: colors of defense against cellular stress. *Am. J. Physiol. Lung Cell. Mol. Physiol.* **279**: 1029−1037

Paek JH, Shin KH, Kang YH, Lee JY, and Lim SS (2013) Rapid identification of aldose reductase inhibitory compounds from Perilla frutescens. *BioMed Res. Int.* **2013**: 679463

Park HC, So YK, Kim JB, Yuk HS, and Jin CH (2016) Comparison of anti-inflammatory activity of extracts with supercritical carbon dioxide from radiation mutant Perilla frutescens (L.) Britton and wild-type. *J. Radiat. Ind.* **10**: 97−104 (in Korean)

Park PH, Kim HS, Jin XY, Jin F, Hur J, Ko G, and Sohn DH (2009a) KB-34, a newly synthesized chalcone derivative, inhibits lipopolysaccharide-stimulated nitric oxide production in RAW264.7 macrophages via heme oxygenase-1 induction and blockade of activator protein-1. *Eur. J. Pharmacol.* **606**: 215−224

Park SH, Paek JH, Shin DK, Lee JY, Lim SS, and Kang YH (2015) Purple perilla extracts with alpha-asarone enhance cholesterol efflux from oxidized LDL-exposed macrophages. *Int. J. Mol. Med.* **35**: 957−965

Park YD, Kang MA, Lee HJ, Jin CH, Choi DS, Kim DS, Kang SY, Byun MW, and Jeong IY (2009b) Inhibition of an inducible nitric oxide synthase expression by a hexane extract from Perilla frutescens cv. Chookyoupjaso mutant induced by mutagenesis with gamma-ray. *J. Radiat. Ind.* **3**: 13−18 (in Korean)

Park YD, Jin CH, Choi DS, Byun MW, and Jeong IY (2011) Biological evaluation of isoegomaketone isolated from Perilla frutescens and its synthetic derivatives as anti-inflammatory agents. *Arch. Pharm. Res.* **34**: 1277−1282

Peng Y, Ye J, and Kong J (2005) Determination of phenolic compounds in Perilla frutescens L. by capillary electrophoresis with electrochemical detection. *J. Agric. Food Chem.* **53**: 8141−8147

Rennie K, Hughes J, Lang R, and Jebb S (2003) Nutritional management of rheumatoid arthritis: a review of the evidence. *J. Hum. Nutr. Dietet.* **16**:97−109

Rojo AI, Salina M, Salazar M, Takahashi S, Suske G, Calvo V, de Sagarra MR, and Cuadrado A (2006) Regulation of heme oxygenase-1 gene expression through the phosphatidylinositol 3-kinase/PKC-ζ pathway and Sp1. *Free Radic. Biol. Med.* **41**: 247−261

Roshak AK, Callahan JF, and Blake SM (2002) Small-molecule inhibitors of NF-κB for the treatment of inflammatory joint disease. *Curr. Opin. Pharmacol.* **2**: 316−321

Rowley MJ, Nandakumar KS, and Holmdahl R (2008) The role of collagen antibodies in mediating arthritis. *Mod. Rheumatol*. **18**: 429−441

Ruan RS (2002) Possible roles of nitric oxide in the physiology and pathophysiology of the mammalian cochlea. *Am. N. Y. Acad. Sci.* **962**: 260−274

Ryter SW, Alam J, and Choi AM (2006) Heme oxygenase-1/carbon monoxide: from basic science to therapeutic application. *Physiol. Rev.* **86**: 583−650

Sachs RK, Hlatky LR, and Trask BJ (2000) Radiation-produced chromosome aberrations. *Trends Genet.* **16**: 483−493

Sangsiri C, Sorajjapinun W, and Srinives P. (2005) Gamma radiation induced mutations in mungbean. *ScienceAsia* **31**, 251−255

Santos LL, Morand EF, Hutchinson P, Boyce NW, and Holdsworth SR (1997) Anti-neutrophil monoclonal antibody therapy inhibits the development of adjuvant arthritis. *Clin. Exp. Immunol*. **107**: 248−253

Sato Y, Shirasawa K, Takahashi Y, Nishimura M, and Nishio T (2006) Mutant selection from progeny of gamma-ray irradiated rice by DNA heteroduplex cleavage using Brassica petiole extract. *Breed Sci.* **56**: 179−183

Scott DL, Wolfe F, Huizinga TW (2010) Rheumatoid arthritis. *Lancet* **376**: 1094−108

Shao P, He J, Sun P, and Zhao P (2012) Analysis of conditions for microwave-assisted extraction of total water-soluble flavonoids from Perilla frutescens leaves. *J. Food Sci. Technol.* **49**: 66–73

Shakibaei M, Csaki C, Nebrich S, and Mobasheri A (2008) Resveratrol suppresses interleukin-1beta-induced inflammatory signaling and apoptosis in human articular chondrocytes: potential for use as a novel nutraceutical for the treatment of osteoarthritis. *Biochem. Pharmacol.* **76**: 1426−1439

Sharma S, Arif M, Nirala RK, Gupta R, and Thakur SC (2016) Cumulative therapeutic effects of phytochemicals in Arnica Montana flower extract alleviated collagen-induced arthritis: Inhibition of both pro-inflammatory mediators and oxidative stress. *J. Sci. Food Agric.* **96**: 1500−1510

Shih RH, Cheng SE, Hsiao LD, Kou YR, and Yang CM (2011) Cigarette smoke extract upregulates heme oxygenase-1 via PKC/NADPH oxidase/ROS/PDGFR/PI3K/Akt pathway in mouse brain endothelial cells. *J. Neuroinflammation* **8**: 104

Shin GC, Kim C, Lee JM, Cho WS, Lee SG, Jeong M, Cho J, and Lee K (2009) Apigenin-induced apoptosis is mediated by reactive oxygen species and activation of ERK1/2 in rheumatoid fibroblast-like synoviocytes. *Chem. Biol. Interact.* **182**: 29−36

Shikazono N, Tanaka A, Watanabe H, and Tano S (2000) Rearrangements of the DNA in carbon ion-induced mutants of Arabidopsis thaliana. *Genetics* **157**: 379–387

Sho P, He J, Sun P, and Zhao P (2012) Analysis of conditions for microwave-assisted extraction of total water-soluble flavonoids from Perilla frutescens leaves. *J. Food Sci. Technol*. **49**: 66–73

Siti Maisurah Z, and Siti Mazlina Mustapa K. (2016) Subcritical water extraction of bioactive compounds from plants and algae: application in pharmaceutical and food ingredients. *Food Eng. Rev.* **8**: 23–34

Smolen JS, Landewe R, Breedveld FC, Buch M, Burmester G, Dougados M, Emery P, Gaujoux-Viala C, Gossec L, and Nam J (2014) EULAR recommedations for the management of rheumatoid arthritis with synthetic and biological disease-modifying antirheumatic drugs: 2013 update. *Ann. Rheum. Dis.* **73**: 492−509

Sookwong P, Suttiarporn P, Boontakham P, Seekhow P, Wangtueai S, and Mahatheeranont S (2016) Simultaneous quantification of vitamin E, r-oryzanols and xanthophylls from rice bran essences extracted by supercritical CO_2. *Food Chem.* **211**: 140−147

So YK, Jo YH, Nam BM, Lee SY, Kim JB, Kang SY, Jeong HG, and Jin CH (2015) Anti-obesity effect of isoegomaketone isolated from Perilla frutescens (L.) Britt. cv. Leaves. *Kor. J. Pharmacogn.* **46**: 1−6

So YK, Lee SY, Han AR, Kim JB, Jeong HG, and Jin CH (2016) Rosmarinic acid methyl ester inhibits LPS-induced NO production via suppression of MyD88-dependent and –independent pathways and induction of HO-1 in RAW 264.7 cells. *Molecules* **21**: 1083

Sotnikova R, Ponist S, Navarova J, Mihalova D, Tomekova V, Strosova M, and Bauerova K (2009) Effects of sesame oil in the model of adjuvant arthritis. *Neuro Endocrinol. Lett.* **30**: 22−24

Stadler LJ (1928) Mutation in barley induced by X-rays and radium. *Science* **67**: 186−187

Suprasanna P, Mirajkar SJ, and Bhagwat SG (2015) Induced mutation and crop improvement. *Plant Biology and Biotechnology.* Chapter 23. 593−617

Sybille BW, Hajime F, Claudia R, and Christiane S (2014) Perilla extract improves gastrointestinal discomfort in a randomized placebo controlled double blind human pilot study. *BMC complement. Altern. Med.* **14**: 173

Takano H, Osakabe N, and Sanbongi C (2004) Extract of Perilla frutescens enriched for rosmarinc acid, a polyphenolic phytochemical, inhibits seasonal allergic rhinoconjunctivitis in human. *Exp. Biol. Med.* **229**: 247−254

Thapa D, Meng P, Bedolla RG, Reddick RL, Kumar AP, and Ghosh R (2014) NQO-1 suppresses NF-κB-p300 interaction to regulate inflammatory mediators associated with prostate tumorigenesis. *Cancer Res.* **74**: 1−12

Torun S, Tunc BD, and Suvak, B (2012) Assessement of neutrophil-to-lymphocyte ratio in ulcerative colitis: A promising marker in predicting disease severity. *Clin. Res. Hepatol. Gastroenterol.* **36**: 491−497

True AL, Olive M, Boehm M, San H, Westrick RJ, Raghavachari N, Xu X, Lynn EG, Sack MN, Munson PJ, Gladwin MT, and Nabel EG (2007) Heme oxygenase-1 deficiency accelerates formation of arterial thrombosis through oxidative damage to the endothelium, which is rescued by inhaled carbon monoxide. *Circ. Res.* **101**: 893−901

Tsoyi K, Kim HJ, Shin JS, Kim DH, Cho HJ, Lee SS, Ahn SK, Yun-Choi HS, Lee JH, Seo HG, and Chang KC (2008) HO-1 and JAK-2/STAT-1 signals are involved in preferential inhibition of iNOS over COX-2 gene expression by newly synthesized tetrahydroisoquinoline alkaloid, CKD712, in cells activated with lipopolysaccharide. *Cell Signal.* **20**: 1839−1847

Turdi S, Han X, Huff AF, Roe ND, Hu N, Gao F, and Ren J (2012) Cardiac-specific overexpression of catalase attenuates lipopolysaccharide-induced myocardial contractile dysfunction: Role of autophagy. *Free Radic. Biol. Med.* **53**: 1327−1338

Tylor BS, Kion YM, Wang QI, Sharpio RA, Billiar TR, and Geller DA (1997) Nitric oxide down regulates hepatocyte-inducible nitric oxide synthase gene expression. *Arch. Surg.* **1**: 1177−1182

Ueda H, and Yamazaki M (1997) Inhibition of tumor necrosis factor-α production by orally administering a Perilla leaf extract. *Biosci. Biotechnol. Biochem*. **61**: 1292−1295

Ueda H, Yamazaki C, and Yamazaki M (2002) Luteolin as an anti-inflammatory and anti-allergic constituent of Perilla frutescens. *Biol. Pharm. Bull.* **25**: 1197−1202

Umar S, Umar K, Sarwar AHMG, Khan A, Ahmad N, Ahmad S, Katiyar CK, Husain SA, and Khan HA (2014) Boswellia serrate extract attenuates inflammatory mediators and oxidative stress in collagen induced arthritis. *Phytomedicine* **21**: 847−856

Wang CY, Wang SY, and Chen C (2008) Increasing antioxidant activity and reducing decay of blueberries by essential oils. *J. Agric. Food Chem.* **56**: 3587−3592

Wang Y, Huang X, Han J, Zheng W, and Ma W (2013) Extract of Perilla frutescens inhibits tumor proliferation of HCC via PI3K/AKT signal pathway. *Afr. J. Tradit. Complement Altern. Med.* **10**: 251−257

Wegener T, and Lupke N (2003) Treatment of patients with arthrosis of hip or knee with an aqueous extract of devil's claw (Harpagophytum procumbens DC.). *Phytother. Res.* **17**: 1165−1172

Woo KW, Han JY, Choi SU, Kim KH, and Lee KR (2014) Triterpenes from Perilla frutescens var. acuta and their cytotoxic activity. *Nat. Product Sci.* **20**: 71−75

Yamada N, Yamaya M, Okinaga S, Nakyama K, Shibahara S, and Sasaki H. (2000) Microsatellite polymorphism in the heme oxygenase-1 gene promoter is associated with susceptibility to emphysema. *Am. J. Hum. Gene.* **66**: 187−195

Yang CLH, Or TCT, Ho MHK, and Lau ASY (2013) Scientific basis of botanical medicine as alternative remedies for rheumatoid arthritis. *Clin. Rev. Allergy Immunol.* **44:** 284−300

Yin X, Xiao Y, Li F, Qi S, Yin Z, and Gao J (2016) Prognostic role of neutrophil-to-lymphocyte ratio in prostate cancer. *Medicine* **95**: e2544

Yoon CH, Chung SJ, Lee SW, Park YB, Lee SK, and Park MC (2013) Gallic acid, a natural polyphenolic acid, induces apoptosis and inhibits proinflammatory gene expressions in rheumatoid arthritis fibroblast like synoviocytes *Joint Bone Spine*. **80**: 274−279

Zhang M, An C, Gao Y, Leak RK, Chen J, and Zhang F (2013) Emerging roles of Nrf2 and phase II antioxidant enzymes in neuroprotection. *Prog. Neurobiol.* **100**: 30−47

Zhang X, Wang G, Gurley EC, and Zhou H (2014) Flavonoid apigenin inhibits lipopolysaccharide-induced inflammatory response through multiple mechanism in macrophages. *PLoS One* **9**: e107072

국문초록

방사선육종 차조기에서 분리한 이소에고마케톤의 항염증 효능

서울대학교 대학원 식품영양학과

진창현

방사선 육종 차조기 165종에 대해 항염증 효능을 탐색한 결과 RAW264.7세포에서 일산화질소 (nitric oxide, NO) 생성 저해 효능이 가장 우수한 품종 하나를 선별하였다. 선발된 돌연변이 차조기의 항염증 효능이 증가한 원인은 이소에고마케톤 성분 함량의 증가로 여겨진다. 이소에고마케톤은 차조기에 존재하는 지질 성분 중의 하나로서 항염증, 항암, 항비만 효능이 보고되었다. 이소에고마케톤이 RAW264.7 세포에서 항염증 효능을 보이는 이유 중의 하나는 항산화 효소인 HO-1 발현을 유도하기 때문이다. 하지만 이소에고마케톤이 어떤 기작을 통해 HO-1의 발현을 증가시키는지에 대한 연구는 미흡하다. 본 연구에서는 방사선육종 차조기에서 분리한 이소에고마케톤의 항염증 효능을 세포 실험 및 동물 모델에서 규명하였다. 또한, 방사선육종 차조기를 기능성 식품으로 활용하기 위한 기초 연구를 수행하였다.

연구 1에서는 RAW264.7 세포에서 이소에고마케톤에 의해 HO-1 효소가 발현되는 기작을 규명하기 위해 이소에고마케톤을 농도별 (5, 10, 15 μM)로 처리하였다.

그 결과 이소에고마케톤은 농도 의존적으로 HO-1 발현을 증가시켰다. 이소에고마케톤에 의한 HO-1 효소 발현과 Nrf2 활성화는 p38 MAPK의 특이 억제제 (SB203580)와 활성산소 제거제 (NAC, GSH)를 처리하였을 때 감소하였다.

연구 2에서는 이소에고마케톤이 동물 모델에서 항관절염 효능을 보이는지 알아보기 위해 콜라겐 항체를 수컷 Balb/c 생쥐에 주입하여 유도한 관절염 동물 모델에서 실험을 진행하였다. Balb/c 생쥐를 다섯 개의 그룹 (정상 그룹, 관절염 유발 그룹, 관절염 유발 뒤 이소에고마케톤을 농도별로 처리한 그룹 (5, 10 mg/kg/day), 관절염 유발 뒤 아피제닌 (16 mg/kg/day) 처리 그룹)으로 나누어 하루 한번 4일 동안 경구 투여하였다. 그 결과 이소에고마케톤을 경구 투여한 생쥐군 (10 mg/kg/day)에서 관절염 질환이 개선되었다. 관절염 유발 7일째에 이소에고마케톤을 경구 투여한 생쥐군이 관절염 수치(73%), 관절 부피(15%), 관절 두께(14%)가 관절염만 유발시킨 대조군에 비해 낮았다. 조직학적 관찰을 통해 이소에고마케톤을 경구 투여한 생쥐군에서 관절부위 염증 세포 침투 및 부종 발생이 감소하였다. 또한 림프구 대비 호중구의 비율 (NLR) 역시 이소에고마케톤을 경구 투여한 생쥐군에서 51.9% 낮았다.

연구 3에서는 방사선육종 차조기를 기능성 식품으로 개발하고자 할 때 최적의 추출방법을 결정하기 위해 초임계 유체 추출법과 주정 추출법을 이용해 추출물을 얻었다. 그 결과 초임계 유체 추출물이 주정 추출물에 비해 이소에고마케톤 함량이 5배 높았다. 또한 두 개의 추출물을 LPS로 자극한 RAW264.7 세포에 25 μg/mL 농도로 처리하였을 때 초임계 유체 추출물이 주정 추출물에 비해 염증 물질 (NO, MCP-1, IL-6, IFN-β, iNOS)의 발현을 효과적으로 억제하였다.

연구 4에서는 방사선육종 차조기의 초임계 유체 추출물이 동물모델에서도 효능을 보이는지 규명하기 위해 콜라겐 항체를 이용해 유도한 관절염 동물 모델을 사용하였다. 방사선육종 차조기와 야생 차조기 잎에서 초임계 유체 추출물을 획득하였다. 수컷 Balb/c 생쥐를 네 개의 그룹 (정상 그룹, 관절염 유발 그룹, 관절염 유발 뒤 방사선육종 차조기 추출물 투여 그룹, 관절염 유발 뒤 야생 차조기 추출물 투여 그룹)으로 나누어 하루 한번 4일 동안 경구 투여하였다. 그 결과 방사선육종 차조기의 초임계 추출물을 경구 투여한 생쥐 그룹에서 관절염 수치, 관절 부피, 관절 두께가 관절염만 유발시킨 생쥐 그룹에 비해 개선되었다. 조직학적 관찰을 통해 이소에고마케톤을 경구 투여한 생쥐군에서 관절부위 염증 세포 침투 및 부종 발생이 감소하였다. 또한 림프구 대비 호중구의 비율 (NLR) 역시 방사선육종 차조기의 초임계 추출물을 경구 투여한 생쥐 그룹에서 37% 낮았다. 하지만 야생 차조기의 초임계 추출물을 투여한 생쥐 그룹은 관절염만 유발시킨 생쥐 그룹과 비교해 유의적인 차이를 보이지 않았다.

이소에고마케톤은 RAW264.7 세포에서 ROS/p38 MAPK/Nrf2 경로를 통해 HO-1을 발현시킴으로써 항염 효과를 나타냈다. 또한 콜라겐 항체를 이용해 유도한 관절염 동물 모델에서 실제로 명확하게 관절염 증상을 개선하였다. 방사선육종 차조기를 기능성 식품으로 개발하고자 할 때 이소에고마케톤 함량이 높은 추출물을 획득할 수 있는 초임계 유체 추출 방법이 가장 적합한 방법이었다. 실제로 방사선육종 차조기의 초임계 추출물은 콜라켄 항체를 이용해 유도한 관절염 동물 모델에서 관절염 증상의 발생률을 낮췄다. 종합적으로, 이번 연구의 결과는 방사선육종 차조기의 초임계 유체 추출물이 관절염과 같은 만성 염증성 질환에 있어서 기능성 식품으로 활용할 가능성이 있음을 제시한다.

주요어: 이소에고마케톤, 항염증, 초임계 유체 추출, 방사선육종 차조기, 콜라겐 항체로 유발된 관절염

학번: 2011-31095